

# Review and Outlook of Hydrogen Production through Catalytic Processes

Ravi Kumar, Rohini Singh, and Suman Dutta\*



Cite This: <https://doi.org/10.1021/acs.energyfuels.3c04026>



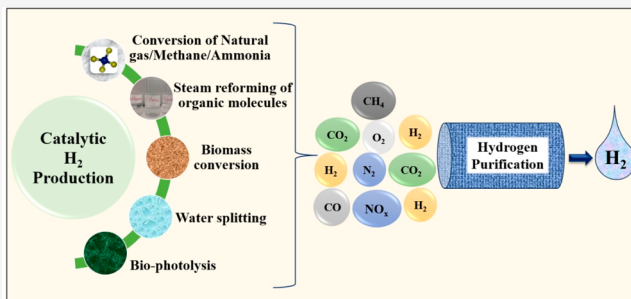
Read Online

ACCESS |

Metrics & More

Article Recommendations

**ABSTRACT:** Hydrogen holds immense potential as a sustainable energy source as a result of its eco-friendliness and high energy density. Thus, hydrogen can solve the energy and environmental challenges. However, it is crucial to produce hydrogen using sustainable approaches in a cost-efficient manner. Currently, hydrogen can be produced by utilizing diverse feedstocks, such as natural gas, methane, ammonia, smaller organic molecules (methanol, ethanol, glycerol, and formic acid), biomass, and water. These feedstocks undergo conversion into hydrogen through different catalytic processes, including steam reforming, pyrolysis, catalytic decomposition, gasification, electrolysis, and photo-assisted methods (photoelectrochemical, photocatalysis, and biophotolysis). Researchers have extensively explored various catalysts, including metals, alloys, oxides, non-oxides, carbon-based materials, and metal–organic frameworks, for these catalytic methods. The primary objectives have been to attain higher activity, selectivity, stability, and cost effectiveness in hydrogen generation. The efficacy of these catalytic processes is significantly dependent upon the performance of the catalysts, emphasizing the need for further research and development to create more efficient catalysts. However, during catalytic hydrogen production, gases like CO<sub>2</sub>, O<sub>2</sub>, CO, N<sub>2</sub>, etc. are produced alongside hydrogen. Separation techniques, such as pressure swing adsorption, metal hydride separation, and membrane separation, are employed to obtain high-purity hydrogen. Furthermore, a techno-economic analysis indicates that catalytic hydrogen production through steam reforming of natural gas/methane is currently viable and commercially successful. Photovoltaic electrolysis has been commercialized, but the cost of hydrogen production is still higher. Meanwhile, other photo-assisted methods are in the development phase and hold the potential for future commercialization.



## 1. INTRODUCTION

In the era of industrialization and technological advancement, energy demand is increasing sharply, and the depletion of fossil fuels and the alarming trend of climate change have given rise to deep concern.<sup>1</sup> Currently, more than 80% of the entire world's energy demand is fulfilled by the supply of carbon-based fuels.<sup>2</sup> This results in the emission of 90% of total CO<sub>2</sub> emitted by the world every year to fulfill the energy demand. Furthermore, the world economy is growing rapidly, indicating the increase in energy consumption in the near future,<sup>4</sup> and hydrogen (H<sub>2</sub>) can play a vital role in fulfilling the energy demand. Hydrogen can be considered an ideal fuel for future generations as a result of its high energy density (143 MJ kg<sup>-1</sup>) and zero emissions.<sup>5,6</sup> In view of this, researchers have explored various catalytic methods for the production of hydrogen. However, almost 90% of hydrogen is produced from non-renewable resources, like fossil fuels,<sup>7</sup> through hydrocarbon reforming, hydrocarbon pyrolysis, and plasma reforming. As a consequence, CO<sub>2</sub> co-production is unavoidable, and approximately 830 million tons of CO<sub>2</sub> per year is produced through these methods.<sup>3</sup> Unfortunately, the widely used method for hydrogen production is steam methane reforming (SMR),

which produces 9 tons of CO<sub>2</sub> for every ton of hydrogen produced.<sup>8</sup> Nowadays, the use of non-fossil feedstocks, such as ethanol, methanol, and glycerol, is essential for the sustainable development of society. The catalytic steam reforming of these smaller organic molecules stands out as one of the most promising methods for hydrogen production.<sup>7</sup> Furthermore, hydrogen can be produced from renewable resources, like biomass or water splitting.<sup>9</sup> Biomass is becoming increasingly favored because it is widely accessible as a renewable energy source and is viewed as an energy option that does not contribute to net carbon emissions. Hence, biomass holds promise as a viable feedstock resource for the production of hydrogen.<sup>10</sup> At present, biomass-based hydrogen production technology mainly includes thermochemical and biological

Received: October 16, 2023

Revised: December 22, 2023

Accepted: December 22, 2023

methods.<sup>11</sup> The thermochemical process includes pyrolysis, gasification, and liquefaction, and this process is gaining attention for producing hydrogen, while biological hydrogen production has low production rates and is difficult to scale up.<sup>12</sup> Another renewable resource for hydrogen production is water, and the water-splitting process is gaining attention worldwide because this process is eco-friendly and produces green hydrogen.<sup>13</sup> There are several methods available for water splitting, including electrolysis, photoelectrochemical, and photocatalysis.<sup>14</sup> However, among these methods, the electrolysis process has been commercialized and produced approximately 4% of total hydrogen production.<sup>15</sup> Other methods, like photoelectrochemical and photocatalysis, utilize solar energy directly and have the potential for large-scale production of hydrogen, but currently, both are in the developmental phase as a result of the unavailability of efficient photocatalysts. Apart from these methods, biophotolysis is another approach through which hydrogen can be produced through the biological process.<sup>16</sup> In the process of biophotolysis, both cyanobacteria and microalgae possess the capability to harness solar energy, producing hydrogen through the reaction of water and CO<sub>2</sub>. The biophotolysis process can be divided into direct and indirect biophotolysis. However, this method suffers from several limitations, like low hydrogen yield and lower light conversion efficiency.<sup>17</sup> The rate of hydrogen production in these catalytic processes is significantly influenced by the choice of catalysts. Consequently, researchers have explored a diverse range of catalysts, including metals (Ni, Fe, Pt, Co, Cu, etc.),<sup>18,19</sup> their alloys, and oxides (CeO<sub>2</sub>, Al<sub>2</sub>O<sub>3</sub>, TiO<sub>2</sub>, BiVO<sub>4</sub>, etc.),<sup>20,21</sup> for hydrogen production. Additionally, from the viewpoint of cost-effectiveness, several non-oxide catalysts based on carbides,<sup>22</sup> nitrides,<sup>23</sup> sulfides,<sup>24</sup> phosphides,<sup>25</sup> and borides<sup>26</sup> have exhibited promising activity toward catalytic hydrogen production. Apart from these catalysts, carbon-based materials, such as carbon nanotubes (CNTs),<sup>27,28</sup> graphene,<sup>29,30</sup> graphitic carbon nitride (g-C<sub>3</sub>N<sub>4</sub>),<sup>1,31</sup> and carbon quantum dots,<sup>32</sup> have been extensively used for catalytic hydrogen production. Nowadays, metal–organic framework (MOF)-based catalysts<sup>13,33,34</sup> have gained attention for their potential in hydrogen production from various sources, including methane, ethanol, and biomass. Unfortunately, the catalytic methods used for hydrogen production often generate several gases along with hydrogen. To obtain hydrogen of fuel-grade quality, various purification techniques, such as pressure swing adsorption (PSA), metal hydride separation, and membrane separation, have been employed.<sup>35</sup> Moreover, for real-life applications of different catalytic hydrogen production processes, conducting a comprehensive techno-economic analysis is crucial to assess the feasibility of these processes.

In this review, the authors have outlined various catalytic methods for hydrogen production, summarizing the catalysts employed in these processes. Additionally, different purification techniques for obtaining fuel-grade hydrogen are discussed, followed by an examination of the techno-economic viability of various catalytic methods.

## 2. ROLE OF CATALYSTS IN VARIOUS CATALYTIC PROCESSES FOR HYDROGEN PRODUCTION

Hydrogen is considered as a sustainable and clean energy source for the future.<sup>36</sup> Various catalytic methods, like reforming of methane,<sup>27,37</sup> reforming of organic compounds,<sup>38–40</sup> biomass conversion,<sup>22</sup> splitting of water,<sup>41,42</sup>

etc., are available for hydrogen generation to achieve economic stability. However, the production of cost-effective and environmentally friendly hydrogen is still challenging. In these catalytic processes, catalysts play a vital role in accelerating the rate of hydrogen generation.<sup>7,18,43</sup> They are directly engaged in the primary transformation, as seen in reforming and electro/photocatalytic water splitting. An efficient catalyst can enhance the activity and selectivity for hydrogen production.

Industrial-scale catalytic decomposition of methane (CDM) to produce hydrogen relies on two essential prerequisites: the development of highly efficient catalysts and the optimization of reactor systems.<sup>44</sup> Nowadays, researchers are considering ammonia as a hydrogen carrier. However, hydrogen production from ammonia requires catalytic processes.<sup>9</sup> The most advanced catalysts currently available for ammonia decomposition involve ruthenium as well as its alloys with elements, like potassium, barium, cesium, etc., and these are supported on various oxide and carbon-based materials. However, it is worth noting that even these catalysts do not exhibit sufficient activity for ammonia decomposition at low temperatures. Moreover, a critical concern is that they may not be economical for large-scale industrial applications.<sup>45</sup> In other catalytic processes, the yield of hydrogen from organic substances, like ethanol, methanol, glycerol, etc., is dependent upon various factors, e.g., the nature of the metal used, catalyst support material, and operating conditions.<sup>46</sup> Thus, catalyst supports play a significant role that influences both hydrogen selectivity and the stability of the catalyst as a result of their inherent characteristics and redox properties. To enhance the efficiency of hydrogen generation via reforming process, it is recommended to develop catalysts that can effectively prevent the formation of coke, a carbonaceous byproduct.<sup>7</sup> Furthermore, the design of efficient catalysts holds the potential to enhance the conversion of biomass, addressing vital considerations, like their stability, recyclability, and effectiveness for practical industrial use. These aspects require more comprehensive exploration and customization through ongoing research endeavors.<sup>12</sup> To realize practical electrocatalytic hydrogen production from water splitting, it is imperative to develop cost-effective catalysts or electrocatalysts that exhibit both high activity and stability.<sup>4,47</sup> Optimizing the efficiency of catalysts for hydrogen generation through photoelectrochemical processes involves precise tuning of various factors. This includes manipulation of the morphology, crystal facet orientation, and energy band structure, as extensively documented in the existing literature. Furthermore, the selection of appropriate electrode materials, such as TiO<sub>2</sub>, WO<sub>3</sub>, Fe<sub>2</sub>O<sub>3</sub>, BiVO<sub>4</sub>, and Cu<sub>2</sub>O, among others, is crucial. These materials should exhibit enhanced stability, photocurrent, and photovoltage properties. Besides, designing a suitable reactor system is equally essential in achieving efficient hydrogen production through these methods.<sup>48</sup> Furthermore, photocatalysis is a simple water-splitting method for hydrogen production. However, developments in the field of photocatalyst materials have been facilitated by a deeper comprehension of the fundamental catalytic mechanisms. This enhanced understanding will allow for a more precise selection of catalytic nanomaterials, resulting in improved overall performance in hydrogen production.<sup>49</sup> Now, in the case of biophotolysis, nitrogenases and hydrogenases are two prominent enzymes involved in photobiological hydrogen production. Hydrogenase enzymes are found across all three

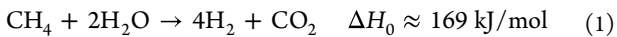
domains of life: eubacteria, archaea (including methanogens and certain extremophiles), and eukaryotes (like green algae). These enzymes play a crucial role in biological hydrogen metabolism and are significant in various biological processes, including microbial hydrogen production.<sup>16</sup>

The discussion above emphasizes the pivotal role of catalysts in hydrogen production through various catalytic processes. The rate of hydrogen production is significantly influenced by the activity and selectivity of the catalysts. Additionally, the stability and reusability of catalysts are crucial parameters in determining their viability for large-scale usage. Furthermore, the development of cost-effective catalysts holds paramount importance for facilitating large-scale industrial production of hydrogen. Sometimes, catalysts play the role of storage materials and purifiers. Therefore, catalysts are also used to purify and store hydrogen after the production process.

### 3. CATALYTIC PROCESSES FOR HYDROGEN GENERATION

Hydrogen production encompasses several methods, each distinguished by the source or feedstock utilized. These methods include the following categories: hydrogen generation from natural gas/methane or ammonia, hydrogen production from smaller organic compounds (methanol, ethanol, formic acid, and glycerol), hydrogen generation from biomass conversion, water-splitting methods (electrolysis, photoelectrochemical, and photocatalysis), and the biophotolysis method.

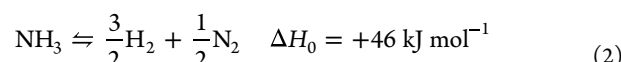
**3.1. Hydrogen Production from Natural Gas/Methane/Ammonia.** Methane is a main constituent of natural gas, and there have been multiple suggested approaches for generating hydrogen from methane, including (a) steam methane reforming, (b) partial oxidation, and (c) autothermal reforming.<sup>50</sup> These methods, which rely on fossil fuels for hydrogen production, are environmentally unfriendly as a result of the high carbon footprint and substantial greenhouse gas emissions. They also release significant pollutants, including carbon monoxide, sulfur compounds, nitrogen oxides, and ash-containing radioactive materials and heavy metals.<sup>51</sup> Among several methods, hydrogen production via reforming of natural gas (methane) is very popular and economical. However, CO<sub>2</sub> capture and sequestration are crucial for steam reforming (SR) of natural gas. Gaseous hydrocarbons, like methane and propane, undergo decomposition through thermocatalytic reactions, employing catalysts based on metals, metal alloys, metal oxides, and carbon-based materials to produce hydrogen.<sup>8</sup> The efficiency of transition metal catalysts declines significantly as a result of carbon deposition on the surface. Consequently, carbon-based catalysts are advantageous for this process because they obviate the necessity for separating carbon from the catalyst. Steam reforming of methane is represented in eq 1.<sup>8</sup>



Steam methane reforming is a mature technology, and it can mitigate environmental problems when coupled with CO<sub>2</sub> capture. Utilization of a membrane reactor can solve the problem. Palladium (Pd)-based membranes are suitable because they have high selectivity for hydrogen and high stability. Habib et al.<sup>52</sup> discussed various methods for the synthesis of Pd alloy membranes and compared them based on their stability and hydrogen permeability. The presence of impurities, such as H<sub>2</sub>S, CO<sub>2</sub>, CO, and O<sub>2</sub>, affects the

performance of the membrane. Various parameters affect the performance of the Pd membrane reactor, such as flow characteristics, temperature, pressure, H<sub>2</sub>O/CH<sub>4</sub> ratio, residence time, etc.

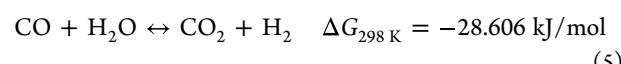
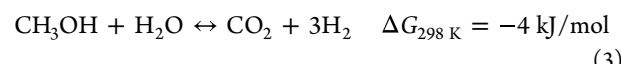
Ammonia is being explored as a promising energy carrier for hydrogen storage and transportation as a result of several advantages.<sup>45</sup> Unlike liquid hydrogen, which requires extremely low temperatures ( $-253^\circ\text{C}$ ) at ambient pressure (1 bar) for liquefaction, ammonia can be easily liquefied at more moderate conditions, making it a more energy-efficient process. Additionally, ammonia is non-flammable, poses no significant safety risks, and has a distinct odor that makes it easy to detect in the case of leaks. Notably, ammonia is a carbon-free molecule, further enhancing its appeal as a hydrogen carrier for addressing challenges related to hydrogen storage and transport. The decomposition of ammonia is a slightly endothermic reaction, and its reaction kinetics are influenced by two key factors: the concentration of ammonia in the feed and the temperature at which the reaction occurs.<sup>53</sup>



Researchers have studied the decomposition of ammonia and other hydrogen-containing materials to find the best storage system for transportation and onboard applications. Hydrogen generation from ammonia via catalytic decomposition at low temperatures ( $<450^\circ\text{C}$ ) is receiving significant consideration because the complete conversion is possible (equilibrium conversion is 99.5% at  $450^\circ\text{C}$ ).<sup>45</sup>

**3.2. Hydrogen Production from Smaller Organic Molecules (Methanol, Ethanol, Formic Acid, and Glycerol).** The steam reforming of smaller organic compounds, like methanol, ethanol, and glycerol, shows significant potential in hydrogen production.<sup>7</sup> The growing demand for economically viable operations at a lower cost of hydrogen production has driven increased research into the utilization of these renewable hydrocarbons. These hydrocarbons are being efficiently converted into hydrogen through process intensification techniques.<sup>54</sup>

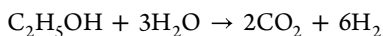
Methanol is a biodegradable substance and is liquid at room temperature, but it possesses toxic properties. One of its notable advantages is its high hydrogen/carbon ratio. In the case of methanol steam reforming (MSR), as depicted in eq 3, the process typically takes place at lower temperatures (200–300 °C) as a result of the presence of only one carbon atom in the methanol structure. This reaction involves multiple steps, including two significant side reactions: methanol decomposition (eq 4) and the water–gas shift reaction (eq 5).<sup>7</sup>



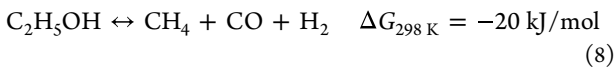
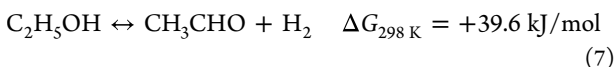
Hydrogen is generated from methanol via aqueous phase reforming. The methanol aqueous phase reforming (MAPR) reaction is conducted under mild conditions (low temperature and normal pressure). Yu et al.<sup>55</sup> have developed N-doped carbon dots/g-C<sub>3</sub>N<sub>4</sub> (NCDs/g-C<sub>3</sub>N<sub>4</sub>; CN-x) composites that can be used as catalysts for the MAPR reaction. The optimized catalyst (NCDs/g-C<sub>3</sub>N<sub>4</sub>; CN-0.7) at 80 °C shows a hydrogen yield of 19.5 μmol g<sup>-1</sup> h<sup>-1</sup>. The surface charge localization was

observed as a result of the incorporation of NCDs. The surface charge localization was helpful for the selective adsorption and polarization activation of polar molecules on the catalyst surface.

Ethanol is another organic compound that offers several benefits as a result of its higher hydrogen content, wide availability, non-toxic nature, ease of handling as a liquid at room temperature, and safety considerations. The process of ethanol steam reforming (ESR) is characterized by an endothermic reaction. During the primary reaction (as described in eq 6), both  $\text{CO}_2$  and  $\text{H}_2$  are generated. Additionally, ESR reactions lead to the formation of other carbon-containing byproducts, including  $\text{CH}_4$ ,  $\text{CO}$ ,  $\text{CH}_3\text{CHO}$ , and  $\text{C}_2\text{H}_4$ , as noted in various studies. Simultaneously, there are secondary reactions, such as dehydrogenation (as shown in eq 7), decomposition (as represented by eq 8), and dehydration (as indicated in eq 9), of ethanol occurring alongside the primary reaction. The production of  $\text{CH}_3\text{CHO}$  primarily results from the dehydrogenation of ethanol.  $\text{C}_2\text{H}_4$  is produced through the dehydration of ethanol and also leads to coke formation.  $\text{CH}_4$  is formed through ethanol decomposition, while ethanol dehydrogenation promotes hydrogen production. Furthermore, the reaction of  $\text{CO}$  with water, as governed by the water–gas shift reaction (eq 5), leads to the production of  $\text{H}_2$ .<sup>7,56</sup>

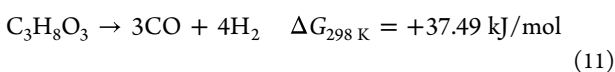
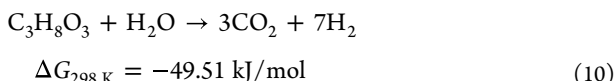


$$\Delta G_{298\text{ K}} = +64 \text{ kJ/mol} \quad (6)$$



Byrd et al.<sup>56</sup> studied the production of hydrogen from ethanol using supercritical water as a reforming media. They have used a continuous tubular reactor with the  $\text{Ru}/\text{Al}_2\text{O}_3$  catalyst to produce hydrogen via ethanol reforming. Supercritical water acts as a dense solvent as well as participates in a reforming reaction. High-pressure hydrogen was produced with low methane and carbon monoxide formation. Authors reported that hydrogen formation was favored at high temperatures and a high water/ethanol ratio. An excellent conversion was achieved in 4 s of reaction time, and coke formation was also negligible.

Apart from methanol and ethanol, glycerol steam reforming (GSR) represents a relatively recent approach to hydrogen production. GSR is characterized by an endothermic nature (eq 10). It is important to note that several side reactions, including glycerol decomposition (eq 11) and the water–gas shift reaction (eq 5), invariably accompany the primary reaction.<sup>7,57</sup>



Glycerol is a byproduct of biodiesel production plants and could be used as a good renewable source to produce hydrogen

fuel. Hydrogen was produced from glycerol via a steam reforming process over nickel-based catalysts, such as  $\text{Ni}/\text{CeO}_2$ ,  $\text{Ni}/\text{MgO}$ , and  $\text{Ni}/\text{TiO}_2$ . The  $\text{Ni}/\text{CeO}_2$  catalyst possesses the highest surface area ( $67.0 \text{ m}^2 \text{ g}^{-1}$ ) and shows the best performance under studied conditions.<sup>58</sup> In another study,  $\text{PtM}$  ( $M = \text{Fe}, \text{Co}, \text{Ni}, \text{or Cu}$ )/ $\gamma\text{-Al}_2\text{O}_3$  catalysts were synthesized for glycerol aqueous phase reforming.<sup>59</sup> The authors reported that the  $\text{Pt}_1\text{Fe}_1/\gamma\text{-Al}_2\text{O}_3$  catalyst has the best performance. Fe facilitated the supply of OH via dissociation of  $\text{H}_2\text{O}$  and helped the reaction with CO adsorbed on Pt, as shown in Figure 1. The  $\text{Pt}_1\text{Fe}_1$  alloy also increases the decomposition/desorption of formate species that tend to block the active sites.

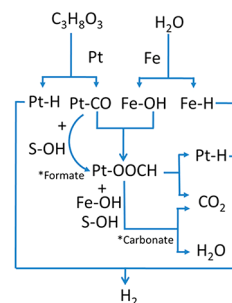
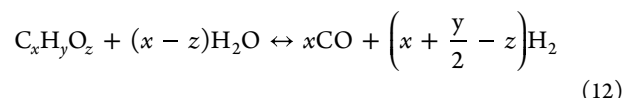
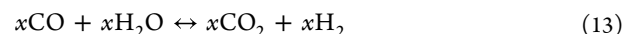


**Figure 1.** Proposed scheme of glycerol aqueous phase reforming over the  $\text{Pt}_1\text{Fe}_1/\gamma\text{-Al}_2\text{O}_3$  catalyst. The symbol “S” refers to the support. This figure was reproduced with permission from ref 59. Copyright 2019 American Chemical Society.

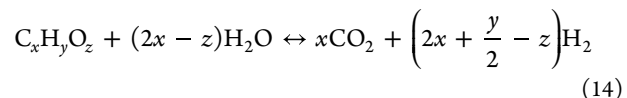
Li et al.<sup>60</sup> have conducted the thermodynamic analysis of steam reforming (SR) of oxygenated fuels (e.g., methanol, ethanol, *n*-propanol, *n*-butanol, *n*-hexanol, ethylene glycol, glycerol, glucose, acetic acid, and acetone). They have considered the Gibbs free energy minimization method for this purpose. The suitable temperature range for the steam reforming process was 600–700 °C. The catalyst may be deactivated as a result of the deposition of carbon. Therefore, a proper steam/carbon ratio should be maintained to minimize carbon deposition. The SR reactions of the above oxygenates can be generally described by the following equations:



By coupling with the water–gas shift reaction (WGSR)



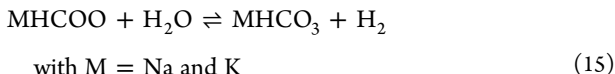
Complete selectivity of  $\text{H}_2$  at the expense of CO takes the form of eq 14



However, the steam reforming of smaller organic molecules encounters challenges like catalyst poisoning caused by coke formation. Therefore, the pivotal aspect for achieving higher hydrogen production from steam reforming lies in developing efficient catalysts that exhibit high catalytic activity, remarkable stability, high selectivity, and regeneration capability.

Additionally, hydrogen can be stored efficiently in the form of formic acid (53 g of  $\text{H}_2/\text{L}$ ). Formic acid is produced via hydrogenation of  $\text{CO}_2$  by various methods.<sup>61</sup> The bicarbonate/

formate approach can release hydrogen. The advantage of this method is that it avoids the handling of gaseous CO<sub>2</sub> (see eq 15). The reaction is also thermodynamically favorable. Cesium salts are effectively utilized because cesium formate and bicarbonate exhibit the highest solubility in water among all alkali metal formates and bicarbonates.<sup>62</sup>



This reversible reaction can be conducted using heterogeneous as well as homogeneous catalysts. The bicarbonate/formate system shows lower power densities. However, improvements in catalysis can solve the problem.<sup>63</sup>

### 3.3. Hydrogen Production by Biomass Conversion.

Biomass conversion is another catalytic process to produce hydrogen. Biomass encompasses a diverse range of organic materials originating from non-fossil sources and formed through the biological process.<sup>12</sup> Additionally, biomass extends to include waste materials generated in agricultural and forestry practices, encompassing agricultural remnants, forest by-products, energy-oriented crops, waste from agro-industries, and municipal waste.<sup>12</sup> Apparently, energy-efficient plant biomass includes forestry wastes, agricultural wastes, and crops, such as sugar cane, corn, and many more.<sup>64</sup> Hydrogen is produced by biomass conversion through two major processes, i.e., thermochemical and biological processes. Figure 2 shows

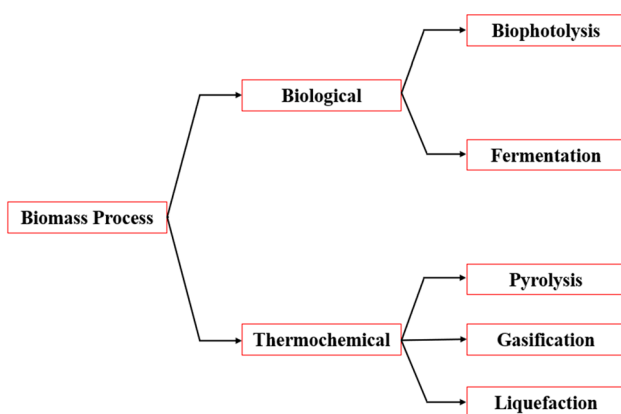


**Figure 2.** Hydrogen production processes through biomass conversion. This figure was partially adapted with permission from ref 18. Copyright 2022 Elsevier.

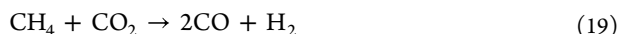
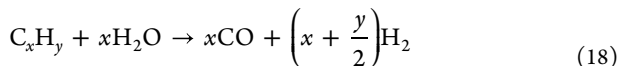
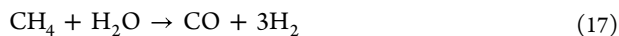
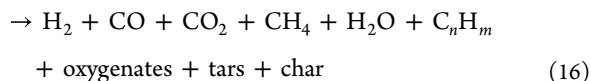
the hydrogen production from biomass through various methods. Hydrogen generation from biomass conversion occurs in two stages. Initially, biomass is converted into an intermediate hydrogen substrate, and then hydrogen generation is performed via catalytic conversion of substrates.

**3.3.1. Thermochemical Process.** Hydrogen production through the thermochemical process is further classified into different methods, such as pyrolysis, gasification, and liquefaction. In these processes, biomass has emerged as a promising feedstock, significantly contributing to the production of value-added materials. Furthermore, higher concentrations of oxygen (35–40%) in the products obtained through these methods have limited miscibility with traditional mineral fuels, making them unsuitable for direct utilization in blending with diesel or gasoline. To meet such standards, further substantial upgrading of the bio-oil is necessary.<sup>65,66</sup> Among

these methods, gasification has the advantage of producing syngas, which can be directly utilized as fuel in furnaces or to obtain pure hydrogen through purification.

Pyrolysis is a thermal degradation process operated at high temperatures (400–900 °C) and short contact times (seconds or less). In this process, dry biomass is processed in the absence of oxygen, which produces gaseous products, liquid (bio-oil), and solids.<sup>66</sup> Biomass pyrolysis represents a straightforward process offering numerous advantages, such as utilizing inexpensive feedstock, being CO<sub>2</sub>-neutral, and facilitating waste recycling. However, this process encounters limitations, such as the formation of charcoal on the catalyst surface, high reactor cost, and seasonal availability of feedstock. This method was employed with nickel-containing BEA zeolite catalysts (NiBEA catalysts) by researchers<sup>67</sup> for the production of hydrogen-rich gas from lignocellulosic biomass. Ni on dealuminated SiBEA zeolite has a large surface area, relatively small pore size, high micropore contribution, and large number of vacant T atom sites. Initially, cellulose and pinewood were pyrolyzed at 500 °C, and vapors were passed through a catalyst bed at 700 °C to upgrade their quality. A mixture of gases can be produced from lignocellulosic biomass, as shown in eq 16.<sup>67</sup>

lignocellulosic biomass



Conversely, the methanation reaction (eq 21) reduces the amount of H<sub>2</sub> production, which is not desirable at all.



Gasification of biomass is another thermochemical method that operates at a higher temperature of around 1000 °C and pressure of about 33 bar depending upon the type of reactor, final product application, and operational scale. In this process, syngas (H<sub>2</sub> and CO) is the main product and obtained in the presence of oxidizing agents, either pure oxygen, air, or steam.<sup>18</sup> In the thermal conversion of lignocellulosic biomass, nickel catalysts play a vital role in promoting the cleavage of carbon–carbon and carbon–oxygen bonds. This results in the increased formation of gaseous compounds and enhances the overall efficiency of hydrogen production. The quantity of hydrogen generated within the gaseous product is contingent upon the operational parameters of biomass gasification. Key factors include the temperature and steam flow, both of which should undergo optimization with regard to economic factors and gasification efficiency. Additionally, the selection of materials plays a pivotal role in determining the effectiveness of the gasification process.<sup>12</sup> However, further studies are necessary to address technical barriers associated with this process, notably the issues related to tar formation and ash accumulation. Among the most promising approaches for tar removal, catalytic gas cleaning stands out as a method that offers several advantages.<sup>68</sup> The gasification process was

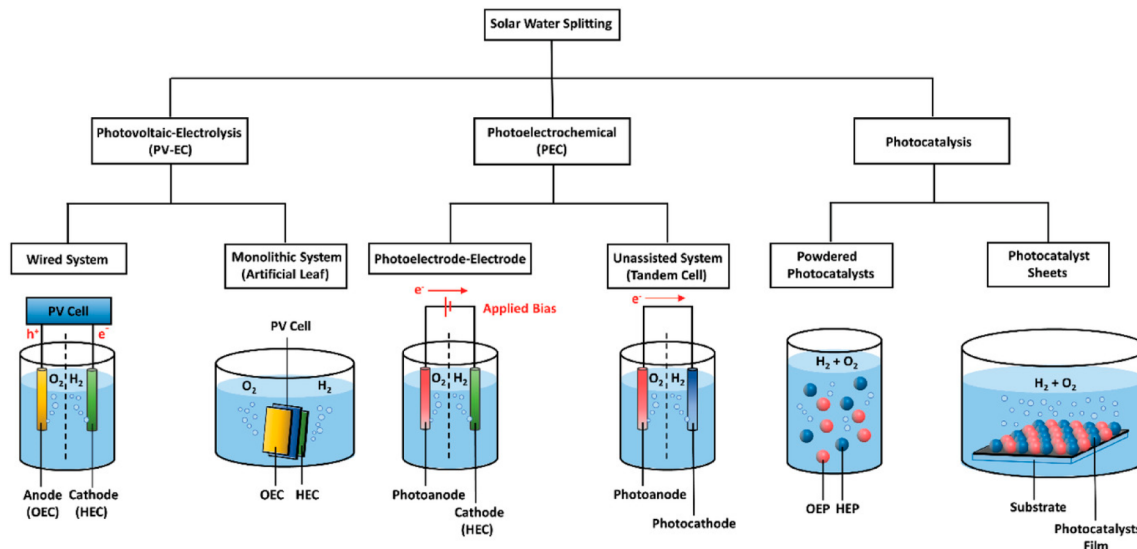


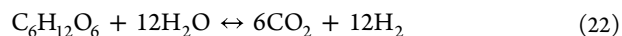
**Figure 3.** Solar water-splitting technologies: PV–E, PEC, and photocatalysis. This figure was reproduced with permission from ref 14. Copyright 2020 Wiley-VCH.

employed by Lu et al.<sup>69</sup> for hydrogen production from miscellaneous sawdust. In this study, authors reported that the Mo–Ni–Co/cordierite monolithic catalyst has reached a hydrogen yield of 49.3 g/kg, gas yield of 1.28 Nm<sup>3</sup>/kg, and tar conversion of 99.2%. Higher tar conversion helps in overcoming the key issue of tar removal from biomass gasification and, thus, reduces the tar content from product gases.

Another thermochemical method known as liquefaction involves a longer retention time at mild temperatures (250–350 °C). It commonly utilizes wet biomass, like sewage sludges and domestic organic waste as feedstock, which reduces the energy required for drying and shows an advantage over the pyrolysis process. Oils produced through liquefaction exhibit greater stability compared to those from pyrolysis, with reduced the oxygen content. Consequently, these oils possess a high heat value (approximately 75–80% of the feedstock) and demonstrate excellent compatibility with mineral fuels.<sup>66</sup> However, this method has some drawbacks, including the relatively low yield of hydrogen obtained from the reformation of the produced oil.<sup>68</sup> In a study, Rajagopal et al.<sup>70</sup> processed household waste for the production of bio-oil and biohydrogen through hydrothermal gasification (HTG) and hydrothermal liquefaction (HTL). The authors employed the bentonite/Nb-TiO<sub>2</sub> catalyst that produced a hydrogen yield from HTG of 39 wt % (catalyst load of 4 wt %) and HTL of 26 wt % (catalyst load of 3 wt %).

**3.3.2. Biological Processes.** Other processes for hydrogen generation via fermentation or photofermentation of biomass pose challenges, such as lower yield and larger reactor volume requirements. However, biological wastes are cheap and abundant, which gives an edge with respect to feedstock. Photofermentation harnesses nitrogenases as catalysts to transform biomass feedstock into hydrogen using solar energy in a nitrogen-deficient medium. However, biohydrogen production through this process has several limitations, like lower solar conversion efficiency, the requirement of a sufficient adenosine triphosphate (ATP) supply, and lower hydrogen production. Equation 22 illustrates the general

reaction involved in the photoproduction of hydrogen from glucose.<sup>18</sup>



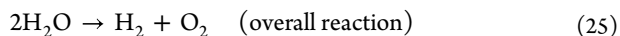
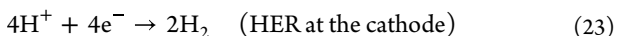
Dark fermentation is one of the most comprehensively understood methods for biohydrogen production among various fermentative approaches. In dark fermentation, micro-organisms utilize substrates to produce hydrogen, primarily as an energy source. In the absence of an electron acceptor, an excess of hydrogen gas molecules is generated alongside other co-products.<sup>51</sup> During this process, anaerobic microorganisms, such as microalgae, generate hydrogen under dark conditions and within a temperature range spanning from 25 to 80 °C. The primary mechanism for hydrogen production in this method is the breakdown of carbohydrates through catabolism.<sup>18</sup> Dark fermentation has attracted researchers as a result of its high energy efficiency, carbon balance, and environmental sustainability. However, it is necessary to improve hydrogen production by enhancing biological activity. Apart from this, the kinetic and thermodynamic constraints of the microbial anaerobic fermentation reactions can be overcome by improving the electron transfer of the microbial fermentation. Some of the researchers enhanced the biological activity as well as electron transfer in the presence of metals (Ni<sup>0</sup> and Fe<sup>0</sup>) or metallic oxide nanoparticles (Fe<sub>2</sub>O<sub>3</sub> and NiO). Additionally, it is essential to pretreat the substrate to improve biodegradability and remove undesired metabolites.

**3.4. Water-Splitting Process.** Another approach for catalytic hydrogen production is based on the photo-assisted method. Figure 3 illustrates three distinct categories, including photovoltaic–electrolysis (PV–E), photoelectrochemical (PEC), and photocatalysis, for solar water splitting.<sup>14</sup> First, there is the photovoltaic-electrolyzer-based setup, where two separate devices are employed to drive the electrolysis process. Second, PEC, which relies on semiconductors serving as photoelectrodes, is separated by a membrane within a cell that is immersed in an aqueous electrolyte. Third, there is the photocatalytic-based setup, which involves the use of photoactive semiconductor particles suspended in a solution, essentially forming a slurry.<sup>71</sup>

**3.4.1. Electrolysis.** Electrocatalytic water splitting involves two key processes: the hydrogen evolution reaction (HER) occurring at the cathode and the oxygen evolution reaction (OER) taking place at the anode.<sup>72</sup> However, from a thermodynamic perspective, the energy requirements for water splitting are highly unfavorable under typical conditions. At 298 K and 1 bar atmospheric pressure, water splitting is non-spontaneous and demands more than 237 kJ/mol of Gibbs free energy ( $\Delta G$ ) to generate hydrogen and oxygen. Consequently, there is a pressing need for innovative electrocatalysts capable of facilitating the electrolysis of water under atmospheric conditions. Various approaches are employed in the fabrication or design of electrocatalysts to reduce overpotential and enhance the production of hydrogen through water splitting.<sup>19</sup> For this purpose, a novel nanohybrid material composed of vertically grown CoS nanosheets on a carbon cloth (CoS/CC) that serves as an effective self-supported cathode was developed by the researchers<sup>73</sup> for hydrogen evolution during water splitting across a broad pH range. This material demonstrates a remarkable current density of 10 mA cm<sup>-2</sup> at a low overpotential of 192 mV in basic conditions and 212 mV in acidic conditions. Furthermore, it exhibits excellent long-term stability, sustaining its performance for over 50 h. In 2015, Chen et al.<sup>74</sup> made a significant advancement by developing metallic Co<sub>4</sub>N porous nanowire arrays directly on flexible substrates, representing a breakthrough as highly active electrocatalysts for the OER. This achievement was made possible by the collaborative advantages of the metallic nature of the material, the one-dimensional porous nanowire arrays, and the unique three-dimensional electrode configuration. Through surface oxidation activation, Co<sub>4</sub>N porous nanowire arrays on carbon cloth achieved an exceptionally low overpotential of 257 mV at a current density of 10 mA cm<sup>-2</sup> in an alkaline medium. Additionally, they demonstrated a low Tafel slope of 44 mV dec<sup>-1</sup>. These results signify the best OER performance among all reported Co-based electrocatalysts until 2015.

While electrolysis offers several advantages, like renewable feedstock and being environmentally friendly, its application is constrained by certain limitations. These include high electricity demand, thus higher electricity costs when non-renewable energy sources are employed, and high initial investments when utilizing renewable sources (PV and wind). Additionally, the use of catalysts as electrode materials presents certain limitations, including expensive catalyst costs and lower catalytic efficiency. Thus, the cost of hydrogen mainly depends upon electricity costs and is anticipated to decrease in the near future with advancements in technology. Furthermore, the development of efficient catalysts can make this process more economical.

**3.4.2. Photoelectrochemical.** Electrochemical water splitting stands out as an exceptionally environmentally friendly method for hydrogen production, because it generates no carbon footprint. This process entails two half-cell reactions, with the HER taking place at the cathode and the OER occurring at the anode. The ultimate electrochemical decomposition of water (H<sub>2</sub>O) into hydrogen (H<sub>2</sub>) and oxygen (O<sub>2</sub>) as a byproduct is represented by eq 25.<sup>15</sup>



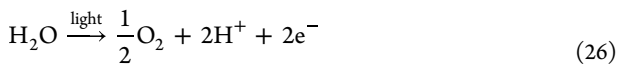
The photoelectrochemical (PEC) cell, typically consisting of a cathode and an anode, can split water into hydrogen (H<sub>2</sub>) and oxygen (O<sub>2</sub>) without requiring an external electrical bias. This can be achieved by initiating half-cell reactions at the anode and cathode, involving oxidation and reduction processes, respectively.<sup>75</sup> Nevertheless, the widespread industrial application of the PEC cell faces numerous limitations and challenges. These include issues like photocorrosion, recombination of electrons and holes, instability of catalysts, and the relatively low solar-to-hydrogen (STH) efficiency, all of which need to be addressed and overcome for the technology to reach its full potential. In a study, a cobalt phosphide (CoP) electrocatalyst serves a dual role in a PEC water-splitting system. This PEC cell was composed solely of earth-abundant elements, eliminating the need for precious metals. During the process, the cathode retains CoP, while CoP on the BiVO<sub>4</sub> photoanode transforms into amorphous CoO<sub>x</sub>–HPO<sub>y</sub>, matching the performance of traditional cobalt phosphate electrocatalysts. Impressively, this system outperforms precious metal-based setups, with the Pt HER electrocatalyst at the cathode replaced by earth-abundant elements.<sup>76</sup>

**3.4.3. Photocatalysis.** Another catalytic process that employs semiconductor materials as catalysts has attracted significant attention as a result of its potential for optimizing solar energy utilization. Photocatalytic reactions take place when semiconductor materials absorb photons with energy ( $h\nu$ ) equal to or exceeding the band gap of the semiconductor. Upon absorbing this energy, electrons are elevated from the valence band to the conduction band, forming an electron–hole pair. These photogenerated electrons in the conduction band subsequently reduce H<sup>+</sup> ions to form H<sub>2</sub>, while the holes on the semiconductor surface participate in the decomposition of H<sub>2</sub>O into O<sub>2</sub> and H<sup>+</sup>.<sup>77</sup> Efficient solar water splitting relies on photocatalysts that exhibit three crucial characteristics: first, a strong capacity to absorb visible light; second, minimal charge recombination, which ensures that separated electrons and holes remain available for reactions; and third, a large surface area conducive to facilitating surface reactions.<sup>49</sup> The design of stable molecular catalysts with low-cost and earth-abundant transition metals is an attractive approach to the hydrogen economy. For this purpose, various transition metal complexes of macrocycles, including porphyrins, have been developed. Transition metal complexes of porphyrins and porphyrin molecules attached to a surface are used as homogeneous and heterogeneous catalysts, respectively.<sup>78</sup> In another study performed by Song et al.,<sup>79</sup> graphitic carbon nitride (g-C<sub>3</sub>N<sub>4</sub>)/WO<sub>3</sub>/WS<sub>2</sub> ternary heterojunctions were synthesized and utilized for hydrogen generation via photocatalytic reaction. The S-scheme heterojunction was formed during the synthesis of the catalyst. The as-prepared ternary photocatalyst shows a hydrogen evolution rate of 29 μmol g<sup>-1</sup> h<sup>-1</sup> even without Pt loaded. Holes were retained on WO<sub>3</sub> and helped to generate •OH. The addition of WS<sub>2</sub> and the presence of oxygen vacancies improved the light absorption as a result of the combined effect of the narrow band gap and the localized surface plasmon resonance (LSPR) effect. WS<sub>2</sub> was also utilized as the co-catalyst to receive electrons.

However, the scalability of this approach is restricted by several factors and necessities to overcome, for example, (i) use of non-scalable sacrificial agents, (ii) lower photocatalytic efficiency, (iii) stability of the photocatalysts, (iv) usage of

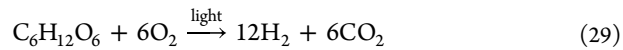
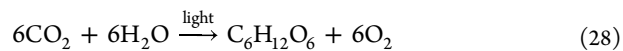
noble metal as a co-catalyst, and (v) narrow light absorption. Thus, the synthesis of a suitable photocatalyst that has a lower electron–hole ( $e^-/h^+$ ) pair recombination along with the high absorption of the visible light spectrum, hence, efficiently works under natural sunlight without the usage of sacrificial reagents. Nowadays, researchers are increasingly concentrating their efforts on developing efficient photocatalysts through the design of heterojunctions and incorporation of co-catalysts.

**3.5. Water Biophotolysis.** Biophotolysis is another emerging technology that produces hydrogen from water via a metabolic pathway of a special type of microorganism. Hydrogen can be produced by direct biophotolysis and indirect biophotolysis.<sup>16</sup> Cyanobacteria are the most promising microorganisms for biological photohydrogen production. Cyanobacteria contain chlorophyll and various carotenoids, which are responsible for light harvesting and photoprotection. They can produce chlorophyll and also have phycobilins, which act as accessory pigments in photosynthesis.<sup>80</sup> Hydrogenases, including [FeFe] and [NiFe] types, play a significant role in catalyzing the biological hydrogen production process. The major limitation in the commercialization of biological processes is the low light-absorbing capacity of the microorganisms. The problem associated with inherent low-light saturation of photosynthesis can be solved using the truncated antenna mutants of *Chlamydomonas* and *Synechocystis*.<sup>81</sup> In a study, the catalytic activity of two key enzymes, i.e., hydrogenase and nitrogenase, were reported for hydrogen production via the biophotolysis (direct and indirect) process.<sup>17</sup> In the process of direct biophotolysis, photoautotrophic organisms utilize light energy under anaerobic conditions to convert water molecules into hydrogen through the catalytic action of the hydrogenase enzyme. The overall reactions can be outlined as follows:



Over the past few decades, there has been significant interest in utilizing the unicellular green algae known as *Chlamydomonas reinhardtii* for the production of hydrogen molecules through direct biophotolysis.<sup>82</sup> The utilization of water as a feed source and sunlight as an energy source for biocatalysts makes this process an attractive option for hydrogen production. However, an efficient photobioreactor with a large area is required for this process to allow for adequate light penetration into the media, supporting algal cultivation. Furthermore, the co-production of oxygen alongside hydrogen leads to the inhibition of hydrogen-related reactions through hydrogenase catalytic activities. The utilization of genetically modified strains represents an advanced method that has been extensively explored to enhance the tolerance of hydrogenase to oxygen. The primary challenge associated with direct biophotolysis, which is the sensitivity of hydrogenase to oxygen, has been successfully addressed and resolved through indirect biophotolysis.<sup>83</sup>

In the indirect biophotolysis process, carbohydrates, like starch and glycogen, are accumulated during the CO<sub>2</sub>-fixation stage, leading to the generation of oxygen (O<sub>2</sub>). These accumulated substrates from the initial stage are then utilized as a carbon source in the subsequent stage, which operates under anaerobic conditions. The sequence of photochemical reactions involved in indirect biophotolysis is outlined below.<sup>36</sup>



Several researchers have extensively explored this area and devoted significant contributions to the biophotolysis process. The photosynthesis efficiency and the algal H<sub>2</sub> production via biophotolysis have been improved through the reduction of the chlorophyll size. Mutation of *C. reinhardtii* was performed by atmospheric and room-temperature plasma (ARTP) to improve hydrogen production. The algal mutant shows 1.8–5.2 times and 2.7–3.1 times higher hydrogen production than the wild type as pure and in a co-culture, respectively.<sup>84</sup> In a study, the algal strain *Chlamydomonas* mutant hpm91 shows an improved H<sub>2</sub> photoproduction (under sulfur deprivation) in terms of sustainability compared to its progenitor strain (CC400, wild type) and other pgr mutants.<sup>85</sup> In another study, Chen et al.<sup>86</sup> studied H<sub>2</sub> photoproduction under sulfur-deprived conditions using both the wild type and hpm91 mutant. The study reveals that the activity of both photosystem II (PSII) and photosystem I (PSI) in the hpm91 variant is significantly improved in comparison to the wild type. Specifically, the effective quantum yield of PSII and PSI in hpm91 shows enhancements of up to 78.9 and 147.6%, respectively, resulting in overall enhanced photochemistry of hpm91. The mutant hpm91 can be used for large-scale applications.

In biological hydrogen production, hydrogenases are utilized efficiently. These hydrogenases have good redox chemical properties and are efficient as a biocatalyst for hydrogen fuel. Researchers are studying the possibility of replacing platinum electrodes with hydrogenase biocatalysts in hydrogen generation systems as well as hydrogen fuel cells.<sup>87</sup> The [FeFe] hydrogenase from *Clostridium acetobutylicum* can be used as the catalyst for the cathodic reaction.<sup>88</sup> In another study, Vincent et al.<sup>89</sup> employed O<sub>2</sub>-tolerant [NiFe] hydrogenase from *Ralstonia eutropha* to coat the pyrolytic graphite edge electrode, which serves as the anode in a fuel cell. This device shows an output voltage of about 1 V, even in the presence of CO. Inorganic–bio hybrid photocatalysts can be used efficiently for hydrogen production. This system is a combination of an inorganic semiconductor and a biocatalyst, where the inorganic semiconductor catalyst captures and converts light energy into chemical energy and the biocatalyst is utilized for hydrogen production.<sup>90</sup> Numerous inorganic–bio hybrid photocatalysts have been developed, including combinations, such as TiO<sub>2</sub> with bacterial hydrogenase and archaeal [NiFe] hydrogenase, TiO<sub>2</sub>-coated p-Si photocathode with [NiFeSe] hydrogenase, nitrogen-doped TiO<sub>2</sub> with [FeFe] hydrogenase, and CdTe or CdS with recombinant clostridial [FeFe] hydrogenase. The major drawbacks of these catalysts are the stability of the enzyme, time and cost associated with cell disruption, and protein purification steps. This problem can be solved by utilizing a whole-cell biocatalyst rather than purified hydrogenases. Honda et al. have developed a system, which was a combination of anatase TiO<sub>2</sub>, methyl viologen (electron mediator), and a whole-cell biocatalyst, which was composed of recombinant *Escherichia coli* that harbors genes for encoding clostridial [FeFe] hydrogenase and maturase, as shown in Figure 4.<sup>91</sup> Cells from a culture were utilized directly as whole-cell biocatalysts and were more stable than purified hydrogenase. In this system, the apparent quantum yield at 300 nm (AQY300) for hydrogen production was only 0.3%. The

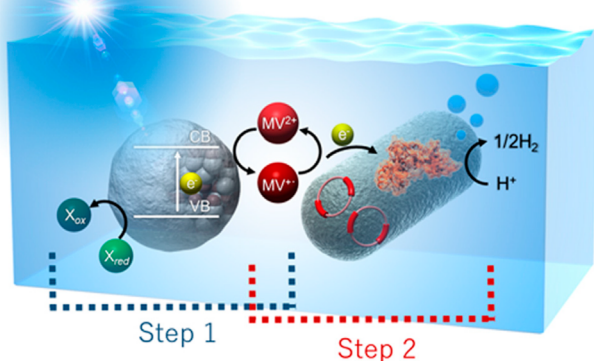
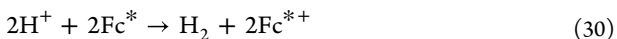


**Figure 4.** Photocatalytic hydrogen production system using the combination of an inorganic semiconductor, an electron mediator, and a whole-cell biocatalyst (recombinant *E. coli*). This figure was reproduced with permission from ref 91. Copyright 2017 Elsevier.

reaction involves two steps: (1) the photocatalytic reduction of methyl viologen (MV) by  $\text{TiO}_2$  and (2) the generation of hydrogen by reduced MV through the utilization of a whole-cell biocatalyst, as illustrated in Figure 4.

Numerous models have been identified for catalyzing the conversion of hydrogen ions into  $\text{H}_2$  when exposed to an acidic environment and a soluble reducing agent.<sup>92</sup> Remarkably, both complexes ( $[1]^0$  and  $[2]^0$ ) can produce  $\text{H}_2$  in the presence of an acid, even in the absence of supplementary reducing agents, marking an unprecedented achievement among hydrogenase models. The catalytic reaction can be concisely described by eq 30.



A suggested mechanism outlining the reaction of  $[1]^0$  with protons to yield  $\text{H}_2$  is illustrated in Figure 5. The catalysts introduced in this study exhibit heightened reactivity as a result of the synergistic interplay of three elements: (i) the presence of the aminodithiolate (adt) cofactor, (ii) the existence of a FeFe core with adequate basicity to facilitate the creation of terminal hydrides, and (iii) the inclusion of a redox-active ligand possessing ample driving force.<sup>92</sup>

#### 4. VARIOUS CATALYSTS USED FOR HYDROGEN GENERATION

The choice of catalyst depends upon the specific hydrogen production method, cost considerations, and environmental factors. Researchers are continually working to develop more efficient and affordable catalysts for sustainable hydrogen production.

**4.1. Metal/Alloy Catalysts.** Metals/alloys are used for catalytic hydrogen production, and the selection of suitable metals/alloys can improve the performance of the catalytic process. Metals utilized for the synthesis of catalysts for various catalytic processes are summarized in Table 1. Key metals and alloys used in these catalysts include nickel (Ni), platinum (Pt), cobalt (Co), iron (Fe), and their combinations. These catalysts are essential for enhancing reaction kinetics, improving selectivity, and ensuring efficient and sustainable hydrogen production. The catalytic decomposition of natural

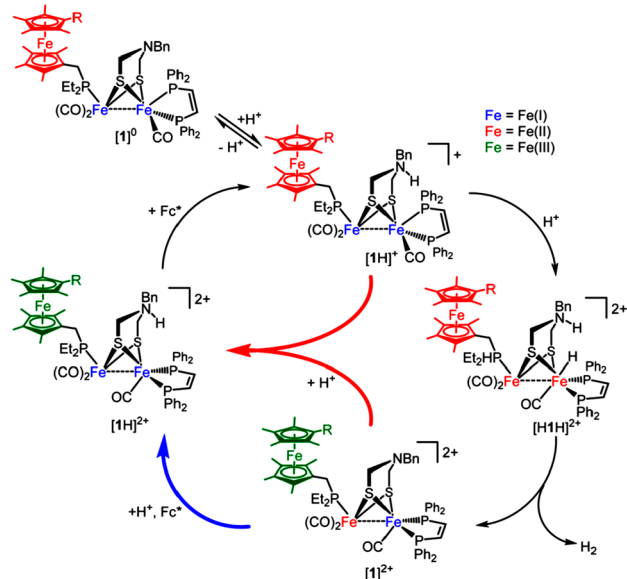


**Figure 5.** Proposed hydrogen evolution mechanism for  $[1]^0$  (and  $[2]^0$ , where R = H) in the presence of excess acid and reducing agent. This figure was reproduced with permission from ref 92. Copyright 2014 American Chemical Society.

gas involves the participation of various transition metals. Among the various metals, Ni-based systems have garnered significant attention as a result of their effectiveness and stability under relatively mild reaction conditions (temperature range of 773–873 K and pressure of 0.1 MPa). However, the utilization of Ni-based catalysts has encountered certain challenges, primarily their limited operational temperature range and susceptibility to oxidative treatments (e.g., burnoff with  $\text{O}_2/\text{air}$  or gasification with  $\text{H}_2\text{O}/\text{CO}_2$ ) commonly employed for coke removal.<sup>93</sup> In a study, Palmer et al.<sup>94</sup> used molten metal Cu- and Bi-based alloy catalysts for methane pyrolysis. In a separate study, a molten mixture of Ni (27 mol %) and Bi (73 mol %) is used for  $\text{CO}_2$ -free hydrogen production via catalytic decomposition in a bubble column reactor from methane, crude petroleum, propane, and benzene at high temperatures (900–1000 °C). For crude oil, benzene, and propane, this reactor shows 100% conversion at a residence time of 1 s.<sup>8</sup> Another alloy based on Ni–Cu–Co was utilized by Lua et al.<sup>95</sup> for methane decomposition. Remarkably, these Ni–Cu–Co catalysts demonstrated exceptional performance, achieving methane conversion rates of up to 82% when operated at 750 °C. Furthermore, for the purpose of ammonia decomposition, a deposition–precipitation process was employed for the synthesis of transition metal (Co, Ni, and Fe) based catalysts that were uniformly distributed on La-promoted MgO surfaces. As a result, the catalysts displayed exceptionally high catalytic activity for ammonia decomposition compared to previous reports on similar compositions, showcasing their potential for advancing this critical process.<sup>96</sup> In another study, Lucentini et al.<sup>97</sup> synthesized bimetallic catalysts (Ni–Ru) supported with ceria using a co-impregnation method, conducted comprehensive characterizations, and assessed their efficacy in hydrogen production via catalytic ammonia decomposition. The catalysts exhibiting the most remarkable performance featured Ni and Ru loadings in the range of 2.4–5 and 0.4–0.6 wt %, respectively, with a Ni/Ru weight percent ratio approximately

**Table 1. Metals and Metal Oxides Used in Various Catalytic Hydrogen Production**

process	catalyst	reference
hydrogen production from natural gas/methane/ammonia	metals Ru, Rh, Pt, Pd, Ir, Na, Co, Mg, Ni, Al, Fe, Mo, Cu, and Zn metal oxides CeO <sub>2</sub> , La <sub>2</sub> O <sub>3</sub> , Y <sub>2</sub> O <sub>3</sub> , ZrO <sub>2</sub> , MgO, CaO, SiO <sub>2</sub> , Al <sub>2</sub> O <sub>3</sub> , and TiO <sub>2</sub>	43 and 110
hydrogen production from organic molecules (methanol, ethanol, formic acid, and glycerol)	metals Ru, Rh, Pd, Pt, Ir, Au, Ni, Co, Cu, Al, Zn, La, and Mn metal oxides Al <sub>2</sub> O <sub>3</sub> , CeO <sub>2</sub> , ZrO <sub>2</sub> , ZnO, MgO, TiO <sub>2</sub> , SiO <sub>2</sub> , CuO, CaO, and Nb <sub>2</sub> O <sub>5</sub>	7, 21, 54, 57, and 111
hydrogen production by biomass conversion	metals Ru, Ag, Pt, Pd, Rh, W, Co, Cr, Ni, Fe, Ca, Zn, Mn, and Cu metal oxides Al <sub>2</sub> O <sub>3</sub> , CeO <sub>2</sub> , CaO, ZnO, MgO, SiO <sub>2</sub> , TiO <sub>2</sub> , and ZrO <sub>2</sub>	10, 12, 18, and 20
electrolysis	metals Ag, Ni, Co, Mo, Mn, Fe, Cu, and Ag metal oxides NiO, FeO <sub>2</sub> , CoO <sub>2</sub> , Co <sub>2</sub> O <sub>4</sub> , Co <sub>3</sub> O <sub>4</sub> , IrO <sub>2</sub> , RuO <sub>2</sub> , CuO, and MoO <sub>2</sub>	15, 19, and 112
photoelectrochemical	metals Pt, Ni, Co, Fe, Cu, and Zn metal oxides TiO <sub>2</sub> , ZnO, BiVO <sub>4</sub> , WO <sub>3</sub> , Fe <sub>2</sub> O <sub>3</sub> , and Cu <sub>2</sub> O	48, 71, and 75
photocatalysis	metals Au, Ag, Pt, Pd, Tb, Sm, Rh, Mn, Cu, Co, Fe, Ni, Cr, and Mo metal oxides TiO <sub>2</sub> , ZnO, CuO, NiO, WO <sub>3</sub> , Co <sub>3</sub> O <sub>4</sub> , and Fe <sub>2</sub> O <sub>3</sub>	49, 77, and 113
water biophotolysis	metals Ni, Fe, and Se metal oxides TiO <sub>2</sub>	16 and 91

equal to 7.0. These catalysts achieved remarkable turnover frequencies for hydrogen production, more than  $2\text{ s}^{-1}$ , thus establishing themselves as one of the efficient catalysts for ammonia decomposition at 400 °C.

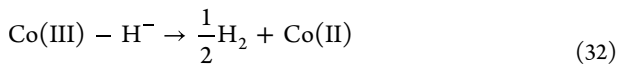
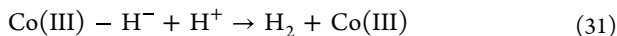
Metals/alloys also play a critical role in hydrogen production from organic compounds. Zhang et al.<sup>98</sup> investigated the steam-reforming reactions of glycerol and ethanol for hydrogen production using ceria-supported catalysts containing Ir, Co, and Ni. This study evaluates the influence of different active metals and their impact on the reaction pathways. Notably, the Ir/CeO<sub>2</sub> catalyst exhibited highly favorable catalytic performance, demonstrating its promise as an efficient catalyst for these processes. In another study,<sup>99</sup> the reforming of methanol was performed for hydrogen production by utilizing a novel Ni/ $\alpha$ -MoC catalyst. Under optimized conditions, the turnover frequency of this catalyst reached an impressive value of 1800 h<sup>-1</sup> at 240 °C. This improved activity was observed as a result of a greater number of isolated Ni atoms, effectively stabilized by carbon bridges within the  $\alpha$ -MoC host. In a review performed by Bepari et al.,<sup>7</sup> Ni-based catalysts supported by various materials were summarized for their role in hydrogen production through the steam reforming of organic molecules, such as ethanol, methanol, and glycerol. The choice of active metal, the catalyst support, and operating conditions influenced the hydrogen yield obtained in these processes. Thus, the nature of these supports is crucial because they impact catalyst stability as well as its selectivity toward hydrogen as a result of their inherent basic properties and redox characteristics.

Hydrogen generation via formic acid decomposition was studied by Yang et al.<sup>100</sup> Pd-based alloy catalysts, such as PdAu and PdAg alloy (Pd<sub>2</sub>L@Pd<sub>1</sub>Ag<sub>1</sub> and Pd<sub>2</sub>L@Pd<sub>1</sub>Au<sub>1</sub>), with specific atomic arrangements were used for hydrogen generation. In another study, Qin et al. produced H<sub>2</sub> at room temperature from formic acid using Pd@Bi/C catalysts.<sup>101</sup>

Apart from these studies, the potential roles of alkali and alkaline earth metals in catalysis were explored by incorporat-

ing typical elements, like Mg, Ca, and K, into Ni/La<sub>0.7</sub>Sr<sub>0.3</sub>AlO<sub>3-x</sub> catalysts for hydrogen production through steam reforming of toluene (serving as a model for biomass tar). The findings revealed that the introduction of Mg, Ca, and K into the Ni/perovskite catalysts significantly enhanced their catalytic performance. Notably, these modifications improved the resistance of catalysts to sintering and carbon deposition, contributing to their effectiveness in the process.<sup>102</sup> The study conducted by Tarifa et al.<sup>103</sup> assessed the performance of Fe-based catalysts adorned with Ni for hydrogen production from biomass gasification streams rich in CO<sub>2</sub>, H<sub>2</sub>, and CH<sub>4</sub>. Alterations in the Ni content had discernible impacts on the structure of catalysts, redox properties, and catalytic behavior. While Ni-rich systems exhibited anticipated optimal performance, particularly at elevated temperatures, like 700 °C, they also exhibited significant carbon deposition issues that posed challenges to the long-term stability of the catalysts. In a separate study, Meng et al.<sup>104</sup> summarize the transition-metal-based catalysts for catalytic biomass gasification conducted in recent decades. A comprehensive review encompasses a wide range of transition metal catalysts, such as mono- and bimetallic Ni-based catalysts, as well as catalysts based on Fe, Co, and Pt. In summary, the majority of monometallic Ni-based catalysts demonstrated superior performance in terms of syngas or hydrogen yield, whereas recent studies have not primarily focused on the influence of loaded Ni on tar reduction.

The role of metals/alloys is also explored for the various photo-assisted methods. Many cobalt complexes reported in the literature catalyze hydrogen evolution via electrocatalytic and photocatalytic hydrogen formation processes. Among different cobalt complexes, Losse et al.<sup>105</sup> utilized tetradeятate polypyridine cobalt complexes and cobalt porphyrins as electrocatalysts. The hydrogen production rate was increased with decreased pH. Two hydrogen generation pathways, such as a proton attack on a cobalt(III) hydride species (eq 31) and a disproportionation reaction of the cobalt hydride (eq 32), have been considered.



In another study, Wang et al.<sup>106</sup> have developed a cobalt complex of bis(methyl thioether)pyridine ( $[(\text{b}_{\text{tep}})\text{CoBr}_2]$ ) that was utilized for hydrogen generation via electro- and photocatalytic reduction of water. The catalyst  $[(\text{b}_{\text{tep}})\text{CoBr}_2]$  generated 591.9 mol of  $\text{H}_2$  mol<sup>-1</sup> of catalyst h<sup>-1</sup> from water, with an overpotential of 837.6 mV. The highest achieved apparent quantum yield (AQY) was approximately 25.5%. Anion modification techniques improve the catalytic activity of electrocatalysts by regulating the physicochemical characteristics.<sup>107</sup> Hydrogen can be produced via the electrolysis of urea using nickel as a catalyst. For this purpose, multimetal catalysts were developed by researchers<sup>108</sup> to improve the catalytic activity of nickel. The poor current densities and the stability of the anode affect the hydrogen production rate during the electrolysis of urea. The synergistic effect of rhodium and nickel reduces the surface blockage, thereby enhancing catalyst stability. During the electro-oxidation of urea, Rh–Ni electrodes reduced the overpotential, and the current density was enhanced by 200 times in comparison to a Ni catalyst. In hydrogen evolution and oxygen evolution reactions, cost-effective catalysts are essential. Non-precious metal catalysts, particularly iron–nickel (Fe and Ni) based catalysts, hold great promise as a result of their synergistic interaction, enhancing these reactions. Several Fe- and Ni-based catalyst categories, including alloys, oxides, fluorides, phosphides, sulfides, layered double hydroxides, tellurides, and selenides, were discussed. Durability and stability are of paramount importance, especially in the face of challenging electrolytic conditions. This emphasizes the need for long-term catalyst stability in practical applications. Hybrid catalysts, combining Fe and Ni, outperform others, benefiting from a synergistic effect. Although it is unclear whether Ni or Fe sites dominate the water-splitting reaction, the hybrid FeNi catalyst significantly enhances catalytic performance by modifying electronic structures, reducing kinetic barriers, and promoting active phase formation for the OER. A range of rhenium, iridium, and ruthenium complexes have been employed as potential photosensitizers for photocatalytic proton reduction.<sup>4</sup> The recent advancements in PEC water-splitting systems have centered on employing cost-effective, abundant, and dependable co-catalysts. To facilitate the hydrogen evolution reaction (HER), various metal complexes, including Mo, Ni, Co, and Fe, have been integrated into the photocathode. While platinum (Pt) is considered the gold standard for HER catalysts, its widespread application is hindered by its high cost and limited availability. Transition metal oxides/hydroxides, specifically those based on iron (Fe), nickel (Ni), and cobalt (Co), have emerged as prevalent and robust co-catalysts. These materials are renowned for their capacity to enhance activity, optimize OER kinetics, and ensure stability, making them competitive with esteemed noble metal co-catalysts, such as  $\text{IrO}_x$  and  $\text{RuO}_x$ , largely as a result of their superior electronic conductivity in metallic form.<sup>75</sup>

For the photocatalysis process, various metals, such as transition metals (Ni, Co, Cu, Fe, etc.), noble metals (Au, Ag, Pt, etc.), and rare earth metals (Tb, Sm, Ce, etc.) have been reported in the literature. These metals are incorporated with various catalysts to improve the photocatalytic activity. In a

study, a terbium (Tb) and samarium (Sm) co-doped ZnO/CNTs composite, with carbon nanotubes (CNTs) acting as a support material, was synthesized using the sol–gel method. The authors noted that the  $\text{H}_2$  evolution of the Tb and Sm co-doped ZnO/CNTs was significantly increased, reaching 47 times higher levels than pure ZnO. A plausible mechanism for the photocatalytic  $\text{H}_2$  evolution over the TS-ZnO/CNTs composite is depicted in Figure 6.<sup>109</sup>

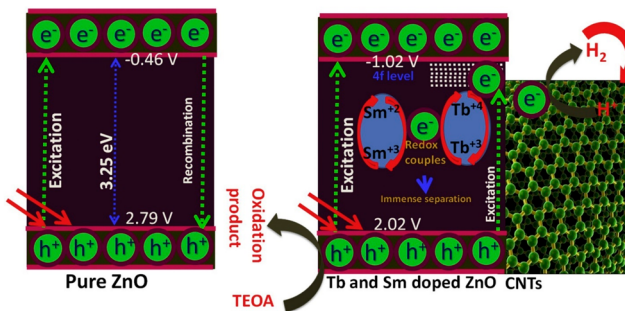


**Figure 6.** Photocatalytic  $\text{H}_2$  evolution mechanism over the TS-ZnO/CNTs photocatalyst. This figure was reproduced with permission from ref 109. Copyright 2022 Elsevier.

**4.2. Oxide/Mixed Oxide Catalysts.** Oxide and mixed oxide catalysts are essential components in various hydrogen production processes, playing a significant role in facilitating chemical reactions that generate hydrogen gas. Oxides used in various catalytic processes for hydrogen production are summarized in Table 1. Among the various oxide catalysts, ceria ( $\text{CeO}_2$ ), alumina ( $\text{Al}_2\text{O}_3$ ), and zirconia ( $\text{ZrO}_2$ ), were extensively explored for hydrogen production through steam reforming of different feedstocks. This may happen as a result of their exceptional attributes, including high-temperature stability, oxygen mobility, substantial surface area, and resistance to carbon deposition.

In the realm of hydrogen production via methane decomposition, a series of catalysts consisting of Ni and Ni-supported materials were synthesized using the sol–gel method. Notably, among these catalysts, Ni– $\text{TiO}_2$  emerged as the frontrunner in terms of catalytic performance. Operating at 575 °C, it achieved a methane conversion rate of 45% and exhibited impressive longevity, with a lifespan of 840 min. Additionally, the catalyst yielded 256 g of carbon/g of Ni, showcasing its promising potential for efficient hydrogen production.<sup>114</sup> Ammonia decomposition stands as an effective means for high-purity hydrogen production, yet enhancing catalytic activity at lower temperatures remains a significant challenge in this process. In this study, a composite of  $\text{CeO}_2$ – $\text{ZrO}_2$  was successfully synthesized using the co-precipitation method. This composite material served as the nickel metal carrier for ammonia decomposition. Notably, the Ni/Al– $\text{Ce}_{0.8}\text{Zr}_{0.2}\text{O}_2$  catalyst achieved complete ammonia decomposition at 580 °C, surpassing the performance of the reference Ni/ $\text{Al}_2\text{O}_3$  catalyst, which achieved only 92% ammonia decomposition at 600 °C.<sup>115</sup>

Steam reforming of methanol was performed by Shanmugam et al.<sup>116</sup> for hydrogen production by utilizing various metal oxide supports ( $\text{ZrO}_2$ ,  $\text{Al}_2\text{O}_3$ , and  $\text{CeO}_2$ ) and  $\text{In}_2\text{O}_3$  co-supported Pt. As anticipated, methanol conversion displayed an upward trend with an increasing temperature, ranging from 300 to 375 °C, across all catalysts, underscoring the profound

**Table 2. Non-oxide Catalysts for Various Catalytic Hydrogen Production**

non-oxide catalyst type	non-oxide catalyst	process	reference
carbides	ZrO <sub>2</sub> -supported Co–Mo carbide	reforming of methane	37
	Ru/SiC	ammonia decomposition	53
	M/Mo <sub>2</sub> C (M = Pt, Fe, Co, and Ni)	methanol reforming	39
	Re <sub>2</sub> C	biomass pyrolysis	22
	WC, W <sub>2</sub> C, and Mo <sub>2</sub> C	electrolysis	72
	g-CN–SiC	photoelectrochemical	129
	SiC NFs–C <sub>x</sub>	photocatalysis	41
nitrides	Mn <sub>6</sub> N <sub>5</sub> –CaNH	ammonia decomposition	145
	(Ni, Cu)/BN	methanol reforming	130
	Co <sub>4</sub> N	electrolysis	74
	InGaN	photoelectrochemical	131
sulfides	Mg/Ta <sub>3</sub> N <sub>5</sub>	photocatalysis	23
	MoS <sub>2</sub>	methane pyrolysis	132
	p-Ni <sub>x</sub> Co <sub>9-x</sub> S <sub>8</sub>	electrolysis	24
phosphides	Co <sub>9</sub> S <sub>8</sub> /ZnIn <sub>2</sub> S <sub>4</sub>	photocatalysis	146
	Ni <sub>2</sub> P and Ni <sub>3</sub> P <sub>4</sub>	dry reforming of methane	25
	N-VGSs@CB/CoP	electrolysis	133
	CoP	photoelectrochemical	76
borides	WP/CdS	photocatalysis	147
	Re <sub>3</sub> B and ReB <sub>2</sub>	biomass pyrolysis	26
	MoB	electrolysis	134
	M–B (M = Ni and Co)	photoelectrochemical	148
	C <sub>3</sub> N <sub>4</sub> /NiB <sub>7.5</sub>	photocatalysis	149

impact of the temperature on catalyst activity. Furthermore, the choice of metal oxide support was found to exert an additional influence on methanol conversion. Notably, among the catalysts investigated, 15 wt % Pt-supported CeO<sub>2</sub> catalysts demonstrated high selectivity for hydrogen with complete methanol conversion at 350 °C. A series of composite materials comprising TiO<sub>2</sub> coupled with metal oxide nanoparticles were synthesized via the sol–gel method, maintaining a consistent molar ratio while varying the compositions. This approach resulted in improved hydrogen generation during glycerol photoreforming compared to standalone TiO<sub>2</sub>. Notably, among the samples, Ag<sub>2</sub>O–TiO<sub>2</sub> demonstrated the most favorable hydrogen production performance, boasting the highest quantum efficiency and light-to-hydrogen energy conversion efficiency, measured at 3.02 and 1.15%, respectively.<sup>117</sup> Researchers<sup>118</sup> have developed palladium-based catalysts that are suitable for hydrogen generation from formic acid at near-ambient pressure and temperature. TiO<sub>2</sub>-supported [PdO/Pd<sup>0</sup>] catalysts were synthesized with various compositions via the sequential-deposition flame spray pyrolysis (SD-FSP) technique. The developed [PdO/Pd<sup>0</sup>/TiO<sub>2</sub>] nanocatalysts with a high [PdO/Pd<sup>0</sup>] ratio (>70%) can produce H<sub>2</sub> at a rate of 534 mmol g<sup>-1</sup> of Pd min<sup>-1</sup>.

A diverse array of metal oxide support materials, including but not limited to Al<sub>2</sub>O<sub>3</sub>, ZrO<sub>2</sub>, CeO<sub>2</sub>, Y<sub>2</sub>O<sub>3</sub>, La<sub>2</sub>O<sub>3</sub>, ZnO, TiO<sub>2</sub>, and MgO, have been increasingly employed in the synthesis of supported transition-metal-based catalysts for the biomass conversion.<sup>20</sup> Supercritical water gasification (SCWG) stands as a promising technology for harnessing wet biomass resources. This study involved the synthesis of Ni and various metal catalysts through wet impregnation techniques, subsequently assessing their catalytic activity in the SCWG process using wheat stalk as the feedstock. The findings indicated a variation in the activity of Ni catalysts supported by different materials, with the order of activity being Ni/MgO > Ni/ZnO > Ni/Al<sub>2</sub>O<sub>3</sub> > Ni/ZrO<sub>2</sub>.<sup>119</sup>

A range of metal-oxide-based catalysts have been reported for the electrocatalysis process. Among those, IrO<sub>2</sub> and RuO<sub>2</sub> are considered superior catalysts for the OER.<sup>47</sup> A few other oxides, like Co<sub>3</sub>O<sub>4</sub>,<sup>120</sup> have been employed for HER. In a recent study conducted by Wang et al.,<sup>121</sup> an IrO<sub>2</sub>-based catalyst was synthesized through boron doping in TiO<sub>2</sub> and then crafted an IrO<sub>2</sub>/TiB<sub>x</sub>O<sub>2</sub> composite using the Adams melting method. This composite catalyst demonstrated a commendable overpotential of 273 mV at a current density of 10 mA cm<sup>-2</sup>, coupled with an impressively low charge transfer resistance of a mere 15 Ω. Notably, the composite catalyst exhibited superior stability compared to pure IrO<sub>2</sub>. In the case of the photoelectrochemical process, most of the researchers focused on the advancement of metal oxide catalysts, like TiO<sub>2</sub>,<sup>122</sup> ZnO,<sup>123</sup> and BiVO<sub>4</sub>,<sup>124</sup> as a result of a suitable band gap. In a study, Tayebi et al.<sup>125</sup> opted BiVO<sub>4</sub> catalysts as the photoelectrode material. BiVO<sub>4</sub> possesses a favorable band gap of 2.37 eV and is an economically viable n-type photocatalyst. BiVO<sub>4</sub>, when employed as a photoanode, exhibits the capability to theoretically harness nearly 10% of solar energy, owing to its appropriate valence band (VB) position, thereby enabling efficient water oxidation with a maximum identified photocurrent of 7.5 mA cm<sup>-2</sup>.

Nanosized semiconductor photocatalysts possess a huge potential for hydrogen generation in a sustainable and environmentally friendly manner via photocatalytic water splitting. For the photocatalysis process, various oxides, like TiO<sub>2</sub>, ZnO, CuO, Co<sub>3</sub>O<sub>4</sub>, etc., have been extensively explored by several researchers. Among these oxides, TiO<sub>2</sub> is a promising photocatalyst for this process. Singh and Dutta<sup>42</sup> described the application of TiO<sub>2</sub>/TiO<sub>2</sub>-assisted catalysts in detail. The efficient utilization of nanosized TiO<sub>2</sub> can generate low-cost and eco-friendly fuel as a photocatalyst via photocatalytic water splitting. TiO<sub>2</sub> possesses enhanced optical and structural properties. It is a chemically stable, non-toxic, and corrosion-resistant photocatalyst. Also, ZnO is a potential

photocatalyst with a wide band gap n-type semiconductor belonging to the II-VI group.<sup>126</sup> It is considered an efficient photocatalyst with high electron mobility, good transparency, and strong luminescence properties at room temperature. In addition to that, it exhibits photocatalytic antibacterial activity in visible light.<sup>127</sup> The morphology of ZnO can be controlled by varying the synthesis technique, process operating conditions, concentration of reactor or precursor, and pH of the system. Zinc oxide is generally categorized as a non-toxic material. However, it causes zinc fever or zinc ague by inhalation or ingestion. Therefore, proper safety precautions must be taken while preparing, packaging, transporting, and handling ZnO.<sup>128</sup>

**4.3. Non-oxide Catalysts.** Non-oxide-based catalysts are gaining prominence in hydrogen production as a result of their distinct advantages. Various non-oxide catalysts based on carbides,<sup>53,129</sup> nitrides,<sup>130,131</sup> sulfides,<sup>132</sup> phosphides,<sup>133</sup> and borides<sup>26,134</sup> have demonstrated promising activity toward catalytic hydrogen production (see Table 2). These materials are based on non-precious elements and are, thus, suitable for the development of cost-effective catalysts.<sup>134</sup> However, these catalysts suffer from thermal instability, rendering them unsuitable for high-temperature processes.<sup>132</sup>

In a study, a series of ruthenium (Ru) catalysts supported on  $\beta$ -SiC were meticulously prepared, featuring varying Ru loadings ranging from 1 to 5% by weight. The optimal intrinsic activity was achieved when the Ru particle size was approximately 5 nm. Remarkably, the catalyst composed of 2.5% Ru, subjected to calcination in a nitrogen ( $N_2$ ) atmosphere and reduction at 673 K, exhibited outstanding performance in hydrogen production via ammonia decomposition. This catalyst achieved nearly complete ammonia conversion at an operating temperature of 623 K, signifying its exceptional catalytic ability. Furthermore, the study highlighted the suitability of porous SiC as a support material for the nanoscale Ru catalyst, showcasing high activity in the context of hydrogen generation through ammonia decomposition.<sup>53</sup>

A variety of transition metals (Ni, Co, Pt, and Fe) were chosen as catalyst supports on molybdenum carbides to enhance the hydrogen production rate from steam reforming of methanol. In comparison to undoped molybdenum carbide, the metal-doped counterparts exhibited superior methanol conversion rates and higher hydrogen yields. Ma et al.<sup>39</sup> reported that Pt-doped molybdenum carbide shows better selectivity as well as stability and achieved complete methanol conversion, even at a low temperature of 200 °C. In a separate study, Re<sub>3</sub>B and ReB<sub>2</sub> catalysts were evaluated in the context of hydrogen (H<sub>2</sub>) production through coconut shell pyrolysis conducted at temperatures ranging from 500 to 800 °C, employing catalyst loadings of 5, 10, and 20 wt %. Remarkably, Re<sub>3</sub>B demonstrated superior catalytic activity, particularly at 800 °C with a 10 wt % catalyst loading. This heightened catalytic performance of Re<sub>3</sub>B can be attributed to factors such as its low surface area, the reactivity of its Re and B catalytic centers, and the high-temperature pyrolysis conditions. Consequently, Re<sub>3</sub>B emerges as a promising catalyst candidate for facilitating H<sub>2</sub> production from biomass with similar compositional proportions of lignin, hemicellulose, and cellulose.<sup>26</sup>

Hydrogen can be produced effectively via electrolytic water splitting by utilizing non-oxide-based catalysts. Currently, catalysts used for electrolytic water splitting are costly and less stable. Utilization of transition metal phosphates can solve

these problems. Cost-effective methods for the synthesis of metal phosphate are the (i) solid state method, (ii) thermolytic molecular precursor (TMP) method, (iii) hydrothermal method, (iv) precipitation method, (v) solution combustion method, (vi) microwave-assisted method, (vii) electrodeposition, and (viii) photodeposition.<sup>135</sup> Cobalt phosphate-based materials have good stability and satisfactory performance during electrolytic water splitting. The unique lattice structure of the phosphate group is beneficial for the adsorption and dissociation of water on the electrode surface. The high overpotential of the electrode leads to increased energy consumption; therefore, a catalyst with low overpotential is preferable for large-scale water electrolysis applications. Thus, efforts to develop efficient, non-noble metal electrocatalysts are crucial for achieving commercial viability. Transition metal phosphates offer numerous advantages, including their natural abundance and cost-effectiveness. Sankar et al.<sup>136</sup> have successfully synthesized porous cobalt phosphate nanoparticles (NPs) through a straightforward wet chemical method. This catalyst exhibits a minimal overpotential of 299 mV at a current density of 10 mA cm<sup>-2</sup> and maintains excellent stability for up to 12 h. For large-scale hydrogen production, the seawater electrocatalytic process should be used to minimize the cost of production. Transition metal phosphide-based catalysts (e.g., phosphorus-doped transition metals and binary metal phosphides) can be utilized for seawater electrolysis.<sup>137</sup> Seawater electrolysis presents significant challenges, primarily stemming from the anodic OER, which has a higher energy barrier compared to freshwater electrolysis. Additionally, there is the issue of the competitive and side chloride evolution reaction (CER), which negatively impacts the activity and stability of catalysts.<sup>138</sup> There are various drawbacks of seawater electrocatalysis, such as the presence of CER and poisoning of electrocatalysts as a result of the presence of calcium and magnesium ions. Therefore, most of the current studies are limited to the laboratory scale. Furthermore, the utilization of renewable energy resources is essential to reduce carbon emissions. Coastal regions are suitable for the production of H<sub>2</sub> via electrolytic processes as a result of the ample access to seawater and intense solar irradiation or strong wind patterns.<sup>139</sup> Apart from the electrolysis process, several researchers explored the non-oxide-based catalysts for the photoelectrochemical process. In a study, Chen et al.<sup>140</sup> constructed efficient Ta<sub>3</sub>N<sub>5</sub> photoanodes by incorporating a continuous CoPi layer and non-continuous Co(OH)<sub>2</sub>. This approach aimed to enhance charge separation, improve catalytic activity, and enhance resistance to self-oxidation properties of Ta<sub>3</sub>N<sub>5</sub> in the context of photoelectrochemical water splitting. Several researchers<sup>131</sup> reported indium gallium nitride (InGaN)-based catalysts for the photoelectrochemical water splitting as a result of suitable alignment of CB and VB with a wide tunable band gap in the range of 0.67–3.4 eV, high mobility of charge carriers, and straddling the redox potentials of the water. Furthermore, researchers have tried to improve the catalytic activity of the photocatalysts by adopting these non-oxide-based catalysts. Researchers<sup>141</sup> discuss recent advancements in visible-light-driven photocatalysts, with a particular emphasis on enhancing non-oxide photocatalysts, including (oxy)nitrides and oxysulfides. Metal heteroanionic compounds, like oxynitrides (TaON and Ga<sub>1-x</sub>Zn<sub>x</sub>N<sub>1-x</sub>O<sub>x</sub>), oxysulfides (Ln<sub>2</sub>Ti<sub>2</sub>S<sub>2</sub>O<sub>5</sub> and Sm<sub>2</sub>Ti<sub>2</sub>S<sub>2</sub>O<sub>5</sub>), and oxyhalides, have lower band gaps compared to conventional oxides and can be utilized as efficient photocatalysts for water splitting.

**Table 3.** Carbon-Based Catalysts for Various Catalytic Hydrogen Production

carbon material	carbon-based catalyst	process	reference
CNT	Ni/CNT and Ni–Cu/CNT	methane decomposition	27
	Ni/CNTs–SF	steam reforming of ethanol	38
	Ru/CNT	steam reforming of glycerol	40
	Ni/CNT	reforming of biomass (bio-oil)	155
	Ni/CNT	electrolysis	156
	Ag/TiO <sub>2</sub> /CNT	photoelectrochemical	28
	MgO-promoted Ni–Si/CNTs	photocatalysis	157
	Ni–W/G	gasification of biomass	29
	Ni/G	electrolysis	30
	BVO/rGO	photoelectrochemical	158
graphene	ZnO–MoS <sub>2</sub> –rGO	photocatalysis	159
	TMs–MCN (TMs = Co, Mn, Fe, Ni, and Cu)	ammonia decomposition	150
	CD/C <sub>3</sub> N <sub>4</sub>	methanol reforming	55
	MGCN	electrolysis	160
	g-C <sub>3</sub> N <sub>4</sub> /WO <sub>3</sub> /WS <sub>2</sub>	photocatalysis	79
	g-C <sub>3</sub> N <sub>4</sub> /ZnO@BiVO <sub>4</sub>	photoelectrochemical	161
	Ru–AC	methane decomposition	162
	Ni–Fe/C	pyrolysis–gasification of biomass and plastic wastes	163
	Ru/3DNPC	electrolysis	164
	C/TiO <sub>2</sub>	photoelectrochemical	165
carbon	carbon quantum dots	photocatalysis	32

This happened as a result of the lower electronegativity of nitrogen and sulfur than oxygen.<sup>142</sup> These materials have some drawbacks, such as unsuitable energy band alignments, surface defects, and photocorrosion, that limit their real-life application. Bismuth-based photocatalysts, like BiOX (X = Cl, Br, and I) and BiVO<sub>4</sub>, can be utilized efficiently for the sluggish water oxidation process as well as for water splitting via Z-schemes.<sup>143</sup> Researchers<sup>144</sup> have developed metal oxychloride intergrowths based on Bi<sub>4</sub>TaO<sub>8</sub>Cl–Bi<sub>2</sub>GdO<sub>4</sub>Cl. These intergrowths were utilized with Ru/SrTiO<sub>3</sub>/Rh as a hydrogen evolution catalyst. The photocatalytic water-splitting activity was optimized by varying the Ta/Gd molar ratio in the intergrowths. This catalyst shows a 4% activity loss after 24 h of operation with visible light illumination.

**4.4. Carbon/Graphene-Based Catalysts.** Carbon-based materials, such as carbon nanotubes (CNTs),<sup>27,28,40</sup> graphene,<sup>29,30</sup> graphitic carbon nitride (g-C<sub>3</sub>N<sub>4</sub>),<sup>79,150</sup> and carbon quantum dots,<sup>32</sup> are extensively used for catalytic hydrogen production (see Table 3). Through precise structural engineering and surface modifications, carbon materials with higher surface areas and significant pore volumes have found widespread applications in various catalytic processes. These modifications enhance the dispersion and stability of nanoparticles (NPs), consequently boosting catalytic performance.<sup>151</sup> Notably, several carbon materials, including carbon black and carbon nanotubes characterized by surface defect sites, have garnered recent attention as effective heterogeneous catalysts for hydrocarbon decomposition. This unique property allows for the generation of pure hydrogen without significant concurrent production of CO<sub>2</sub>.<sup>152</sup> In a study, Nishii et al.<sup>50</sup> performed methane decomposition experiments employing various carbon structures, including mesoporous carbon (MC), carbon black (CB), activated carbon (AC), and carbon nanofiber (CNF). The findings of this study revealed that the carbon generated during methane decomposition not only diminishes catalyst activity by coating the catalyst but also exhibits catalytic properties independently, regardless of the initial carbon catalyst type. Surprisingly, all catalysts sustained a

consistent methane conversion rate of approximately 17% as they continued to catalyze the carbon produced, even after their activity had declined. In another study, a novel composite material consisting of CNTs and silica fibers (SFs) was successfully synthesized through the steam reforming of ethanol using a Ni/silica fiber catalyst prepared via electro-spinning. The study investigated the impact of the temperature within the range of 300–500 °C on ethanol conversion and product distribution. Among the catalysts tested, NiCNTs–SF exhibited the most favorable performance, characterized by exceptional stability and high activity, especially at lower reaction temperatures. This remarkable catalytic performance of NiCNTs–SF can be attributed to its excellent dispersion of metallic components and easy accessibility for reactants.<sup>38</sup> In another study, Gallegos-Suárez et al.<sup>40</sup> developed ruthenium catalysts supported on carbon materials for hydrogen production through glycerol steam reforming. The investigation encompassed a range of carbon-based materials, including activated carbon, Pyrograph III carbon nanofibers, and carbon nanotubes. The study delved into the intricate effects of these diverse carbon substrates on the steam reforming process. Furthermore, carbon-based catalysts were also utilized for the biomass conversion. In this case, authors applied an ultrasound-assisted wet impregnation technique to deposit Ni and W metal particles onto the graphene support, both with and without the inclusion of Pt particles. A comprehensive chemical and thermal reduction process of biomass-derived compounds followed this deposition. Saquic et al.<sup>29</sup> suggest that, when metals deposited on the graphene support with their unique properties, these metals hold great potential as catalysts. Several other researchers also explored the carbon-based catalysts for the photo-assisted process. In a study, authors synthesized a catalyst with an ultrafine vanadium nitride (VN) nanoparticle (2–4 nm) dispersedly confined in Co-encapsulated N-doped carbon nanotubes (VN/Co@NCNTs).<sup>153</sup> The catalyst developed with non-precious metals having a long catalytic durability (60 h). This catalyst also has a quite low overpotential (180 mV at 10 mA cm<sup>-2</sup>). Therefore,

this catalyst is suitable for large-scale green hydrogen production via the HER. In a separate study by Han et al.<sup>154</sup> in 2021, they explored the use of Ni/NiO nanocomposite supported on N-doped carbon nanoweb (Ni/NiO/NCW) hybrid materials as efficient electrocatalysts for the HER in alkaline conditions. The developed catalysts exhibited outstanding electrocatalytic properties, including a lower overpotential of 105.3 mV [versus reversible hydrogen electrode (RHE)] at 10 mA cm<sup>-2</sup>, a reduced Tafel slope of 55.2 mV dec<sup>-1</sup>, and nearly 100% faradaic efficiency, and demonstrated good stability. This improved electrocatalytic performance in the HER was attributed to the synergistic effects arising from the three-dimensional (3D) N-doped carbon nanoweb morphology and the Ni/NiO heterostructure, with an optimal Ni/NiO ratio. In a study conducted by Chaudhary et al.,<sup>28</sup> the photoelectrochemical process was employed for water splitting under visible light exposure. Researchers created a photoanode using CNTs and enhanced it by grafting silver (Ag) nanoparticles onto the surface of a TiO<sub>2</sub>/CNT nanocomposite. The improved photocurrent density observed in the Ag/TiO<sub>2</sub>/CNT photoanode results from enhanced visible light absorption and a reduction in band bending. The combination of Ag nanoparticles and CNTs promotes efficient interfacial electron transfer, leading to the observed synergy in performance. For the photocatalysis process, a S-type heterojunction photocatalyst was synthesized with Co<sub>3</sub>S<sub>4</sub> nanoparticles supported on g-C<sub>3</sub>N<sub>4</sub>/ $\alpha$ -Fe<sub>2</sub>O<sub>3</sub>.<sup>1</sup> The photocatalyst (g-C<sub>3</sub>N<sub>4</sub>/ $\alpha$ -Fe<sub>2</sub>O<sub>3</sub>/Co<sub>3</sub>S<sub>4</sub>) exhibited exceptional stability and outstanding photoelectrochemical activity, resulting in a significant amount of hydrogen evolution (191.41  $\mu$ mol). This amount was approximately 30 times higher than that achieved by pure Co<sub>3</sub>S<sub>4</sub> (6.38  $\mu$ mol). The efficiency was improved as a result of the synergistic/synergistic effect of various components of the composite material. The mechanism of the photocatalytic hydrogen generation is shown in Figure 7.

**4.5. MOF-Based Catalysts.** Metal–organic framework (MOF)-based catalysts have gained attention in recent years for their potential in hydrogen production from various sources, including methane, ethanol, and biomass. MOFs are porous materials composed of metal ions or clusters

coordinated with organic ligands.<sup>33,166</sup> The utilization of MOFs in the realm of catalysts is a prevalent practice, where they are employed either independently or as a supportive component.<sup>167</sup> Moreover, MOFs exhibit the capability to serve as templates for the synthesis of metal oxides, owing to their exceptional attributes, including notable porosity, precise structural characteristics, and a high surface area.<sup>168</sup> Metal oxide nanoparticles derived from MOFs display exceptional properties when compared to their conventionally synthesized counterparts.<sup>34</sup> What is particularly interesting is that the morphology and porosity inherent to the MOF precursor are typically retained in the resultant metal oxide nanoparticles.<sup>169</sup> Because of their adjustable porous structures, MOFs have been employed as platforms for regulating the dimensions of metal nanoparticles (NPs).<sup>170</sup> Thus, their high surface area, tunable structure, and diverse metal–organic combinations make MOFs promising candidates for catalytic applications.

In a study, authors synthesized NiCo@C nanocomposites derived from a NiCo-based bimetallic metal–organic framework. These nanocomposites exhibited exceptional catalytic performance in the dry reforming of methane (DRM) process. They achieved remarkable turnover frequencies (TOFs) even at relatively low temperatures, surpassing 5.7 s<sup>-1</sup> at 600 °C. Additionally, these catalysts exhibited excellent product selectivity, with a hydrogen/carbon monoxide (H<sub>2</sub>/CO) ratio of 0.9 at 700 °C. The introduction of cobalt (Co) into the nickel (Ni) catalysts significantly enhances both operational stability and light-off stability, further enhancing their catalytic efficiency and durability.<sup>171</sup> Ultrapure hydrogen can be produced from ammonia–borane (NH<sub>3</sub>·BH<sub>3</sub>, AB), hydrazine (NH<sub>2</sub>NH<sub>2</sub>), lithium borohydride [Li(BH<sub>4</sub>)], and sodium alanate [Na(AlH<sub>4</sub>)] via pyrolysis or hydrolysis. To assist both processes, a series of homogeneous and heterogeneous catalysts were synthesized by utilizing MOFs. Composite material (hydride@MOF) was synthesized via nanoconfinement of lightweight hydrides in MOFs. During pyrolysis, the catalyst lowers the hydrogen evolution temperature as a result of the presence of MOF and, thus, increases the hydrogen production rate. During hydrolysis, the reaction between the hydride and water was catalyzed by the NPs@MOF.<sup>172</sup> In a study conducted by Kamyar et al. in 2020, copper-based catalysts were investigated in the context of hydrogen production through methanol steam reforming. The catalysts were prepared over aluminum spinels derived from AS20 MOF. AS20 MOF was chosen as a template as a result of its advantageous characteristics, notably its production feasibility in water on an industrial scale, reaching as high as 3600 kg m<sup>-3</sup> day<sup>-1</sup>, even under mild conditions as low as 60 °C. The findings of the study underscore the potential benefits of using MOF templates for fabricating supports and their subsequent application in heterogeneous catalysts.<sup>173</sup> Furthermore, Cu- and In-doped ZnS (abbreviated as CIZS) was synthesized using a MOF precursor, specifically, a Cu- and In-doped zeolitic imidazolate framework known as ZIF-8. This prepared CIZS exhibits remarkable efficiency in hydrogen production during the photoreforming reaction of lignocellulosic biomass under simulated sunlight conditions. Notably, its catalytic activity surpasses that of undoped ZnS prepared using the same procedure by a substantial factor, achieving a 125-fold enhancement.<sup>174</sup> Several MOF-based catalysts for hydrogen production from the photo-assisted method are reported in the literature. For the electrolysis process, Co-MOF nanorods (NRs) were prepared at room temperature. After that, the

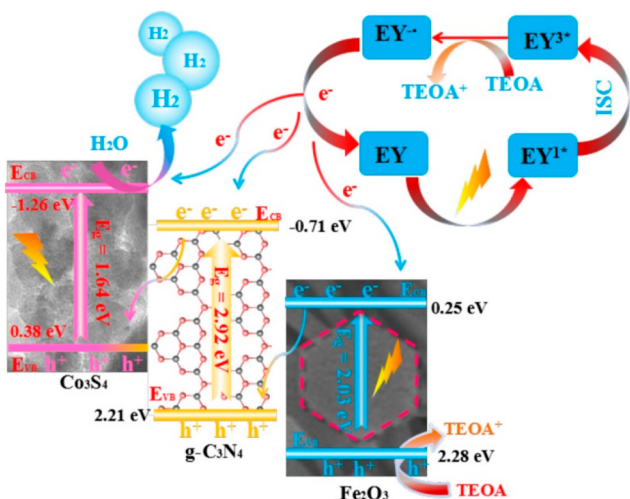


**Figure 7.** S-Scheme mechanism of the photocatalytic H<sub>2</sub> evolution of EY-sensitized CNFS-20 composites. This figure was reproduced with permission from ref 1. Copyright 2021 American Chemical Society.

MOF was transformed into CoS NRs on carbon cloth (CoS/CC) by the calcination and hydrothermal sulfurization process. The synergistic interplay between the structure and composition of the synthesized catalysts (CoS@CoNi-LDH/CC) leads to enhanced electrocatalytic performance for the HER. This catalyst exhibited long-term stability, with only a 17 mV increase in overpotential even after 50 h.<sup>175</sup> MOFs and MOF-derived materials can be used efficiently for hydrogen generation via electrochemical and photoelectrochemical water splitting. Their optical, electrical, and catalytic properties can be fine-tuned to enhance their performance. By modifying the organic ligands and/or metal centers, we can improve properties like surface area, band gap, current density, electrochemical active surface area, and overpotential.<sup>176</sup> Most of the MOF-based photocatalysts are ultraviolet (UV)-light-active. Therefore, the development of solar photoactive catalysts is essential.<sup>177</sup> MOF/MOF heterojunctions were constructed by Kampouri et al.<sup>178</sup> to enhance the photocatalytic activity of MOF-based systems. The MIL-167/MIL-125-NH<sub>2</sub> heterojunction was formed by combining MIL-167 and MIL-125-NH<sub>2</sub>, which provides improved optoelectronic properties, visible light absorption, and efficient charge separation. Figure 8 depicts the plausible mechanisms for hydrogen production from MOF-based photocatalysts.

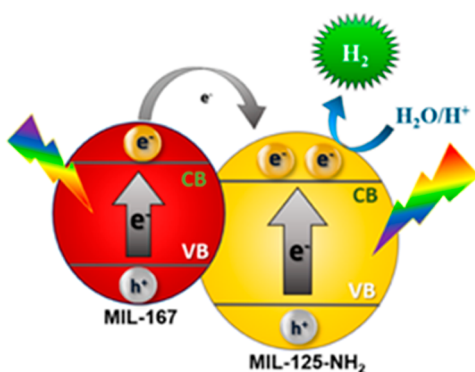


**Figure 8.** Schematic representation of a type II heterojunction with MIL-167 and MIL-125-NH<sub>2</sub>. This figure was reproduced with permission from ref 178. Copyright 2021 American Chemical Society.

Several other researchers also explored MOF-based catalysts, such as Morshed et al.<sup>179</sup> successfully synthesizing two distinct MOF structures, Yang et al.<sup>180</sup> reporting a composite of CdS nanorods (CdS-NRs) and hierarchical Ni-based MOF (NMOF-Ni), Horiuchi et al.<sup>181</sup> synthesizing a Ti-MOF-NH<sub>2</sub> catalyst, etc., for photocatalytic hydrogen production.

## 5. PURIFICATION OF HYDROGEN

Hydrogen production through various catalytic methods can indeed result in the generation of additional gases alongside hydrogen. For instance, when hydrogen is produced from methane through processes like steam methane reforming (SMR), catalytic cracking, partial oxidation of methane, etc., byproducts, such as carbon dioxide (CO<sub>2</sub>) and carbon monoxide (CO), are often formed.<sup>182,183</sup> In the context of ammonia decomposition, it is essential to separate the generated N<sub>2</sub> (nitrogen) and H<sub>2</sub> (hydrogen) gases to obtain purified hydrogen that meets the composition requirements established by the International Organization for Standardization (ISO) for use as a fuel.<sup>110</sup> Similarly, the reforming

of organic molecules (ethanol/methanol/glycerol) results in the production of various gases as byproducts.<sup>21</sup> In contemporary practices, hydrogen production from biomass typically yields a gas mixture known as syngas. Syngas consists of several gases, including hydrogen, carbon dioxide (CO<sub>2</sub>), carbon monoxide (CO), water vapor (steam), methane, and various other species. This diverse gas mixture arises from the complex chemical reactions involved in the gasification or pyrolysis of biomass feedstock. These reactions not only produce hydrogen, which is the desired product, but also result in the formation of these coexisting gases.<sup>184</sup> However, pure hydrogen can be generated through water-splitting processes, such as electrolysis and photoelectrochemical methods.<sup>185</sup> However, in the case of photocatalysis and biophotolysis, both hydrogen (H<sub>2</sub>) and oxygen (O<sub>2</sub>) are produced simultaneously.<sup>186</sup> Thus, the purification of hydrogen from these gases is required. Figure 9 illustrates various gas separation methods in which pressure swing adsorption (PSA) and membrane separation are widely employed for purifying hydrogen produced through various catalytic processes.

### 5.1. Pressure Swing Adsorption (PSA) Method.

Pressure swing adsorption is a cyclic adsorption process that relies on the selective adsorption of impurities on a solid adsorbent at a high pressure and their subsequent desorption at a low pressure.<sup>187</sup> Various materials, including silica gel, activated alumina, activated carbon, and zeolite, can be employed as solid adsorbents.<sup>188</sup> PSA technology can achieve a hydrogen purity level higher than 99.0%.<sup>189</sup> However, its hydrogen recovery rate typically ranges from 65 to 90%. PSA is most effective when applied to gas mixtures containing 60–90 mol % hydrogen.<sup>190</sup> A two-stage vacuum/pressure swing adsorption (VSA/PSA) process was explored for CO<sub>2</sub> capture, followed by H<sub>2</sub> production from a steam methane reforming (SMR) gas mixture. The findings revealed that the initial stage of the process yielded 95.31% pure CO<sub>2</sub> with a recovery rate of 90.93%, while the subsequent stage resulted in 99.9952% pure H<sub>2</sub> with an overall recovery efficiency of 71.16%.<sup>191</sup> A similar type of scheme was reported by Antonini et al.<sup>192</sup> for H<sub>2</sub> purification and CO<sub>2</sub> capture. A study conducted by Relvas et al.<sup>193</sup> involved the PSA to process a synthetic reformate mixture composed of 70% H<sub>2</sub>, 25% CO<sub>2</sub>, 4% CH<sub>4</sub>, and 1% CO to produce exceptionally pure hydrogen using an activated carbon-based catalyst. Following the optimization process, they successfully achieved hydrogen purity exceeding 99.97%, with a minimal CO content of 0.17 ppm, while maintaining a recovery rate of 76.2%.

**5.2. Metal Hydride Separation Method.** Metal hydrides, which are compounds formed by combining metals with hydrogen, selectively adsorb hydrogen molecules from the gas mixture, separating them from impurities. In the absence of any poisonous components, a metal hydride can serve as a hydrogen purification and storage material that selectively captures and stores hydrogen when supplied with a gas mixture.<sup>194</sup> Sometimes, we need to separate hydrogen from a dilute mixture with methane. For the purification of lean mixtures, metal hydride has an advantage over conventional PSA technology because metal hydrides selectively absorb hydrogen from the mixture. Hydrogen was successfully separated from the mixture of hydrogen (10%) and methane (90%) using the LaNi<sub>4.8</sub>Mn<sub>0.3</sub>Fe<sub>0.1</sub> intermetallic compound.<sup>195</sup> Purification methods employing metal hydrides for hydrogen have proven to be a versatile and cost-effective alternative to more expensive PSA systems, offering reduced initial capital

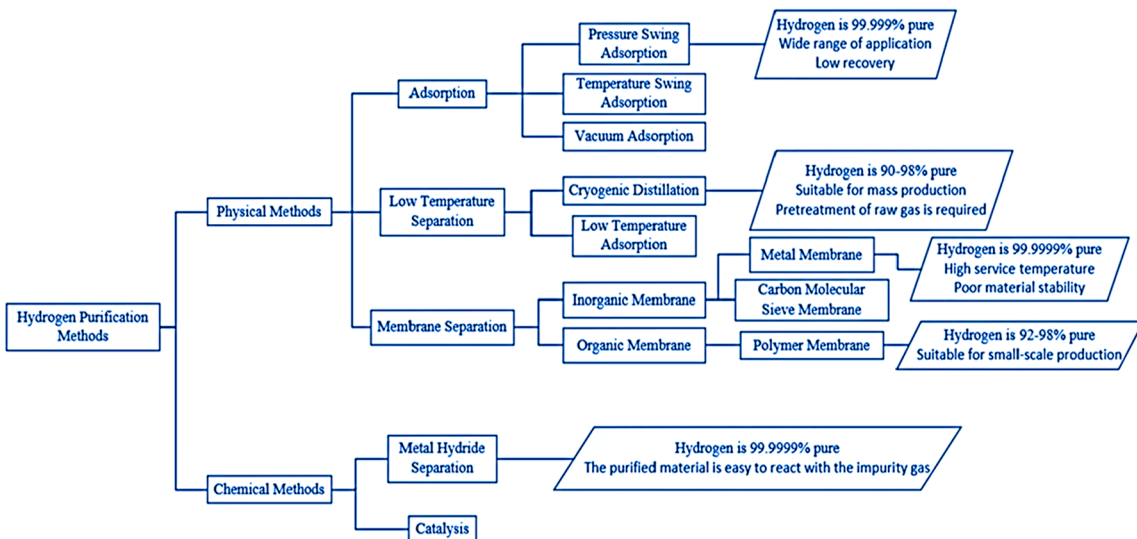


**Figure 9.** Classification of hydrogen purification technologies. This figure was reproduced with permission from ref 35. Copyright 2021 MDPI.

expenses and lower operational and maintenance demands.<sup>196</sup> Miura et al.<sup>197</sup> present a novel hydrogen purification and storage system comprising a CO-selective adsorbent and an ABS-type metal hydride. The laboratory-scale apparatus, operating at a flow rate of 100 NL h<sup>-1</sup>, was subjected to daily start and stop cycles over 100 operational cycles, totaling 150 h of continuous operation, demonstrating satisfactory efficiency throughout the testing period.

**5.3. Membrane Separation.** Membrane separation is a physical process used to purify hydrogen gas based on differences in molecular sizes and diffusion rates. Semi-permeable membranes are employed to selectively separate hydrogen from other gases. In this method, pressurized hydrogen gas is introduced on one side of the membrane, while impurities, such as carbon dioxide (CO<sub>2</sub>), methane (CH<sub>4</sub>), and nitrogen (N<sub>2</sub>), are present on the other side. This approach is characterized by its simplicity, cost-effectiveness, eco-friendliness, and low energy consumption.<sup>188</sup> Various membrane separation methods, such as polymeric, dense material, and micropores, are explored by the researchers.

**5.3.1. Polymeric Membrane.** Polymeric membranes are synthesized from a variety of polymers, including cellulose acetate (CA), polysulfone, polyimide, polyamide, and others, and they play a crucial role in gas separation processes.<sup>198,199</sup> These membranes offer a compelling choice for hydrogen separation, primarily because they offer benefits, such as cost-effectiveness, enhanced energy efficiency, user-friendliness, and reduced environmental footprint, when compared to conventional separation methods.<sup>199</sup> Polymeric-based membranes can be classified into two categories, namely, polymeric glass and rubbery membranes.<sup>200</sup> Luo et al.<sup>201</sup> developed a selective and permeable polymeric membrane by introducing a hierarchical triptycene unit into thermally rearranged polybenzoxazole (TR-PBO) structures. This membrane exhibits substantial potential for hydrogen purification and carbon dioxide extraction from natural gas, showcasing the highest gas selectivity levels for hydrogen separations [e.g.,  $\alpha(\text{H}_2/\text{N}_2) = 96$  and  $\alpha(\text{H}_2/\text{CH}_4) = 203$ ] and the removal of carbon dioxide from natural gas [e.g.,  $\alpha(\text{CO}_2/\text{CH}_4) = 68$ ] compared to existing glassy polymeric membranes. In another study, Li et al.<sup>202</sup> developed polymeric membranes using sulfonated

poly(ether sulfone) (SPES) with incorporated transition metals for applications in hydrogen recovery and natural gas separation. In comparison to conventional flat, dense PES membranes, the SPES membrane enriched with Zn<sup>2+</sup> demonstrated substantial enhancements in selectivity, with improvements of about 140, 86, 18, and 57% observed for gas pairs He/N<sub>2</sub>, H<sub>2</sub>/N<sub>2</sub>, O<sub>2</sub>/N<sub>2</sub>, and CO<sub>2</sub>/CH<sub>4</sub>, respectively. Shao et al.<sup>203</sup> conducted a comprehensive review of polymeric membranes employed in hydrogen purification. Their study encompassed an examination of various polymers utilized in synthesizing these membranes as well as an assessment of diverse strategies aimed at improving the inherent gas separation capabilities. These polymeric membranes designed for hydrogen enrichment exhibit selectivity toward either H<sub>2</sub> or CO<sub>2</sub>, a distinction contingent on the prevailing kinetic or thermodynamic determinants.

**5.3.2. Dense Material Membrane.** Elements belonging to groups III–V, such as platinum (Pt), nickel (Ni), palladium (Pd), and their respective alloys, are commonly employed in the fabrication of dense metal membranes.<sup>204,205</sup> One of the notable characteristics of these membranes is their exceptionally elevated hydrogen selectivity, making them a prevalent choice for generating highly purified hydrogen.<sup>184</sup> In contrast to other metals, palladium exhibits enhanced catalytic capability for breaking down molecular hydrogen and displays increased permeability to atomic hydrogen.<sup>206</sup> In a study, Roses et al.<sup>207</sup> conducted research on palladium-based membrane reactor technologies aimed at pure hydrogen production from natural gas. This membrane reactor facilitates simultaneous reactions and separation processes. It utilizes thin Pd alloy materials, typically ranging from 2 to 50 μm in thickness, as hydrogen perm-selective membranes for the extraction of pure hydrogen from the reactor. In another study, Lim et al.<sup>208</sup> synthesized composite membranes consisting of Pd–Cu and SiO<sub>2</sub>–Al<sub>2</sub>O<sub>3</sub> for the purification of hydrogen derived from ethanol steam reforming. These membrane composites exhibited a selectivity (H<sub>2</sub>/CO<sub>2</sub>) range spanning from 200 to 1000, along with a hydrogen permeance range from  $5.2 \times 10^{-8}$  to  $3.9 \times 10^{-6}$  mol m<sup>-2</sup> s<sup>-1</sup> Pa<sup>-1</sup> at 623 K. For more insight about dense material membranes, Habib et al.<sup>52</sup> performed a review on the fabrication of palladium alloy-based

membrane reactors for hydrogen production and purification. During hydrogen separation, pure Pd membranes face various problems, such as poisoning, embrittlement, and phase transition. Authors indicate that Pd alloy membranes exhibit improved durability and greater hydrogen selectivity when compared to Pd membranes. Various techniques are employed to produce these membranes, including electroless plating (ELP), chemical vapor deposition (CVD), physical vapor deposition (PVD), and electroplating deposition (EPD).<sup>199</sup>

**5.3.3. Micropore Membrane.** Membranes possessing pores measuring less than 2 nm in size fall under the category of microporous membranes. Microporous membranes can be categorized into two main groups according to their structures: amorphous and crystalline. Amorphous membranes consist of silica membranes, carbon membranes, and other metal oxide membranes, whereas crystalline membranes encompass zeolite membranes and MOF membranes.<sup>184</sup> A permeable hydrogen separation membrane was synthesized through a sol–gel technique employing bis(triethoxysilyl)ethane (BTESE) as the silica source. These hybrid silica membranes exhibited remarkable resistance to hydrothermal conditions, primarily attributed to the existence of Si–C–C–Si bonds within their silica structures.<sup>209</sup> In a study, Lei et al.<sup>210</sup> synthesized amorphous carbon molecular sieve (CMS) membranes to separate H<sub>2</sub> from CO<sub>2</sub> using cellulose hollow fiber precursors. Their research demonstrated the potential of two-stage carbon membrane systems for achieving H<sub>2</sub> purity levels exceeding 99.5%. Zeolites are crystalline aluminosilicate materials with molecular-level pores, effective adsorption capabilities, and remarkable thermal and chemical stability.<sup>211</sup> The gas separation capabilities of the ZIF-9 membrane were assessed through both single gas permeation and the separation of gas mixtures, including H<sub>2</sub>/CO<sub>2</sub>, H<sub>2</sub>/N<sub>2</sub>, and H<sub>2</sub>/CH<sub>4</sub>. The membrane demonstrated impressive mixture separation factors, with values of 21.5 for H<sub>2</sub>/CO<sub>2</sub>, 8.2 for H<sub>2</sub>/CH<sub>4</sub>, and 14.7 for H<sub>2</sub>/N<sub>2</sub>. Thus, the ZIF-9 membrane displayed exceptional stability over a relatively wide range of operating temperatures.<sup>212</sup> Furthermore, MOFs represent an emerging category of hybrid porous materials that feature precisely defined geometric and crystallographic structures. They are assembled from metal ions or clusters connected by organic linkers. MOFs offer a range of inherent benefits, including structural adaptability, extraordinarily high porosity, consistently tunable pore sizes, and adaptable internal surface characteristics.<sup>213</sup> The influence of organic ligands on the separation capabilities of Zr-based metal–organic framework (Zr-MOF) membranes was explored.<sup>214</sup> These MOF membranes exhibited impressive separation factors for gas mixtures, with values of 26, 13, and 11 for H<sub>2</sub>/CO<sub>2</sub>, H<sub>2</sub>/N<sub>2</sub>, and H<sub>2</sub>/CH<sub>4</sub>, respectively.

## 6. TECHNO-ECONOMIC ANALYSIS OF VARIOUS CATALYTIC HYDROGEN PRODUCTION METHODS

For real-life applications of various catalytic hydrogen production processes, a thorough techno-economic analysis is required to judge the feasibility of the process. Approximately 90% of the global demand for hydrogen is met through the utilization of natural gas and byproducts from refineries.<sup>132</sup> Steam methane reforming (SMR) stands as the established technology for converting natural gas and various hydrocarbons into syngas, consisting of hydrogen (H<sub>2</sub>) and carbon monoxide (CO), on a commercial scale.<sup>215</sup> A techno-economic analysis was performed by Salkuyeh et al.<sup>216</sup> for hydrogen

production through chemical looping reforming (CLR) and SMR processes, considering both scenarios with and without carbon capture, respectively. Notably, the CLR process stands out as the most efficient in terms of natural gas consumption, exhibiting a remarkable reduction of 11–38% when compared to alternative configurations. This enhanced efficiency translates into a substantial decrease in the quantity of CO<sub>2</sub> that necessitates capture when employing carbon capture systems. The CO<sub>2</sub> production rate in the CLR process is up to 37% lower than that observed in other available options. The minimum hydrogen selling price for the CLR process was the lowest at \$0.98/kg of H<sub>2</sub>, followed closely by the SMR process at \$1.07/kg of H<sub>2</sub>. However, when carbon capture measures were incorporated into these technologies, the impact on pricing varied significantly. For the CLR process, the minimum hydrogen selling price increases modestly by just \$0.13/kg of H<sub>2</sub>, reaching \$1.11/kg of H<sub>2</sub>. In contrast, the introduction of carbon capture to the SMR process results in a substantial price escalation, soaring to \$2.16/kg of H<sub>2</sub>.<sup>217</sup> In the realm of hydrogen production, plasma pyrolysis technologies exhibit distinct characteristics. Specifically, they yield hydrogen at a rate of €5.00/kg of H<sub>2</sub> in the case of a self-sustaining process and €2.55/kg of H<sub>2</sub> when incorporating renewable energy inputs. However, within the current regulatory and economic landscape in Germany, the production of hydrogen through SMR and SMR with carbon capture and storage (CCS) emerges as significantly more economically viable. Both the SMR and SMR with CCS processes offer substantial cost advantages, amounting to approximately €1.5/kg of H<sub>2</sub> in savings when compared to plasma pyrolysis with an external energy supply. Remarkably, the cost savings widen to an impressive €3.0/kg of H<sub>2</sub> when compared to water electrolysis.<sup>218</sup> In another study, a comprehensive techno-economic evaluation was undertaken, covering a broad spectrum of system scales ranging from 10 kW to 10 MW. This extensive assessment provided insights into the considerable impact of scale on the reduction of minimum hydrogen selling prices, showcasing a substantial decrease from \$7.03/kg of H<sub>2</sub> at small modular scales to \$3.98/kg of H<sub>2</sub> at larger industrial scales. Notably, sensitivity analyses underscore the potential for even more significant reductions in hydrogen selling prices, with the potential for reductions of up to 50%. Furthermore, the proposed hydrogen production pathway utilizing green NH<sub>3</sub> exhibits noteworthy advantages in terms of carbon dioxide (CO<sub>2</sub>) reduction. This process achieved a superior CO<sub>2</sub> reduction rate, ranging from 78 to 95% in terms of kilograms of CO<sub>2</sub> per kilogram of H<sub>2</sub> produced when compared to alternative methods, such as biomass gasification and steam methane reforming.<sup>218</sup>

Numerous investigations have been carried out concerning technical aspects, process simulation, mathematical modeling, and feasibility assessments regarding the production of hydrogen from organic compounds. Over time, as technology advances and economies of scale are realized, the cost of hydrogen production from these feedstocks is expected to become more competitive with traditional methods. Byun et al.<sup>223</sup> conducted a thorough economic feasibility analysis for hydrogen (H<sub>2</sub>) production via methanol steam reforming (MSR) using packed-bed reactors (PBRs) and membrane reactors (MRS) across a range of production capacities. Detailed cost estimations of this study revealed that, for H<sub>2</sub> production capacities of 30, 100, 300, and 700 m<sup>3</sup> h<sup>-1</sup>, the H<sub>2</sub> production costs were \$10.41, \$8.41, \$7.55, and \$7.24/kg of

$\text{H}_2$ , respectively, for the PBR and \$8.82, \$7.24, \$6.61, and \$6.43/kg of  $\text{H}_2$ , respectively, for the MR. These findings provide a comprehensive economic perspective on MSR-based  $\text{H}_2$  production, accounting for varying capacities and reactor types, with the MR showing favorable cost efficiencies compared to the PBR at each capacity level. In a separate study, Khamhaeng et al.<sup>222</sup> conducted a comparative analysis between two distinct processes for hydrogen ( $\text{H}_2$ ) production using ethanol as a starting material. The first process involved steam reforming of ethanol, while the second process encompassed the dehydrogenation of ethanol, with valuable byproducts, including ethyl acetate and acetaldehyde. Specifically, the steam reforming of ethanol emerged as the most cost-efficient option, with  $\text{H}_2$  production cost as low as \$1.58/kg of  $\text{H}_2$ . In contrast, the dehydrogenation of ethanol led to different cost outcomes, with costs amounting to \$3.24 and \$1.97/kg of  $\text{H}_2$ , respectively, depending upon the specific process conditions. A comprehensive techno-economic assessment of hydrogen production through glycerol reforming was performed by Khodabandehloo et al.,<sup>223</sup> comparing processes conducted in both aqueous and gaseous phases. Equipment procurement costs and a hydrogen production rate of 80 kg/h were considered for the estimation of the total cost of hydrogen production. Specifically, for steam reforming and aqueous phase reforming plants, the estimated costs were \$3.65 and \$3.55/kg of  $\text{H}_2$ , respectively. Furthermore, the authors considered installation expenses within the equipment costs, and this led to the total cost of hydrogen production being \$7.49 and \$7.45/kg of  $\text{H}_2$  for steam reforming and aqueous phase reforming plants, respectively. These studies suggest that reforming is the most common process for hydrogen production from organic molecules, and production costs vary from \$1.58 to \$10.41/kg (see Table 4).

**Table 4. Estimated Cost of Hydrogen Production from Various Catalytic Processes**

catalytic process/ feed	method	cost (\$/kg of $\text{H}_2$ )	reference
natural gas/ methane	steam reforming	0.98–1.62	219
	pyrolysis	2.37–5.27 <sup>a</sup>	215
ammonia	dissociation of ammonia	3.98–7.03	218 and 220
ethanol	steam reforming	8.87	221
		1.58	222
methanol		6.43–10.41	223 and 224
	glycerol	5.36–7.49	225

<sup>a</sup>1 euro equals to 1.05 U.S. dollar.

Nowadays, hydrogen produced through biomass conversion involves transforming biomass feedstocks, such as agricultural residues, wood, or dedicated energy crops, into hydrogen gas.

This process can be accomplished through various technologies, each with its economic considerations. The sensitivity analysis reveals that the most influential factors affecting the minimum selling price of hydrogen in production are the price of the feedstock and labor costs.<sup>226</sup> The cost of hydrogen production from biomass through various processes is depicted in Table 5. A comprehensive techno-economic analysis was conducted for a hydrogen production plant with a daily capacity of 100 kg of  $\text{H}_2$ , focusing on hydrogen production from two biomass-derived feedstocks: biogas and biomethane. The analysis evaluated key system design parameters, including the reactor size, membrane quantity, and operating pressures. The results showed that biomethane outperformed biogas, achieving higher efficiencies in both the reactor (97.4% versus 97.0%) and the overall system (63.7% versus 62.7%). Nevertheless, when considering the ultimate leveled cost of hydrogen (LCOH), the added expense associated with biomethane procurement results in a slightly higher cost for the produced hydrogen (€4.62/kg of  $\text{H}_2$  at 20 bar versus €4.39/kg of  $\text{H}_2$  at 20 bar). This suggests that, at current pricing levels, biogas stands as the more economically advantageous choice for hydrogen production.<sup>227</sup> Biomass pyrolysis emerges as a viable method for hydrogen production, boasting an energy demand that is 15–20% lower than that of traditional steam methane reforming technology. In a comprehensive comparative analysis of renewable and conventional hydrogen production processes, the cost of hydrogen ( $\text{H}_2$ ) via biomass pyrolysis was found to range from \$1.77 to \$2.05/kg of  $\text{H}_2$ , a range that proved to be cost-competitive when juxtaposed with methane pyrolysis, which ranged from \$1.25 to \$2.20/kg of  $\text{H}_2$ .<sup>228</sup> Biomass gasification is increasingly recognized as an environmentally friendly and sustainable method for producing green hydrogen. The methodology employed entails the development of three biomass gasification process models (conventional, plasma, and supercritical water) using Aspen Plus to estimate maximum hydrogen yields via a comprehensive parametric study. Remarkably, the study establishes a minimum selling price of €7.0, €10.0, and €13.0/kg for green hydrogen derived from the conventional, supercritical water, and plasma gasification processes, respectively.<sup>226</sup> The cost of hydrogen production is closely associated with the operational expenses incurred by the fermentation reactor systems. Optimization of hydrogen production via dark fermentation is performed by some researchers,<sup>229</sup> and it shows that hydrogen production is very low in comparison to the resource treated. The estimated investment reported by the authors was \$18.2 M, and the production cost was \$37.6/kg of  $\text{H}_2$  produced when 1 kg s<sup>-1</sup> of biomass was treated. This research delves into a comprehensive techno-economic assessment of an innovative bioprocess, amalgamating solid-state fermentation and dark fermentation, to harness hydrogen ( $\text{H}_2$ ) from

**Table 5. Estimated Cost of Hydrogen Production from Various Catalytic Biomass Conversion Processes<sup>a</sup>**

process	method	energy efficiency (%)	$\text{H}_2$ yield (g/kg of feedstock)	cost (\$/kg of $\text{H}_2$ )	reference
biomass conversion	dark fermentation	60–80	4–44	1.68–2.57	3 and 232
	photofermentation	0.1–12	9–49	2.57–2.83	3, 233, and 234
	pyrolysis	35–50	25–65	1.77–2.05	228
	gasification	30–60	40–190	1.52–3.4	216, 219, and 235
	steam reforming	74–85	40–130	1.25–14.9	219
	microbial electrolysis cell	26.1–60	70	1.1–4.5	219 and 233

<sup>a</sup>Modified data were taken from ref 3.

**Table 6.** Estimated Cost of Hydrogen Production from Various Catalytic Water-Splitting Processes

process	energy source	cost (\$/kg of H <sub>2</sub> )	STH efficiency	maturity	reference
electrolysis	solar	3.59–6.67	1.03–1.87	commercial	245 and 246
	wind	5.10–6.46	-	commercial	247 and 248
	nuclear	2.18–5.92	-	commercial	237
photoelectrochemical	solar	4.15–18.98	1.64	R&D	236 and 242–244
photocatalysis	solar	18.32	<1.0	R&D	236
direct biophotolysis	solar/microorganism metabolism	2.13–18.45	2.0	R&D	236 and 249
indirect biophotolysis	solar/microorganism metabolism	1.42–36.39	0.1–2.5	R&D	249

food waste (FW). The study entails the design of a H<sub>2</sub> production facility boasting a daily capacity of 10 tons and an anticipated operational lifespan of 10 years. The analysis leveraged Aspen Plus to meticulously model the mass and energy balances within the plant. Among the key determinants, the prevailing H<sub>2</sub> market price and the associated operating labor costs emerged as pivotal factors influencing the net present value of the plant. Notably, the unit cost of H<sub>2</sub> production was established at \$2.29/m<sup>3</sup>.<sup>230</sup> In a study, authors determined the specific cost of photofermentative hydrogen production using an established outdoor pilot-scale photobioreactor system with a capacity of 20 L. The specific hydrogen production cost was calculated at \$2.7/mol (equivalent to \$1362/kg of H<sub>2</sub>), and when equipment cost subsidies are factored in, it amounted to \$395/kg of H<sub>2</sub>. Observing the MECs based on their techno-economic possibilities, two critical challenges have been identified: the electrode materials and the reactor design.

The technological advancements, scale, and availability of energy sources influence the economic aspects of green hydrogen production through water splitting. Currently, the process of water splitting through electrolysis stands as a sustainable and commercially viable method for hydrogen production.<sup>236</sup> The cost of producing hydrogen depends upon the source of electricity used and ranges from \$2.18 to \$6.67/kg of hydrogen, as detailed in Table 6. Apart from the source of electricity, several other variables contribute to the cost variability of green hydrogen, including the chosen production method (e.g., AWE, PEM, SOEC, AEM, and photocatalysis) as well as the capacity and operational lifespan of the facility. As it stands, the current cost range for green hydrogen production spans from approximately \$2.28 to \$7.39/kg of H<sub>2</sub> generated through the electrolysis process with renewable energy sources.<sup>237,238</sup> Green hydrogen production through the electrolysis process, harnessing renewable energy sources, like wind and solar, was studied by Zhou et al.<sup>239</sup> The findings of the authors revealed the cost of green hydrogen in the range of \$2.12 to \$10.82/kg when wind energy was utilized as the electricity source, with H<sub>2</sub> production capacities ranging from 0.012 to 1.36 tons/day. However, when photovoltaic systems were employed as the electricity source, the cost of green hydrogen varied from \$3.17 to \$25.17/kg, with production capacities spanning from 0.0024 to 13.25 tons/day. Three distinct electrolysis techniques, alkaline water electrolysis, proton exchange membrane (PEM) electrolysis, and solid oxide electrolysis cells (SOECs), were explored by Pinsky et al.<sup>240</sup> for hydrogen production utilizing electricity generated from a nuclear power plant. The cost of hydrogen production ranged from \$2.24 to \$5.92/kg. Notably, among the different electrolysis processes studied, SOECs emerged as the most economically favorable option for hydrogen production. In another study, Nasser et al.<sup>241</sup> present a comprehensive

techno-economic evaluation focused on harnessing a hybrid renewable energy system comprising wind turbines and photovoltaic (PV) panels for hydrogen production. The overall system efficiency ranges from 7.69 to 9.37%, while the production cost spans from \$4.54 to \$7.48/kg of H<sub>2</sub> in five distinct Egyptian cities. These results shed light on the potential of this hybrid renewable energy system for sustainable hydrogen production across diverse climatic conditions while also considering the associated economic aspects. These studies suggest that the cost of hydrogen production through the electrolysis process greatly depends upon the source of electricity and the electrolysis methods. As these factors align and improve, the cost competitiveness of green hydrogen is expected to increase, making it an attractive and sustainable energy carrier for the future.

As an alternative to PV-E, photoelectrochemical (PEC) hydrogen production has garnered significant attention in recent years. PEC technology directly converts solar radiation into hydrogen, representing a promising approach in the field.<sup>242</sup> In 2016, Shaner et al.<sup>243</sup> conducted a comprehensive techno-economic analysis focusing on the production of solar hydrogen through two distinct methods: PEC and PV-E processes. Their investigation targeted a substantial daily hydrogen output of 10 000 kg (equivalent to 3.65 kilotonnes annually) to rigorously assess the economic viability of each technology. The plant-gate levelized costs for hydrogen production (LCH) were determined to be \$11.4/kg for the PEC system and \$12.1/kg for the PV-E system in the base-case scenarios without considering taxation. Photocatalysis emerges as a potentially viable alternative to avoid the complexity and high production costs associated with hydrogen production through PV-E and PEC methods. Photocatalytic water splitting is presently in its early stages of development, with significant ongoing research dedicated to the analysis and fabrication of photocatalytic materials.<sup>244</sup> In a recent study conducted by Maurya et al.,<sup>244</sup> four distinct pathways were explored for hydrogen production through the process of photocatalysis. These pathways included TiO<sub>2</sub> nanorods, fluorine-doped carbon nitride quantum dot-embedded TiO<sub>2</sub> (CNF = TNRs/TiO<sub>2</sub>), g-C<sub>3</sub>N<sub>4</sub>, and the g-C<sub>3</sub>N<sub>4</sub>/BiOI composite. The analysis revealed a levelized cost of hydrogen (LCOH) spanning from \$4.15 to \$9.8/kg of H<sub>2</sub> produced across these pathways. Notably, capital investment and labor costs were identified as the primary contributors, constituting 75% of the total cost in this process. At present, neither photoelectrochemical nor photocatalysis methods have been adopted for commercial use as a result of their lower solar-to-hydrogen efficiency. The majority of research on these solar-to-hydrogen (STH) methods continues to be conducted in laboratory settings rather than in real-world outdoor environments.<sup>236</sup> Frowijn et al.<sup>236</sup> reported various green hydrogen production methods and revealed that, among

various hydrogen production methods, photovoltaic-based electrolysis emerges as the most cost-effective option, with a production cost of \$9.31/kg of H<sub>2</sub>. In contrast, production costs based on photocatalytic and photoelectrochemical water splitting were comparatively higher, standing at \$18.32 and \$18.98/kg of H<sub>2</sub>, respectively. It is worth noting that these costs are expected to experience substantial reductions in the future. Specifically, photocatalytic water splitting shows significant potential for cost reduction, with potential costs estimated at \$3.12/kg of H<sub>2</sub>, making them potential candidates to surpass the cost efficiency of photovoltaic-based electrolysis.

Water biophotolysis is another photo-assisted method for hydrogen production. However, both the direct biophotolysis (DBP) and indirect biophotolysis (IBP) methods have not yet reached commercialization. While both methods hold promise for hydrogen production, they have remained largely confined to laboratory settings and small-scale outdoor environments up to the present day.<sup>236</sup> The major drawbacks of the biophotolysis process are the complex bioreactor design with large surface areas for light capturing and low H<sub>2</sub> conversion yields.<sup>249</sup> In the study conducted by Qureshi et al.,<sup>249</sup> a comprehensive overview of data about direct and indirect biophotolysis was presented. Their findings indicated that the costs for direct biophotolysis span a range from \$2.13 to \$7.24/kg of H<sub>2</sub>, while indirect biophotolysis costs encompass a spectrum from \$1.42 to \$7.54/kg of H<sub>2</sub>. However, in another study, the leveled cost of hydrogen (LCOH) for the DBP process was meticulously computed at \$18.45/kg of H<sub>2</sub>. An intriguing finding was that nearly 75% of the LCOH was attributed to the bioreactor cost, within which the expenses related to bioreactor materials and nutrients dominate, accounting for a substantial 63% of the LCOH. Interestingly, when shifting the focus to IBP, the LCOH noticeably doubles in comparison to DBP, reaching \$36.39/kg of H<sub>2</sub>.<sup>236</sup> Biophotolysis has the potential to be self-sustaining and can utilize wastewater as a resource for hydrogen production. This approach holds significant promise and could play a crucial role in advancing sustainable hydrogen production in the near future.<sup>236</sup>

## 7. CHALLENGES AND PROSPECTIVES

Various catalytic processes for hydrogen production have been reviewed in this study. However, steam reforming of methane remains the dominant and cost-effective method for hydrogen production, with costs ranging from \$0.98 to \$1.62/kg of hydrogen. This process has a significant drawback as it produces substantial amounts of greenhouse gases, approximately 5–10 kg of CO<sub>2</sub> for every kilogram of hydrogen produced.<sup>219</sup> To mitigate this issue, the carbon capture and storage (CCS) method has been adopted. Various alternative methods for hydrogen production are emerging. One such method involves the steam reforming of organic compounds derived as byproducts from biomass conversion and various industries. However, steam reforming reactions face challenges, including catalyst deactivation and the highly endothermic nature of the reactions. Catalyst deactivation may happen as a result of active metal sintering and coke formation. To address these challenges, various strategies have been developed, including modifying the catalyst with promoters, reducing particle size, incorporating lattice oxygen, and increasing the water/alcohol ratio in the reactions. These approaches aim to enhance the efficiency and longevity of catalysts in the steam reforming process for hydrogen production. Moreover, the cost

of catalysts is high and needs to be reduced for economic operation of these processes.

Hydrogen production through water splitting can be achieved using various methods. Presently, electrolysis is a viable approach for hydrogen production, utilizing electric energy generated from sources, such as solar, wind, nuclear, and fossil fuels. However, nuclear and fossil fuels are not sustainable options, and wind energy is location-dependent and relatively costly. In contrast, solar energy is a renewable and green source, making it an attractive choice for hydrogen production. Nonetheless, the efficiency of solar panels and the catalysts used in the electrodes of electrolysis units contribute to the higher cost of hydrogen production. This can be overcome by developing more efficient catalysts from earth-abundant materials. Disposal and recycling of spent/used solar panels may pose a threat in the near future. In this regard, panels with a longer life are preferred, and regeneration/recycling of panel materials should also be studied.

In addition to electrolysis, there are other photo-assisted methods in the development phase, such as photoelectrochemical, photocatalysis, and biophotolysis. While these methods hold significant potential for green hydrogen production, they have not been commercialized as a result of their lower solar-to-hydrogen (STH) efficiency at the current stage of development. Researchers are actively working on improving the efficiency of photocatalysts to better harness sunlight. Photocatalysis is considered a potential method for hydrogen production as a result of its simplicity, and it may become commercially viable once it reaches a STH efficiency of around 10% with a production cost below \$4.0/kg of hydrogen. This progress could significantly reduce the cost and environmental impact of hydrogen production, making it a more sustainable and accessible energy source.

Separating mixed gases to obtain purified hydrogen fuel presents a significant challenge. Pressure swing adsorption (PSA) technology is renowned for its low operating costs and long lifespan. However, it has limitations with recovery rates that typically range from 65 to 90%, making it most suitable for large-scale applications exceeding 10 000 Nm<sup>3</sup> h<sup>-1</sup>. PSA is most effective when processing gas mixtures containing 60–90 mol % hydrogen. An alternative to the PSA method is metal hydride separation, which is particularly suited for gas mixtures with lower hydrogen concentrations. Nonetheless, a major issue in metal hydride separation is the deterioration of hydrogen charging performance as a result of surface chemical interactions with electrophilic gases. This issue can be addressed through surface modification to enhance poisoning tolerance. In recent years, emerging membrane technologies, including polymeric, dense material, and microscopic membranes, have shown great potential for large-scale industrial applications in the field of gas separation, offering a promising avenue for efficient hydrogen purification.

## 8. CONCLUSION

Hydrogen, an exceptionally promising alternative energy source, possesses the highest energy density. It is environmentally friendly and causes less environmental pollution. This review summarizes various catalytic processes for hydrogen production. Catalysts play a crucial role in these processes. Catalysts based on metals (e.g., Ni, Fe, and Pd) have been extensively explored by several researchers. Various supports, like CeO<sub>2</sub>, TiO<sub>2</sub>, Al<sub>2</sub>O<sub>3</sub>, La<sub>2</sub>O<sub>3</sub>, Y<sub>2</sub>O<sub>3</sub>, and  $\beta$ -zeolite, have been investigated to ensure active metal dispersion, stability, and

participation in catalytic reactions. Metals along with various oxides (e.g.,  $\text{TiO}_2$ ,  $\text{WO}_3$ ,  $\text{Co}_3\text{O}_4$ , and  $\text{Fe}_2\text{O}_3$ ) are also used for hydrogen production. Additionally, various non-oxide-based catalysts have been studied by several researchers. Carbon-based catalysts and MOFs exhibit significant potential for catalytic hydrogen production. Most of the catalytic processes generate  $\text{CO}_2$  gases that impact the environment. Therefore, several CCS methods have been adopted to reduce carbon emissions in the environment. Photo-assisted methods have the potential to produce green hydrogen, but currently, PV electrolysis is the only viable process. The hydrogen purification process needs to be adopted because most catalytic processes release other gases along with hydrogen. Currently, only PSA is an economical separation process for large-scale applications. However, other methods, like metal hydride and membrane separation, hold potential for hydrogen purification. With respect to economic viability, steam reforming of methane remains the dominant and cost-effective method for hydrogen production, with costs ranging from \$0.98 to \$1.62/kg. PV-electrolysis is another method that produces green hydrogen, but its cost is higher than that of SRM. Other catalytic hydrogen production methods, such as steam reforming of organic compounds and biomass conversion, have been explored by researchers but have not been commercialized. Photo-assisted methods have the potential to produce green hydrogen but are currently in the development phase. The non-commercial boundaries of the process are attributed to catalyst limitations. Overall, the catalytic process is a promising method for hydrogen production, and with the advancement of technology and efficient catalysts, green hydrogen can be produced at a viable cost.

## AUTHOR INFORMATION

### Corresponding Author

**Suman Dutta** – Department of Chemical Engineering, Indian Institute of Technology (ISM) Dhanbad, Dhanbad, Jharkhand 826004, India;  [orcid.org/0000-0002-2695-8108](https://orcid.org/0000-0002-2695-8108); Email: [ss.dutta@hotmail.com](mailto:ss.dutta@hotmail.com), [suman@iitism.ac.in](mailto:suman@iitism.ac.in)

### Authors

**Ravi Kumar** – Department of Chemical Engineering, Indian Institute of Technology (ISM) Dhanbad, Dhanbad, Jharkhand 826004, India;  [orcid.org/0000-0002-0802-2365](https://orcid.org/0000-0002-0802-2365)

**Rohini Singh** – Department of Chemical Engineering, Indian Institute of Technology (ISM) Dhanbad, Dhanbad, Jharkhand 826004, India

Complete contact information is available at:  
<https://pubs.acs.org/10.1021/acs.energyfuels.3c04026>

### Notes

The authors declare no competing financial interest.

### Biographies

Ravi Kumar is currently pursuing his Ph.D. in the Department of Chemical Engineering, Indian Institute of Technology (ISM) Dhanbad, India. He obtained his bachelor's degree from Birla Institute of Technology, Mesra, Ranchi, India. His research area includes renewable energy, photocatalysis, and the drying of agricultural products. Notably, he was awarded by the honorable President of India, Shri Ramnath Kovind, on September 24, 2019, at the President's House in New Delhi, India.

Rohini Singh received Ph.D. degree from Indian Institute of Technology (ISM) Dhanbad, India. Her research area includes wastewater purification, solid waste management, photocatalysis, and hydrogen generation.

Suman Dutta is working as an associate professor in the Department of Chemical Engineering, Indian Institute of Technology (ISM) Dhanbad, India. He received a Ph.D. degree from Jadavpur University, Kolkata, India. His research area includes renewable energy, wastewater treatment, photocatalysis, and membrane technology. He is actively associated with the research of synthesis and utilization of photocatalytic materials. He edited the book "Sustainable Fuel Technologies Handbook" and authored the book "Optimization in Chemical Engineering".

## REFERENCES

- (1) Yan, T.; Liu, H.; Jin, Z. g-C<sub>3</sub>N<sub>4</sub>/α-Fe<sub>2</sub>O<sub>3</sub> Supported Zero-Dimensional Co<sub>3</sub>S<sub>4</sub> Nanoparticles Form S-Scheme Heterojunction Photocatalyst for Efficient Hydrogen Production. *Energy Fuels* **2021**, *35* (1), 856–867.
- (2) Nagappan, S.; Yang, S.; Adhikari, A.; Patel, R.; Kundu, S. A Review on Consequences of Flexible Layered Double Hydroxide-Based Electrodes: Fabrication and Water Splitting Application. *Sustainable Energy Fuels* **2023**, *7*, 3741–3775.
- (3) Megia, P. J.; Vizcaino, A. J.; Calles, J. A.; Carrero, A. Hydrogen Production Technologies: From Fossil Fuels toward Renewable Sources. A Mini Review. *Energy Fuels* **2021**, *35* (20), 16403–16415.
- (4) Li, D.; Liu, H.; Feng, L. A Review on Advanced FeNi-Based Catalysts for Water Splitting Reaction. *Energy Fuels* **2020**, *34* (11), 13491–13522.
- (5) Ma, X.; Liu, Y.; Wang, Y.; Jin, Z. Amorphous CoS<sub>x</sub> Growth on CaTiO<sub>3</sub> Nanocubes Formed S-Scheme Heterojunction for Photocatalytic Hydrogen Production. *Energy Fuels* **2021**, *35* (7), 6231–6239.
- (6) Karmakar, A.; Karthick, K.; Sankar, S. S.; Kumaravel, S.; Madhu, R.; Kundu, S. A Vast Exploration of Improvising Synthetic Strategies for Enhancing the OER Kinetics of LDH Structures: A Review. *J. Mater. Chem. A* **2021**, *9*, 1314–1352.
- (7) Bepari, S.; Kuila, D. Steam Reforming of Methanol, Ethanol and Glycerol over Nickel-Based Catalysts-A Review. *Int. J. Hydrogen Energy* **2020**, *45* (36), 18090–18113.
- (8) Palmer, C.; Bunyan, E.; Gelinas, J.; Gordon, M. J.; Metiu, H.; McFarland, E. W. CO<sub>2</sub>-free Hydrogen Production by Catalytic Pyrolysis of Hydrocarbon Feedstocks in Molten Ni-Bi. *Energy Fuels* **2020**, *34* (12), 16073–16080.
- (9) Chen, C.; Wu, K.; Ren, H.; Zhou, C.; Luo, Y.; Lin, L.; Au, C.; Jiang, L. Ru-Based Catalysts for Ammonia Decomposition: A Mini-Review. *Energy Fuels* **2021**, *35* (15), 11693–11706.
- (10) Setiabudi, H. D.; Aziz, M. A. A.; Abdullah, S.; Teh, L. P.; Jusoh, R. Hydrogen Production from Catalytic Steam Reforming of Biomass Pyrolysis Oil or Bio-Oil Derivatives: A Review. *Int. J. Hydrogen Energy* **2020**, *45* (36), 18376–18397.
- (11) Aryal, P.; Tanksale, A.; Hoadley, A. Mini Review of Catalytic Reactive Flash Volatilization of Biomass for Hydrogen-Rich Syngas Production. *Energy Fuels* **2022**, *36* (9), 4640–4652.
- (12) Cao, L.; Yu, I. K. M.; Xiong, X.; Tsang, D. C. W.; Zhang, S.; Clark, J. H.; Hu, C.; Ng, Y. H.; Shang, J.; Ok, Y. S. Biorenewable Hydrogen Production through Biomass Gasification: A Review and Future Prospects. *Environ. Res.* **2020**, *186*, 109547.
- (13) Ali, M.; Pervaiz, E.; Sohail, U. Rational Design of the CdS/Fe-MOF Hybrid for Enhanced Hydrogen Evolution Reaction Catalysis. *Energy Fuels* **2023**, *37* (11), 7919–7926.
- (14) Ng, B. J.; Putri, L. K.; Kong, X. Y.; Teh, Y. W.; Pasbakhsh, P.; Chai, S. P. Z-Scheme Photocatalytic Systems for Solar Water Splitting. *Adv. Sci.* **2020**, *7* (7), 1903171.
- (15) Anwar, S.; Khan, F.; Zhang, Y.; Djire, A. Recent Development in Electrocatalysts for Hydrogen Production through Water Electrolysis. *Int. J. Hydrogen Energy* **2021**, *46* (63), 32284–32317.

- (16) Dutta, S. Review on Solar Hydrogen: Its Prospects and Limitations. *Energy Fuels* **2021**, *35* (15), 11613–11639.
- (17) Akhlaghi, N.; Najafpour-Darzi, G. A Comprehensive Review on Biological Hydrogen Production. *Int. J. Hydrogen Energy* **2020**, *45* (43), 22492–22512.
- (18) Taipabu, M. I.; Viswanathan, K.; Wu, W.; Hattu, N.; Atabani, A. E. A Critical Review of the Hydrogen Production from Biomass-Based Feedstocks: Challenge, Solution, and Future Prospect. *Process Saf. Environ. Prot.* **2022**, *164*, 384–407.
- (19) Lee, J. E.; Jeon, K. J.; Show, P. L.; Lee, I. H.; Jung, S. C.; Choi, Y. J.; Rhee, G. H.; Lin, K. Y. A.; Park, Y. K. Mini Review on H<sub>2</sub> Production from Electrochemical Water Splitting According to Special Nanostructured Morphology of Electrocatalysts. *Fuel* **2022**, *308*, 122048.
- (20) Su, H.; Yan, M.; Wang, S. Recent Advances in Supercritical Water Gasification of Biowaste Catalyzed by Transition Metal-Based Catalysts for Hydrogen Production. *Renewable Sustainable Energy Rev.* **2022**, *154*, 111831.
- (21) Ranjekar, A. M.; Yadav, G. D. Steam Reforming of Methanol for Hydrogen Production: A Critical Analysis of Catalysis, Processes, and Scope. *Ind. Eng. Chem. Res.* **2021**, *60* (1), 89–113.
- (22) Granados-Fitch, M. G.; Quintana-Melgoza, J. M.; Juarez-Arellano, E. A.; Avalos-Borja, M. Mechanism to H<sub>2</sub> Production on Rhenium Carbide from Pyrolysis of Coconut Shell. *Int. J. Hydrogen Energy* **2019**, *44* (5), 2784–2796.
- (23) Zhao, T.; Ye, Z.; Zeng, M.; Li, W.; Luo, W.; Xiao, Q.; Xu, J. Molten Salt Synthesis of Mg-Doped Ta<sub>3</sub>N<sub>5</sub> Nanoparticles with Optimized Surface Properties for Enhanced Photocatalytic Hydrogen Evolution. *Energy Fuels* **2023**, *37* (23), 18194–18203.
- (24) Zhang, D.; Yao, J.; Wang, G.; Yin, J.; Zhu, K.; Yan, J.; Cao, D.; Zhu, M. Efficient Hydrogen Evolution Catalysts Based on Hierarchical Flowerlike Ni<sub>x</sub>Co<sub>9-x</sub> XS8Nanosheets. *Energy Fuels* **2023**, *37* (12), 8531–8538.
- (25) Kim, H.; Robertson, A. W.; Kwon, G.-h.; O, J.-w.; Warner, J. H.; Kim, J. M. Biomass-Derived Nickel Phosphide Nanoparticles as a Robust Catalyst for Hydrogen Production by Catalytic Decomposition of C<sub>2</sub>H<sub>2</sub> or Dry Reforming of CH<sub>4</sub>. *ACS Appl. Energy Mater.* **2019**, *2* (12), 8649–8658.
- (26) Granados-Fitch, M. G.; Quintana-Melgoza, J. M.; Juarez-Arellano, E. A.; Avalos-Borja, M. Rhenium Borides (Re<sub>3</sub>B and ReB<sub>2</sub>) Mechanosynthesis and Their Use as a Catalyst for H<sub>2</sub> Production from Biomass Pyrolysis. *Mater. Res. Bull.* **2021**, *137*, 111180.
- (27) Shen, Y.; Lua, A. C. Synthesis of Ni and Ni-Cu Supported on Carbon Nanotubes for Hydrogen and Carbon Production by Catalytic Decomposition of Methane. *Appl. Catal., B* **2015**, *164*, 61–69.
- (28) Chaudhary, D.; Singh, S.; Vankar, V. D.; Khare, N. A Ternary Ag/TiO<sub>2</sub>/CNT Photoanode for Efficient Photoelectrochemical Water Splitting under Visible Light Irradiation. *Int. J. Hydrogen Energy* **2017**, *42* (12), 7826–7835.
- (29) Saquic, B. E. B.; Irmak, S.; Wilkins, M. Enhancement of Catalytic Performance of Graphene Supported Pt Catalysts by Ni and W for Hydrogen Gas Production by Hydrothermal Gasification of Biomass-Derived Compounds. *Fuel* **2022**, *308*, 122079.
- (30) Qiu, H.-J.; Ito, Y.; Cong, W.; Tan, Y.; Liu, P.; Hirata, A.; Fujita, T.; Tang, Z.; Chen, M. Nanoporous Graphene with Single-Atom Nickel Dopants: An Efficient and Stable Catalyst for Electrochemical Hydrogen Production. *Angew. Chem.* **2015**, *127* (47), 14237–14241.
- (31) Wu, G.; Liu, Q.; Tai, G.; Zhou, C.; Yan, Z.; Han, J.; Xing, W. 0D/2D van der Waals Heterojunction of N,S-Organic Dots/g-C<sub>3</sub>N<sub>4</sub> Nanosheets for Boosted Photocatalytic Hydrogen Evolution. *Energy Fuels* **2022**, *36* (20), 12763–12771.
- (32) Martindale, B. C. M.; Hutton, G. A. M.; Caputo, C. A.; Reisner, E. Solar Hydrogen Production Using Carbon Quantum Dots and a Molecular Nickel Catalyst. *J. Am. Chem. Soc.* **2015**, *137* (18), 6018–6025.
- (33) Nishigaki, K.; Katagiri, M.; Matsuoka, M.; Horiuchi, Y. A Synthetic Route to MoS<sub>2</sub> Catalysts Supported on a Metal–Organic Framework for Electrochemical Hydrogen Evolution Reaction Utilizing Chemical Vapor Deposition. *Energy Fuels* **2022**, *36* (1), 548–553.
- (34) El Hanafi, M.; BaQais, A.; Saadi, M.; Ait Ahsaine, H. Advances and Outlook of Metal–Organic Frameworks as High-Performance Electrocatalysts for Hydrogen Evolution Reaction: A Minireview. *Energy Fuels* **2023**, *37* (15), 10869–10885.
- (35) Du, Z.; Liu, C.; Zhai, J.; Guo, X.; Xiong, Y.; Su, W.; He, G. A Review of Hydrogen Purification Technologies for Fuel Cell Vehicles. *Catalysts* **2021**, *11* (3), 393.
- (36) Das, D.; Veziroglu, T. N. Advances in Biological Hydrogen Production Processes. *Int. J. Hydrogen Energy* **2008**, *33* (21), 6046–6057.
- (37) Du, X.; France, L. J.; Kuznetsov, V. L.; Xiao, T.; Edwards, P. P.; AlMegren, H.; Bagabas, A. Dry Reforming of Methane over ZrO<sub>2</sub>-Supported Co-Mo Carbide Catalyst. *Appl. Petrochem. Res.* **2014**, *4* (1), 137–144.
- (38) Prasongthum, N.; Xiao, R.; Zhang, H.; Tsubaki, N.; Natewong, P.; Reubroycharoen, P. Highly Active and Stable Ni Supported on CNTs-SiO<sub>2</sub> Fiber Catalysts for Steam Reforming of Ethanol. *Fuel Process. Technol.* **2017**, *160*, 185–195.
- (39) Ma, Y.; Guan, G.; Shi, C.; Zhu, A.; Hao, X.; Wang, Z.; Kusakabe, K.; Abudula, A. Low-Temperature Steam Reforming of Methanol to Produce Hydrogen over Various Metal-Doped Molybdenum Carbide Catalysts. *Int. J. Hydrogen Energy* **2014**, *39* (1), 258–266.
- (40) Gallegos-Suárez, E.; Guerrero-Ruiz, A.; Rodríguez-Ramos, I. Efficient Hydrogen Production from Glycerol by Steam Reforming with Carbon Supported Ruthenium Catalysts. *Carbon N. Y.* **2016**, *96*, 578–587.
- (41) Wang, B.; Wang, Y.; Lei, Y.; Wu, N.; Gou, Y.; Han, C.; Xie, S.; Fang, D. Mesoporous Silicon Carbide Nanofibers with in Situ Embedded Carbon for Co-Catalyst Free Photocatalytic Hydrogen Production. *Nano Res.* **2016**, *9* (3), 886–898.
- (42) Singh, R.; Dutta, S. Synthesis and Characterization of Solar Photoactive TiO<sub>2</sub> Nanoparticles with Enhanced Structural and Optical Properties. *Adv. Powder Technol.* **2018**, *29* (2), 211–219.
- (43) Syed Muhammad, A. F. ad; Awad, A.; Saidur, R.; Masiran, N.; Salam, A.; Abdullah, B. Recent Advances in Cleaner Hydrogen Productions via Thermo-Catalytic Decomposition of Methane: Admixture with Hydrocarbon. *Int. J. Hydrogen Energy* **2018**, *43* (41), 18713–18734.
- (44) Qian, J. X.; Chen, T. W.; Enakonda, L. R.; Liu, D. B.; Mignani, G.; Basset, J.-M.; Zhou, L. Methane Decomposition to Produce CO<sub>x</sub>-Free Hydrogen and Nano-Carbon over Metal Catalysts: A Review. *Int. J. Hydrogen Energy* **2020**, *45* (15), 7981–8001.
- (45) Mukherjee, S.; Devaguptapu, S. V.; Sviripa, A.; Lund, C. R. F.; Wu, G. Low-Temperature Ammonia Decomposition Catalysts for Hydrogen Generation. *Appl. Catal., B* **2018**, *226*, 162–181.
- (46) Haryanto, A.; Fernando, S.; Murali, N.; Adhikari, S. Current Status of Hydrogen Production Techniques by Steam Reforming of Ethanol: A Review. *Energy Fuels* **2005**, *19* (5), 2098–2106.
- (47) Wang, S.; Lu, A.; Zhong, C. J. Hydrogen Production from Water Electrolysis: Role of Catalysts. *Nano Convergence* **2021**, *8*, 4.
- (48) Clarizia, L.; Nadagouda, M. N.; Dionysiou, D. D. Recent Advances and Challenges of Photoelectrochemical Cells for Hydrogen Production. *Curr. Opin. Green Sustainable Chem.* **2023**, *41*, 100825.
- (49) Kahng, S.; Yoo, H.; Kim, J. H. Recent Advances in Earth-Abundant Photocatalyst Materials for Solar H<sub>2</sub> Production. *Adv. Powder Technol.* **2020**, *31* (1), 11–28.
- (50) Nishii, H.; Miyamoto, D.; Umeda, Y.; Hamaguchi, H.; Suzuki, M.; Tanimoto, T.; Harigai, T.; Takikawa, H.; Suda, Y. Catalytic Activity of Several Carbons with Different Structures for Methane Decomposition and By-Produced Carbons. *Appl. Surf. Sci.* **2019**, *473*, 291–297.
- (51) Łukaitis, R.; Hołowacz, I.; Kucharska, K.; Glinka, M.; Rybarczyk, P.; Przyjazny, A.; Kamiński, M. Hydrogen Production from Biomass Using Dark Fermentation. *Renewable Sustainable Energy Rev.* **2018**, *91*, 665–694.

- (52) Habib, M. A.; Harale, A.; Paglieri, S.; Alrashed, F. S.; Al-Sayoud, A.; Rao, M. V.; Nemitallah, M. A.; Hossain, S.; Hussien, M.; Ali, A.; Haque, M. A.; Abuelyamen, A.; Shakeel, M. R.; Mokheimer, E. M. A.; Ben-Mansour, R. Palladium-Alloy Membrane Reactors for Fuel Reforming and Hydrogen Production: A Review. *Energy Fuels* **2021**, *35* (7), 5558–5593.
- (53) Pinzón, M.; Sánchez, P.; de la Osa, A. R.; Romero, A.; de Lucas-Consuegra, A. Recent Insights into Low-Surface-Area Catalysts for Hydrogen Production from Ammonia. *Energies* **2022**, *15* (21), 8143.
- (54) Bac, S.; Keskin, S.; Avci, A. K. Recent Advances in Materials for High Purity H<sub>2</sub> Production by Ethanol and Glycerol Steam Reforming. *Int. J. Hydrogen Energy* **2020**, *45* (60), 34888–34917.
- (55) Yu, J.; Li, X.; Wu, Q.; Wang, H.; Liu, Y.; Huang, H.; Liu, Y.; Shao, M.; Fan, J.; Li, H.; Kang, Z. Effective Low-Temperature Methanol Aqueous Phase Reforming with Metal-Free Carbon Dots/C<sub>3</sub>N<sub>4</sub> Composites. *ACS Appl. Mater. Interfaces* **2021**, *13* (21), 24702–24709.
- (56) Byrd, A. J.; Pant, K. K.; Gupta, R. B. Hydrogen Production from Ethanol by Reforming in Supercritical Water Using Ru/Al<sub>2</sub>O<sub>3</sub> Catalyst. *Energy Fuels* **2007**, *21* (6), 3541–3547.
- (57) Qureshi, F.; Yusuf, M.; Pasha, A. A.; Khan, H. W.; Imteyaz, B.; Irshad, K. Sustainable and Energy Efficient Hydrogen Production via Glycerol Reforming Techniques: A Review. *Int. J. Hydrogen Energy* **2022**, *47* (98), 41397–41420.
- (58) Adhikari, S.; Fernando, S. D.; To, S. D. F.; Bricka, R. M.; Steele, P. H.; Haryanto, A. Conversion of Glycerol to Hydrogen via a Steam Reforming Process over Nickel Catalysts. *Energy Fuels* **2008**, *22* (2), 1220–1226.
- (59) Guo, Y.; Liu, X.; Wang, Y. Catalytic and DRIFTS Studies of Pt-Based Bimetallic Alloy Catalysts in Aqueous-Phase Reforming of Glycerol. *Ind. Eng. Chem. Res.* **2019**, *58* (8), 2749–2758.
- (60) Li, J.; Yu, H.; Yang, G.; Peng, F.; Xie, D.; Wang, H.; Yang, J. Steam Reforming of Oxygenate Fuels for Hydrogen Production: A Thermodynamic Study. *Energy Fuels* **2011**, *25* (6), 2643–2650.
- (61) Schmidt, I.; Müller, K.; Arlt, W. Evaluation of Formic-Acid-Based Hydrogen Storage Technologies. *Energy Fuels* **2014**, *28* (10), 6540–6544.
- (62) Sordakis, K.; Dalebrook, A. F.; Laurenczy, G. A Viable Hydrogen Storage and Release System Based on Cesium Formate and Bicarbonate Salts: Mechanistic Insights into the Hydrogen Release Step. *ChemCatChem* **2015**, *7* (15), 2332–2339.
- (63) Müller, K.; Brooks, K.; Autrey, T. Hydrogen Storage in Formic Acid: A Comparison of Process Options. *Energy Fuels* **2017**, *31* (11), 12603–12611.
- (64) Tanksale, A.; Beltramini, J. N.; Lu, G. Q. M. A Review of Catalytic Hydrogen Production Processes from Biomass. *Renewable Sustainable Energy Rev.* **2010**, *14* (1), 166–182.
- (65) Mandal, S.; Daggupati, S.; Majhi, S.; Thakur, S.; Bandyopadhyay, R.; Das, A. K. Catalytic Gasification of Biomass in Dual-Bed Gasifier for Producing Tar-Free Syngas. *Energy Fuels* **2019**, *33* (3), 2453–2466.
- (66) Perego, C.; Bosetti, A.; Ricci, M.; Millini, R. Zeolite Materials for Biomass Conversion to Biofuel. *Energy Fuels* **2017**, *31* (8), 7721–7733.
- (67) Grams, J.; Ryczkowski, R.; Sadek, R.; Chalupka, K.; Przybysz, K.; Casale, S.; Dzwigaj, S. Hydrogen-Rich Gas Production by Upgrading of Biomass Pyrolysis Vapors over Nibeia Catalyst: Impact of Dealumination and Preparation Method. *Energy Fuels* **2020**, *34* (12), 16936–16947.
- (68) Jara-Cobos, L.; Abril-González, M.; Pinos-Vélez, V. Production of Hydrogen from Lignocellulosic Biomass: A Review of Technologies. *Catalysts* **2023**, *13* (4), 766.
- (69) Lu, M.; Xiong, Z.; Lv, P.; Yuan, Z.; Guo, H.; Chen, Y. Catalytic Purification of Raw Gas from Biomass Gasification on Mo-Ni-Co/Cordierite Monolithic Catalyst. *Energy Fuels* **2013**, *27* (4), 2099–2106.
- (70) Rajagopal, J.; Gopinath, K. P.; Neha, R.; Aakriti, K.; Jayaraman, R. S.; Arun, J.; Pugazhendhi, A. Processing of Household Waste via Hydrothermal Gasification and Hydrothermal Liquefaction for Bio-Oil and Bio-Hydrogen Production: Comparison with RSM Studies. *J. Environ. Chem. Eng.* **2022**, *10* (2), 107218.
- (71) Ahmed, M.; Dincer, I. A Review on Photoelectrochemical Hydrogen Production Systems: Challenges and Future Directions. *Int. J. Hydrogen Energy* **2019**, *44* (5), 2474–2507.
- (72) Esposito, D. V.; Hunt, S. T.; Kimmel, Y. C.; Chen, J. G. A New Class of Electrocatalysts for Hydrogen Production from Water Electrolysis: Metal Monolayers Supported on Low-Cost Transition Metal Carbides. *J. Am. Chem. Soc.* **2012**, *134* (6), 3025–3033.
- (73) Li, N.; Liu, X.; Li, G. D.; Wu, Y.; Gao, R.; Zou, X. Vertically Grown CoS Nanosheets on Carbon Cloth as Efficient Hydrogen Evolution Electrocatalysts. *Int. J. Hydrogen Energy* **2017**, *42* (15), 9914–9921.
- (74) Chen, P.; Xu, K.; Fang, Z.; Tong, Y.; Wu, J.; Lu, X.; Peng, X.; Ding, H.; Wu, C.; Xie, Y. Metallic Co<sub>4</sub>N Porous Nanowire Arrays Activated by Surface Oxidation as Electrocatalysts for the Oxygen Evolution Reaction. *Angew. Chem.* **2015**, *127* (49), 14923–14927.
- (75) Kumar, M.; Meena, B.; Subramanyam, P.; Suryakala, D.; Subrahmanyam, C. Recent Trends in Photoelectrochemical Water Splitting: The Role of Cocatalysts. *NPG Asia Mater.* **2022**, *14*, 88.
- (76) Kim, J. H.; Han, S.; Jo, Y. H.; Bak, Y.; Lee, J. S. A Precious Metal-Free Solar Water Splitting Cell with a Bifunctional Cobalt Phosphide Electrocatalyst and Doubly Promoted Bismuth Vanadate Photoanode. *J. Mater. Chem. A* **2018**, *6* (3), 1266–1274.
- (77) Rafique, M.; Hajra, S.; Irshad, M.; Usman, M.; Imran, M.; Assiri, M. A.; Ashraf, W. M. Hydrogen Production Using TiO<sub>2</sub>-Based Photocatalysts: A Comprehensive Review. *ACS Omega* **2023**, *8* (29), 25640–25648.
- (78) Beyene, B. B.; Hung, C. H. Recent Progress on Metalloporphyrin-Based Hydrogen Evolution Catalysis. *Coord. Chem. Rev.* **2020**, *410*, 213234.
- (79) Song, T.; Xie, C.; Matras-Postolek, K.; Yang, P. 2D Layered g-C<sub>3</sub>N<sub>4</sub>/WO<sub>3</sub>/WS<sub>2</sub> S-Scheme Heterojunctions with Enhanced Photocatalytic Performance. *J. Phys. Chem. C* **2021**, *125* (35), 19382–19393.
- (80) Ghiasian, M. Biophotolysis-Based Hydrogen Production by Cyanobacteria. In *Prospects of Renewable Bioprocessing in Future Energy Systems*; Rastegari, A. A., Yadav, A. N., Gupta, A., Eds.; Springer International Publishing: Cham, Switzerland, 2019; Vol. 10, pp 161–184, DOI: [10.1007/978-3-030-14463-0\\_5](https://doi.org/10.1007/978-3-030-14463-0_5).
- (81) Ghirardi, M. L.; King, P. W.; Mulder, D. W.; Eckert, C.; Dubini, A.; Maness, P.-C.; Yu, J. Hydrogen Production by Water Biophotolysis. In *Microbial BioEnergy: Hydrogen Production*; Zannoni, D., De Philippis, R., Eds.; Springer: Dordrecht, Netherlands, 2014; Vol. 38, pp 101–135, DOI: [10.1007/978-94-017-8554-9\\_5](https://doi.org/10.1007/978-94-017-8554-9_5).
- (82) Tamburic, B.; Zemichael, F. W.; Maitland, G. C.; Hellgardt, K. A Novel Nutrient Control Method to Deprive Green Algae of Sulphur and Initiate Spontaneous Hydrogen Production. *Int. J. Hydrogen Energy* **2012**, *37* (11), 8988–9001.
- (83) Eroglu, E.; Melis, A. Photobiological Hydrogen Production: Recent Advances and State of the Art. *Bioresour. Technol.* **2011**, *102* (18), 8403–8413.
- (84) Ban, S.; Lin, W.; Luo, Z.; Luo, J. Improving Hydrogen Production of *Chlamydomonas Reinhardtii* by Reducing Chlorophyll Content via Atmospheric and Room Temperature Plasma. *Bioresour. Technol.* **2019**, *275*, 425–429.
- (85) Steinbeck, J.; Nikolova, D.; Weingarten, R.; Johnson, X.; Richaud, P.; Peltier, G.; Hermann, M.; Magneschi, L.; Hippler, M. Deletion of Proton Gradient Regulation 5 (PGRS) and PGRS-Like 1 (PGRL1) Proteins Promote Sustainable Light-Driven Hydrogen Production in *Chlamydomonas Reinhardtii* Due to Increased PSII Activity under Sulfur Deprivation. *Front. Plant Sci.* **2015**, *6*, 892.
- (86) Chen, M.; Liu, P.; Zhang, J.; Peng, L.; Huang, F. Photochemical Characteristics of *Chlamydomonas* Mutant Hpm91 Lacking Proton Gradient Regulation 5 (PGRS) during Sustained H<sub>2</sub> Photoproduction under Sulfur Deprivation. *Int. J. Hydrogen Energy* **2019**, *44* (60), 31790–31799.

- (87) Kim, S.; Lu, D.; Park, S.; Wang, G. Production of Hydrogenases as Biocatalysts. *Int. J. Hydrogen Energy* **2012**, *37* (20), 15833–15840.
- (88) Hambourger, M.; Gervaldo, M.; Svedruzic, D.; King, P. W.; Gust, D.; Ghirardi, M.; Moore, A. L.; Moore, T. A. [FeFe]-Hydrogenase-Catalyzed H<sub>2</sub> Production in a Photoelectrochemical Biofuel Cell. *J. Am. Chem. Soc.* **2008**, *130* (6), 2015–2022.
- (89) Vincent, K. A.; Cracknell, J. A.; Lenz, O.; Zebger, I.; Friedrich, B.; Armstrong, F. A. Electrocatalytic Hydrogen Oxidation by an Enzyme at High Carbon Monoxide or Oxygen Levels. *Proc. Natl. Acad. Sci. U. S. A.* **2005**, *102*, 16951–16954.
- (90) Honda, Y.; Hagiwara, H.; Ida, S.; Ishihara, T. Application to Photocatalytic H<sub>2</sub> Production of a Whole-Cell Reaction by Recombinant Escherichia Coli Cells Expressing [FeFe]-Hydrogenase and Maturases Genes. *Angew. Chem.* **2016**, *128* (28), 8177–8180.
- (91) Honda, Y.; Watanabe, M.; Hagiwara, H.; Ida, S.; Ishihara, T. Inorganic/Whole-Cell Biohybrid Photocatalyst for Highly Efficient Hydrogen Production from Water. *Appl. Catal., B* **2017**, *210*, 400–406.
- (92) Lansing, J. C.; Camara, J. M.; Gray, D. E.; Rauchfuss, T. B. Hydrogen Production Catalyzed by Bidirectional, Biomimetic Models of the [FeFe]-Hydrogenase Active Site. *Organometallics* **2014**, *33* (20), 5897–5906.
- (93) Italiano, G.; Espiro, C.; Arena, F.; Parmaliana, A.; Frusteri, F. Doped Ni Thin Layer Catalysts for Catalytic Decomposition of Natural Gas to Produce Hydrogen. *Appl. Catal., A* **2009**, *365* (1), 122–129.
- (94) Palmer, C.; Tarazkar, M.; Kristoffersen, H. H.; Gelinas, J.; Gordon, M. J.; McFarland, E. W.; Metiu, H. Methane Pyrolysis with a Molten Cu-Bi Alloy Catalyst. *ACS Catal.* **2019**, *9* (9), 8337–8345.
- (95) Lua, A. C.; Wang, H. Y. Hydrogen Production by Catalytic Decomposition of Methane over Ni-Cu-Co Alloy Particles. *Appl. Catal., B* **2014**, *156–157*, 84–93.
- (96) Hu, X. C.; Wang, W. W.; Jin, Z.; Wang, X.; Si, R.; Jia, C. J. Transition Metal Nanoparticles Supported La-Promoted MgO as Catalysts for Hydrogen Production via Catalytic Decomposition of Ammonia. *J. Energy Chem.* **2019**, *38*, 41–49.
- (97) Lucentini, I.; García Colli, G.; Luzi, C. D.; Serrano, I.; Martínez, O. M.; Llorca, J. Catalytic Ammonia Decomposition over Ni-Ru Supported on CeO<sub>2</sub> for Hydrogen Production: Effect of Metal Loading and Kinetic Analysis. *Appl. Catal., B* **2021**, *286*, 119896.
- (98) Zhang, B.; Tang, X.; Li, Y.; Xu, Y.; Shen, W. Hydrogen Production from Steam Reforming of Ethanol and Glycerol over Ceria-Supported Metal Catalysts. *Int. J. Hydrogen Energy* **2007**, *32* (13), 2367–2373.
- (99) Lin, L.; Yu, Q.; Peng, M.; Li, A.; Yao, S.; Tian, S.; Liu, X.; Li, A.; Jiang, Z.; Gao, R.; Han, X.; Li, Y. W.; Wen, X. D.; Zhou, W.; Ma, D. Atomically Dispersed Ni/α-MoC Catalyst for Hydrogen Production from Methanol/Water. *J. Am. Chem. Soc.* **2021**, *143* (1), 309–317.
- (100) Yang, Y.; Xu, H.; Cao, D.; Zeng, X. C.; Cheng, D. Hydrogen Production via Efficient Formic Acid Decomposition: Engineering the Surface Structure of Pd-Based Alloy Catalysts by Design. *ACS Catal.* **2019**, *9* (1), 781–790.
- (101) Qin, X.; Li, H.; Xie, S.; Li, K.; Jiang, T.; Ma, X.-Y.; Jiang, K.; Zhang, Q.; Terasaki, O.; Wu, Z.; Cai, W.-B. Mechanistic Analysis-Guided Pd-Based Catalysts for Efficient Hydrogen Production from Formic Acid Dehydrogenation. *ACS Catal.* **2020**, *10* (6), 3921–3932.
- (102) Zhang, Z.; Ou, Z.; Qin, C.; Ran, J.; Wu, C. Roles of Alkali/Alkaline Earth Metals in Steam Reforming of Biomass Tar for Hydrogen Production over Perovskite Supported Ni Catalysts. *Fuel* **2019**, *257*, 116032.
- (103) Tarifa, P.; Ramirez Reina, T.; González-Castaño, M.; Arellano-García, H. Catalytic Upgrading of Biomass-Gasification Mixtures Using Ni-Fe/MgAl<sub>2</sub>O<sub>4</sub> as a Bifunctional Catalyst. *Energy Fuels* **2022**, *36* (15), 8267–8273.
- (104) Meng, S.; Li, W.; Li, Z.; Song, H. Recent Progress of the Transition Metal-Based Catalysts in the Catalytic Biomass Gasification: A Mini-Review. *Fuel* **2023**, *353*, 129169.
- (105) Losse, S.; Vos, J. G.; Rau, S. Catalytic Hydrogen Production at Cobalt Centres. *Coord. Chem. Rev.* **2010**, *254* (21–22), 2492–2504.
- (106) Wang, C. L.; Liu, W. X.; Zhan, S. Z. A Cobalt Complex of Bis(Methylthioether)Pyridine, a New Catalyst for Hydrogen Evolution. *Polyhedron* **2020**, *192*, 114863.
- (107) Jin, H.; Liu, X.; Chen, S.; Vasileff, A.; Li, L.; Jiao, Y.; Song, L.; Zheng, Y.; Qiao, S. Z. Heteroatom-Doped Transition Metal Electrocatalysts for Hydrogen Evolution Reaction. *ACS Energy Lett.* **2019**, *4* (4), 805–810.
- (108) King, R. L.; Botte, G. G. Investigation of Multi-Metal Catalysts for Stable Hydrogen Production via Urea Electrolysis. *J. Power Sources* **2011**, *196* (22), 9579–9584.
- (109) Ahmad, I.; Shukrullah, S.; Naz, M. Y.; Ahmed, E.; Ahmad, M. Rare Earth Metals Co-Doped ZnO/CNTs Composite as High Performance Photocatalyst for Hydrogen Production from Water-triethanolamine Mixture. *Int. J. Hydrogen Energy* **2022**, *47* (15), 9283–9294.
- (110) Lamb, K. E.; Dolan, M. D.; Kennedy, D. F. Ammonia for Hydrogen Storage: A Review of Catalytic Ammonia Decomposition and Hydrogen Separation and Purification. *Int. J. Hydrogen Energy* **2019**, *44* (7), 3580–3593.
- (111) Contreras, J. L.; Salernes, J.; Colín-Luna, J. A.; Nuño, L.; Quintana, B.; Córdova, I.; Zeifert, B.; Tapia, C.; Fuentes, G. A. Catalysts for H<sub>2</sub> Production Using the Ethanol Steam Reforming (a Review). *Int. J. Hydrogen Energy* **2014**, *39* (33), 18835–18853.
- (112) Li, R.; Li, Y.; Yang, P.; Wang, D.; Xu, H.; Wang, B.; Meng, F.; Zhang, J.; An, M. Electrodeposition: Synthesis of Advanced Transition Metal-Based Catalyst for Hydrogen Production via Electrolysis of Water. *J. Energy Chem.* **2021**, *57*, 547–566.
- (113) Yang, Q.; Dong, L.; Su, R.; Hu, B.; Wang, Z.; Jin, Y.; Wang, Y.; Besenbacher, F.; Dong, M. Nanostructured Heterogeneous Photo-Catalysts for Hydrogen Production and Water Splitting: A Comprehensive Insight. *Appl. Mater. Today* **2019**, *17*, 159–182.
- (114) Shen, Y.; Lua, A. C. Sol-Gel Synthesis of Ni and Ni Supported Catalysts for Hydrogen Production by Methane Decomposition. *RSC Adv.* **2014**, *4* (79), 42159–42167.
- (115) Sima, D.; Wu, H.; Tian, K.; Xie, S.; Foo, J. J.; Li, S.; Wang, D.; Ye, Y.; Zheng, Z.; Liu, Y. Q. Enhanced Low Temperature Catalytic Activity of Ni/Al-Ce<sub>0.8</sub>Zr<sub>0.2</sub>O<sub>2</sub> for Hydrogen Production from Ammonia Decomposition. *Int. J. Hydrogen Energy* **2020**, *45* (16), 9342–9352.
- (116) Shanmugam, V.; Neuberg, S.; Zapf, R.; Pennemann, H.; Kolb, G. Hydrogen Production over Highly Active Pt Based Catalyst Coatings by Steam Reforming of Methanol: Effect of Support and Co-Support. *Int. J. Hydrogen Energy* **2020**, *45* (3), 1658–1670.
- (117) Wang, C.; Cai, X.; Chen, Y.; Cheng, Z.; Luo, X.; Mo, S.; Jia, L.; Lin, P.; Yang, Z. Improved Hydrogen Production from Glycerol Photoreforming over Sol-Gel Derived TiO<sub>2</sub> Coupled with Metal Oxides. *Chem. Eng. J.* **2017**, *317*, 522–532.
- (118) Deligiannakis, Y.; Tsikourkitoudi, V.; Stathi, P.; Wegner, K.; Papavasiliou, J.; Louloudi, M. PdO/Pd<sup>0</sup>/TiO<sub>2</sub> Nanocatalysts Engineered by Flame Spray Pyrolysis: Study of the Synergy of PdO/Pd<sup>0</sup> on H<sub>2</sub> Production by HCOOH Dehydrogenation and the Deactivation Mechanism. *Energy Fuels* **2020**, *34* (11), 15026–15038.
- (119) Lu, Y.; Jin, H.; Zhang, R. Evaluation of Stability and Catalytic Activity of Ni Catalysts for Hydrogen Production by Biomass Gasification in Supercritical Water. *Carbon Resour. Convers.* **2019**, *2* (1), 95–101.
- (120) Yang, L.; Zhou, H.; Qin, X.; Guo, X.; Cui, G.; Asiri, A. M.; Sun, X. Cathodic Electrochemical Activation of Co<sub>3</sub>O<sub>4</sub> Nanoarrays: A Smart Strategy to Significantly Boost the Hydrogen Evolution Activity. *Chem. Commun.* **2018**, *54* (17), 2150–2153.
- (121) Wang, T.; Zeng, Y.; Xu, M.; Zhang, J.; Wu, S.; Mu, S.; Yu, J. Effect of B-Doping and Manifestation on TiO<sub>2</sub>-Supported IrO<sub>2</sub> for Oxygen Evolution Reaction in Water Electrolysis. *Langmuir* **2023**, *39* (11), 4005–4014.
- (122) Samsudin, M. F. R.; Sufian, S.; Mohamed, N. M.; Bashiri, R.; Wolfe, F.; Ramli, R. M. Enhancement of Hydrogen Production over Screen-Printed TiO<sub>2</sub>/BiVO<sub>4</sub> Thin Film in the Photoelectrochemical Cells. *Mater. Lett.* **2018**, *211*, 13–16.

- (123) Maity, D.; Karmakar, K.; Pal, D.; Saha, S.; Khan, G. G.; Mandal, K. One-Dimensional p-ZnCo<sub>2</sub>O<sub>4</sub>/n-ZnO Nanoheterojunction Photoanode Enabling Photoelectrochemical Water Splitting. *ACS Appl. Energy Mater.* **2021**, *4* (10), 11599–11608.
- (124) Chen, D.; Xie, Z.; Tong, Y.; Huang, Y. Review on BiVO<sub>4</sub>-Based Photoanodes for Photoelectrochemical Water Oxidation: The Main Influencing Factors. *Energy Fuels* **2022**, *36* (17), 9932–9949.
- (125) Tayebi, M.; Lee, B. K. Recent Advances in BiVO<sub>4</sub> Semiconductor Materials for Hydrogen Production Using Photoelectrochemical Water Splitting. *Renewable Sustainable Energy Rev.* **2019**, *111*, 332–343.
- (126) Sudha, D.; Sivakumar, P. Review on the Photocatalytic Activity of Various Composite Catalysts. *Chem. Eng. Process.* **2015**, *97*, 112–133.
- (127) Podporska-Carroll, J.; Myles, A.; Quilty, B.; McCormack, D. E.; Fagan, R.; Hinder, S. J.; Dionysiou, D. D.; Pillai, S. C. Antibacterial Properties of F-Doped ZnO Visible Light Photocatalyst. *J. Hazard. Mater.* **2017**, *324*, 39–47.
- (128) Moezzi, A.; McDonagh, A. M.; Cortie, M. B. Zinc Oxide Particles: Synthesis, Properties and Applications. *Chem. Eng. J.* **2012**, *185–186*, 1–22.
- (129) Baig, U.; Khan, A.; Gondal, M. A.; Dastageer, M. A.; Akhtar, S. Single-Step Synthesis of Silicon Carbide Anchored Graphitic Carbon Nitride Nanocomposite Photo-Catalyst for Efficient Photoelectrochemical Water Splitting under Visible-Light Irradiation. *Colloids Surf., A* **2021**, *611*, 125886.
- (130) Kovalskii, A. M.; Matveev, A. T.; Popov, Z. I.; Volkov, I. N.; Sukhanova, E. V.; Lytkina, A. A.; Yaroslavtsev, A. B.; Konopatsky, A. S.; Leybo, D. V.; Bondarev, A. V.; Shchetinin, I. V.; Firestein, K. L.; Shtansky, D. V.; Golberg, D. V. (Ni, Cu)/Hexagonal BN Nano-hybrids—New Efficient Catalysts for Methanol Steam Reforming and Carbon Monoxide Oxidation. *Chem. Eng. J.* **2020**, *395*, 125109.
- (131) Chen, H.; Wang, P.; Wang, X.; Wang, X.; Rao, L.; Qian, Y.; Yin, H.; Hou, X.; Ye, H.; Zhou, G.; Nötzel, R. 3D InGaN Nanowire Arrays on Oblique Pyramid-Textured Si (311) for Light Trapping and Solar Water Splitting Enhancement. *Nano Energy* **2021**, *83*, 105768.
- (132) McConnachie, M.; Sheil, A.; Konarova, M.; Smart, S. Evaluation of Heterogeneous Metal-Sulfide Molten Salt Slurry Systems for Hydrogen Production through Methane Pyrolysis. *Int. J. Hydrogen Energy* **2024**, *49*, 981–991.
- (133) Wu, Q.; Huang, Y.; Yu, J. Cobalt Phosphide Nanoparticles Supported by Vertically Grown Graphene Sheets on Carbon Black with N-Doping Treatment as Bifunctional Electrocatalysts for Overall Water Splitting. *Energy Fuels* **2023**, *37* (23), 19156–19165.
- (134) Vrubel, H.; Hu, X. Molybdenum Boride and Carbide Catalyze Hydrogen Evolution in Both Acidic and Basic Solutions. *Angew. Chem., Int. Ed.* **2012**, *51* (51), 12703–12706.
- (135) Rekha, P.; Yadav, S.; Singh, L. A Review on Cobalt Phosphate-Based Materials as Emerging Catalysts for Water Splitting. *Ceram. Int.* **2021**, *47* (12), 16385–16401.
- (136) Sankar, S. S.; Rathishkumar, A.; Geetha, K.; Kundu, S. A Simple Route for the Synthesis of Cobalt Phosphate Nanoparticles for Electrocatalytic Water Oxidation in Alkaline Medium. *Energy Fuels* **2020**, *34* (10), 12891–12899.
- (137) Feng, S.; Yu, Y.; Li, J.; Luo, J.; Deng, P.; Jia, C.; Shen, Y.; Tian, X. Recent Progress in Seawater Electrolysis for Hydrogen Evolution by Transition Metal Phosphides. *Catal. Commun.* **2022**, *162*, 106382.
- (138) Wu, L.; Yu, L.; Zhang, F.; McElhenny, B.; Luo, D.; Karim, A.; Chen, S.; Ren, Z. Heterogeneous Bimetallic Phosphide Ni<sub>2</sub>P-Fe<sub>2</sub>P as an Efficient Bifunctional Catalyst for Water/Seawater Splitting. *Adv. Funct. Mater.* **2021**, *31* (1), 2006484.
- (139) Ke, S. C.; Chen, R.; Chen, G. H.; Ma, X. L. Mini Review on Electrocatalyst Design for Seawater Splitting: Recent Progress and Perspectives. *Energy Fuels* **2021**, *35* (16), 12948–12956.
- (140) Chen, R.; Zhen, C.; Yang, Y.; Sun, X.; Irvine, J. T.; Wang, L.; Liu, G.; Cheng, H. M. Boosting Photoelectrochemical Water Splitting Performance of Ta<sub>2</sub>N<sub>5</sub> Nanorod Array Photoanodes by Forming a Dual Co-Catalyst Shell. *Nano Energy* **2019**, *59*, 683–688.
- (141) Maeda, K.; Domen, K. New Non-Oxide Photocatalysts Designed for Overall Water Splitting under Visible Light. *J. Phys. Chem. C* **2007**, *111* (22), 7851–7861.
- (142) Wang, Q.; Domen, K. Particulate Photocatalysts for Light-Driven Water Splitting: Mechanisms, Challenges, and Design Strategies. *Chem. Rev.* **2020**, *120* (2), 919–985.
- (143) Iwase, A.; Yoshino, S.; Takayama, T.; Ng, Y. H.; Amal, R.; Kudo, A. Water Splitting and CO<sub>2</sub> Reduction under Visible Light Irradiation Using Z-Scheme Systems Consisting of Metal Sulfides, CoOx-Loaded BiVO<sub>4</sub>, and a Reduced Graphene Oxide Electron Mediator. *J. Am. Chem. Soc.* **2016**, *138* (32), 10260–10264.
- (144) Chatterjee, K.; Dos Reis, R.; Harada, J. K.; Mathiesen, J. K.; Bueno, S. L. A.; Jensen, K. M. Ø.; Rondinelli, J. M.; Dravid, V.; Skrabalak, S. E. Durable Multimetal Oxychloride Intergrowths for Visible Light-Driven Water Splitting. *Chem. Mater.* **2021**, *33* (1), 347–358.
- (145) Yu, P.; Guo, J.; Liu, L.; Wang, P.; Wu, G.; Chang, F.; Chen, P. Ammonia Decomposition with Manganese Nitride-Calcium Imide Composites as Efficient Catalysts. *ChemSusChem* **2016**, *9* (4), 364–369.
- (146) Li, Q.; Lu, Q.; Guo, E.; Wei, M.; Pang, Y. Hierarchical Co<sub>9</sub>S<sub>8</sub>/ZnIn<sub>2</sub>S<sub>4</sub>Nanoflower Enables Enhanced Hydrogen Evolution Photocatalysis. *Energy Fuels* **2022**, *36* (8), 4541–4548.
- (147) Zhang, J.; Yao, W.; Huang, C.; Shi, P.; Xu, Q. High Efficiency and Stable Tungsten Phosphide Cocatalysts for Photocatalytic Hydrogen Production. *J. Mater. Chem. A* **2017**, *5* (24), 12513–12519.
- (148) Yang, Y.; Wang, M.; Zhang, P.; Wang, W.; Han, H.; Sun, L. Evident Enhancement of Photoelectrochemical Hydrogen Production by Electroless Deposition of M–B (M = Ni, Co) Catalysts on Silicon Nanowire Arrays. *ACS Appl. Mater. Interfaces* **2016**, *8* (44), 30143–30151.
- (149) Zhu, Q.; Qiu, B.; Du, M.; Xing, M.; Zhang, J. Nickel Boride Cocatalyst Boosting Efficient Photocatalytic Hydrogen Evolution Reaction. *Ind. Eng. Chem. Res.* **2018**, *57* (24), 8125–8130.
- (150) Lin, J.; Wang, Y.; Tian, W.; Zhang, H.; Sun, H.; Wang, S. Macroporous Carbon-Nitride-Supported Transition-Metal Single-Atom Catalysts for Photocatalytic Hydrogen Production from Ammonia Splitting. *ACS Catal.* **2023**, *13* (17), 11711–11722.
- (151) Bulushev, D. A.; Zacharska, M.; Shlyakhova, E. V.; Chuvalin, A. L.; Guo, Y.; Beloshapkin, S.; Okotrub, A. V.; Bulusheva, L. G. Single Isolated Pd<sup>2+</sup> Cations Supported on N-Doped Carbon as Active Sites for Hydrogen Production from Formic Acid Decomposition. *ACS Catal.* **2016**, *6* (2), 681–691.
- (152) Lee, S. Y.; Kim, M. S.; Kwak, J. H.; Han, G. Y.; Park, J. H.; Lee, T. J.; Yoon, K. J. Catalytic Characteristics of Carbon Black for Decomposition of Ethane. *Carbon N. Y.* **2010**, *48* (7), 2030–2036.
- (153) Feng, L.; Feng, L.; Huang, J.; Cao, L.; Kajiyoshi, K. Ultrafine VN Nanoparticles Confined in Co@N-Doped Carbon Nanotubes for Boosted Hydrogen Evolution Reaction. *J. Alloys Compd.* **2021**, *853*, 157257.
- (154) Han, H.; Park, S.; Jang, D.; Kim, W. B. N-Doped Carbon Nanoweb-Supported Ni/NiO Heterostructure as Hybrid Catalysts for Hydrogen Evolution Reaction in an Alkaline Phase. *J. Alloys Compd.* **2021**, *853*, 157338.
- (155) Hou, T.; Yuan, L.; Ye, T.; Gong, L.; Tu, J.; Yamamoto, M.; Torimoto, Y.; Li, Q. Hydrogen Production by Low-Temperature Reforming of Organic Compounds in Bio-Oil over a CNT-Promoting Ni Catalyst. *Int. J. Hydrogen Energy* **2009**, *34* (22), 9095–9107.
- (156) Yu, X.; Hua, T.; Liu, X.; Yan, Z.; Xu, P.; Du, P. Nickel-Based Thin Film on Multiwalled Carbon Nanotubes as an Efficient Bifunctional Electrocatalyst for Water Splitting. *ACS Appl. Mater. Interfaces* **2014**, *6* (17), 15395–15402.
- (157) Islam, A.; Teo, S. H.; Awual, M. R.; Taufiq-Yap, Y. H. Improving the Hydrogen Production from Water over MgO Promoted Ni-Si/CNTs Photocatalyst. *J. Cleaner Prod.* **2019**, *238*, 117887.
- (158) Soltani, T.; Tayyebi, A.; Lee, B. K. Enhanced Photoelectrochemical (PEC) and Photocatalytic Properties of Visible-

- Light Reduced Graphene-Oxide/Bismuth Vanadate. *Appl. Surf. Sci.* **2018**, *448*, 465–473.
- (159) Kumar, S.; Reddy, N. L.; Kushwaha, H. S.; Kumar, A.; Shankar, M. V.; Bhattacharyya, K.; Halder, A.; Krishnan, V. Efficient Electron Transfer across a ZnO-MoS<sub>2</sub>-Reduced Graphene Oxide Heterojunction for Enhanced Sunlight-Driven Photocatalytic Hydrogen Evolution. *ChemSusChem* **2017**, *10* (18), 3588–3603.
- (160) Idris, M. B.; Devaraj, S. Mesoporous Graphitic Carbon Nitride Synthesized Using Biotemplate as a High-Performance Electrode Material for Supercapacitor and Electrocatalyst for Hydrogen Evolution Reaction in Acidic Medium. *J. Energy Storage* **2019**, *26*, 101032.
- (161) Mohamed, N. A.; Safaei, J.; Ismail, A. F.; Khalid, M. N.; Mohd Jailani, M. F. A.; Noh, M. F. M.; Arzaee, N. A.; Zhou, D.; Sagu, J. S.; Teridi, M. A. M. Boosting Photocatalytic Activities of BiVO<sub>4</sub> by Creation of g-C<sub>3</sub>N<sub>4</sub>/ZnO@BiVO<sub>4</sub> Heterojunction. *Mater. Res. Bull.* **2020**, *125*, 110779.
- (162) Harun, K.; Adhikari, S.; Jahromi, H. Hydrogen Production: Via Thermocatalytic Decomposition of Methane Using Carbon-Based Catalysts. *RSC Adv.* **2020**, *10* (67), 40882–40893.
- (163) Zhang, S.; Zhu, S.; Zhang, H.; Liu, X.; Xiong, Y. High Quality H<sub>2</sub>-Rich Syngas Production from Pyrolysis-Gasification of Biomass and Plastic Wastes by Ni-Fe@Nanofibers/Porous Carbon Catalyst. *Int. J. Hydrogen Energy* **2019**, *44* (48), 26193–26203.
- (164) Wang, H.; Xu, C.; Chen, Q.; Ming, M.; Wang, Y.; Sun, T.; Zhang, Y.; Gao, D.; Bi, J.; Fan, G. Nitrogen-Doped Carbon-Stabilized Ru Nanoclusters as Excellent Catalysts for Hydrogen Production. *ACS Sustainable Chem. Eng.* **2019**, *7* (1), 1178–1184.
- (165) Chu, D.; Yuan, X.; Qin, G.; Xu, M.; Zheng, P.; Lu, J.; Zha, L. Efficient Carbon-Doped Nanostructured TiO<sub>2</sub> (Anatase) Film for Photoelectrochemical Solar Cells. *J. Nanopart. Res.* **2008**, *10* (2), 357–363.
- (166) Nagappan, S.; Dhandapani, H. N.; Karmakar, A.; Kundu, S. Recent Advancement of 2D Bi-Metallic Hydroxides with Various Strategical Modification for the Sustainable Hydrogen Production through Water Electrolysis. *ES Mater. Manuf.* **2023**, *19*, 830.
- (167) Xu, W.; Thapa, K. B.; Ju, Q.; Fang, Z.; Huang, W. Heterogeneous Catalysts Based on Mesoporous Metal–Organic Frameworks. *Coord. Chem. Rev.* **2018**, *373*, 199–232.
- (168) Meera, M. S.; Hossain, A.; Shafna, M. A.; Vaishnavi, A. K. L.; Anil, A.; Asif, A.; Henaish, A. M. A.; Shibli, S. M. A. Tuning and Sustainment of High Surface Area of Nano CeO<sub>2</sub>-Anchored NiMOF Flake Heterojunctions for Efficient Photocatalytic Hydrogen Generation. *Energy Fuels* **2023**, *37* (17), 13011–13024.
- (169) Cui, L.; Zhao, D.; Yang, Y.; Wang, Y.; Zhang, X. Synthesis of Highly Efficient  $\alpha$ -Fe<sub>2</sub>O<sub>3</sub> Catalysts for CO Oxidation Derived from MIL-100(Fe). *J. Solid State Chem.* **2017**, *247*, 168–172.
- (170) Yao, Q.; DiNg, Y.; Lu, Z. H. Noble-Metal-Free Nanocatalysts for Hydrogen Generation from Boron- And Nitrogen-Based Hydrides. *Inorg. Chem. Front.* **2020**, *7*, 3837–3874.
- (171) Liang, T. Y.; Senthil Raja, D.; Chin, K. C.; Huang, C. L.; Sethupathi, S. A.; Leong, L. K.; Tsai, D. H.; Lu, S. Y. Bimetallic Metal–Organic Framework-Derived Hybrid Nanostructures as High-Performance Catalysts for Methane Dry Reforming. *ACS Appl. Mater. Interfaces* **2020**, *12* (13), 15183–15193.
- (172) Rossin, A.; Tuci, G.; Luconi, L.; Giambastiani, G. Metal–Organic Frameworks as Heterogeneous Catalysts in Hydrogen Production from Lightweight Inorganic Hydrides. *ACS Catal.* **2017**, *7* (8), 5035–5045.
- (173) Kamyar, N.; Khani, Y.; Amini, M. M.; Bahadoran, F.; Safari, N. Copper-Based Catalysts over AS20-MOF Derived Aluminum Spinels for Hydrogen Production by Methanol Steam Reforming: The Role of Spinal Support on the Performance. *Int. J. Hydrogen Energy* **2020**, *45* (41), 21341–21353.
- (174) Nagakawa, H.; Nagata, M. Highly Efficient Hydrogen Production in the Photoreforming of Lignocellulosic Biomass Catalyzed by Cu,In-Doped ZnS Derived from ZIF-8. *Adv. Mater. Interfaces* **2022**, *9* (2), 2101581.
- (175) Ao, K.; Wei, Q.; Daoud, W. A. MOF-Derived Sulfide-Based Electrocatalyst and Scaffold for Boosted Hydrogen Production. *ACS Appl. Mater. Interfaces* **2020**, *12* (30), 33595–33602.
- (176) Ali, M.; Pervaiz, E.; Noor, T.; Rabi, O.; Zahra, R.; Yang, M. Recent Advancements in MOF-Based Catalysts for Applications in Electrochemical and Photoelectrochemical Water Splitting: A Review. *Int. J. Energy Res.* **2021**, *45* (2), 1190–1226.
- (177) Liu, S.; Zhang, C.; Sun, Y.; Chen, Q.; He, L.; Zhang, K.; Zhang, J.; Liu, B.; Chen, L. F. Design of Metal–Organic Framework-Based Photocatalysts for Hydrogen Generation. *Coord. Chem. Rev.* **2020**, *413*, 213266.
- (178) Kampouri, S.; Ebrahim, F. M.; Fumanal, M.; Nord, M.; Schouwink, P. A.; Elzein, R.; Addou, R.; Herman, G. S.; Smit, B.; Ireland, C. P.; Stylianou, K. C. Enhanced Visible-Light-Driven Hydrogen Production through MOF/MOF Heterojunctions. *ACS Appl. Mater. Interfaces* **2021**, *13* (12), 14239–14247.
- (179) Morshed, A. S.; Abd El Salam, H. M.; El Naggar, A. M. A.; Zaki, T. Hydrogen Production and in Situ Storage through Process of Water Splitting Using Mono/Binary Metal–Organic Framework (MOF) Structures as New Chief Photocatalysts. *Energy Fuels* **2020**, *34* (9), 11660–11669.
- (180) Yang, H.; Yang, C.; Zhang, N.; Mo, K.; Li, Q.; Lv, K.; Fan, J.; Wen, L. Drastic Promotion of the Photoreactivity of MOF Ultrathin Nanosheets towards Hydrogen Production by Deposition with CdS Nanorods. *Appl. Catal., B* **2021**, *285*, 119801.
- (181) Horiuchi, Y.; Toyao, T.; Saito, M.; Mochizuki, K.; Iwata, M.; Higashimura, H.; Anpo, M.; Matsuoka, M. Visible-Light-Promoted Photocatalytic Hydrogen Production by Using an Amino-Functionalyzed Ti(IV) Metal–Organic Framework. *J. Phys. Chem. C* **2012**, *116* (39), 20848–20853.
- (182) Gao, X.; Wen, Y.; Tan, R.; Huang, H.; Kawi, S. A Review of Catalyst Modifications for a Highly Active and Stable Hydrogen Production from Methane. *Int. J. Hydrogen Energy* **2023**, *48* (16), 6204–6232.
- (183) Catalan, L. J. J.; Rezaei, E. Modelling the Hydrodynamics and Kinetics of Methane Decomposition in Catalytic Liquid Metal Bubble Reactors for Hydrogen Production. *Int. J. Hydrogen Energy* **2022**, *47* (12), 7547–7568.
- (184) Yin, H.; Yip, A. C. K. A Review on the Production and Purification of Biomass-Derived Hydrogen Using Emerging Membrane Technologies. *Catalysts* **2017**, *7* (10), 297.
- (185) Zhang, F.; Wang, Q. Redox-Mediated Water Splitting for Decoupled H<sub>2</sub> Production. *ACS Mater. Lett.* **2021**, *3* (5), 641–651.
- (186) Srinivasan, N.; Sakai, E.; Miyachi, M. Balanced Excitation between Two Semiconductors in Bulk Heterojunction Z-Scheme System for Overall Water Splitting. *ACS Catal.* **2016**, *6* (4), 2197–2200.
- (187) Chozhavendhan, S.; Rajamehala, M.; Karthigadevi, G.; Praveen Kumar, R.; Bharathiraja, B. A Review on Feedstock, Pretreatment Methods, Influencing Factors, Production and Purification Processes of Bio-Hydrogen Production. *Case Stud. Chem. Environ. Eng.* **2020**, *2*, 100038.
- (188) Singla, S.; Shetti, N. P.; Basu, S.; Mondal, K.; Aminabhavi, T. M. Hydrogen Production Technologies—Membrane Based Separation, Storage and Challenges. *J. Environ. Manage.* **2022**, *302*, 113963.
- (189) Barelli, L.; Bidini, G.; Gallorini, F.; Servili, S. Hydrogen Production through Sorption-Enhanced Steam Methane Reforming and Membrane Technology: A Review. *Energy* **2008**, *33* (4), 554–570.
- (190) Schorer, L.; Schmitz, S.; Weber, A. Membrane Based Purification of Hydrogen System (MEMPHYS). *Int. J. Hydrogen Energy* **2019**, *44* (25), 12708–12714.
- (191) Liu, B.; Yu, X.; Shi, W.; Shen, Y.; Zhang, D.; Tang, Z. Two-Stage VSA/PSA for Capturing Carbon Dioxide (CO<sub>2</sub>) and Producing Hydrogen (H<sub>2</sub>) from Steam-Methane Reforming Gas. *Int. J. Hydrogen Energy* **2020**, *45* (46), 24870–24882.
- (192) Antonini, C.; Treier, K.; Streb, A.; van der Spek, M.; Bauer, C.; Mazzotti, M. Hydrogen Production from Natural Gas and

- Biomethane with Carbon Capture and Storage—A Techno-Environmental Analysis. *Sustainable Energy Fuels* **2020**, *4* (6), 2967–2986.
- (193) Relvas, F.; Whitley, R. D.; Silva, C.; Mendes, A. Single-Stage Pressure Swing Adsorption for Producing Fuel Cell Grade Hydrogen. *Ind. Eng. Chem. Res.* **2018**, *57* (14), 5106–5118.
- (194) Fujisawa, A.; Miura, S.; Mitsutake, Y.; Monde, M. Simulation Study of Hydrogen Purification Using Metal Hydride. *J. Alloys Compd.* **2013**, *580*, S423–S426.
- (195) Dunikov, D.; Blinov, D. Extraction of Hydrogen from a Lean Mixture with Methane by Metal Hydride. *Int. J. Hydrogen Energy* **2020**, *45* (16), 9914–9926.
- (196) Borzone, E. M.; Baruj, A.; Meyer, G. O. Design and Operation of a Hydrogen Purification Prototype Based on Metallic Hydrides. *J. Alloys Compd.* **2017**, *695*, 2190–2198.
- (197) Miura, S.; Fujisawa, A.; Ishida, M. A Hydrogen Purification and Storage System Using Metal Hydride. *Int. J. Hydrogen Energy* **2012**, *37*, 2794–2799.
- (198) Huang, X.; Yao, H.; Cheng, Z. Hydrogen Separation Membranes of Polymeric Materials. In *Nanostructured Materials for Next-Generation Energy Storage and Conversion: Hydrogen Production, Storage, and Utilization*; Chen, Y.-P., Bashir, S., Liu, J. L., Eds.; Springer: Berlin, Germany, 2017; pp 85–116, DOI: [10.1007/978-3-662-53514-1\\_3](https://doi.org/10.1007/978-3-662-53514-1_3).
- (199) Pal, N.; Agarwal, M.; Maheshwari, K.; Solanki, Y. S. A Review on Types, Fabrication and Support Material of Hydrogen Separation Membrane. *Mater. Today: Proc.* **2020**, *28*, 1386–1391.
- (200) Teplyakov, V. Polymeric Membranes for Hydrogen Separation/Purification. In *Current Trends and Future Developments on (Bio-) Membranes: New Perspectives on Hydrogen Production, Separation, and Utilization*; Elsevier: Amsterdam, Netherlands, 2020; Chapter 12, pp 281–304, DOI: [10.1016/B978-0-12-817384-8.00012-1](https://doi.org/10.1016/B978-0-12-817384-8.00012-1).
- (201) Luo, S.; Zhang, Q.; Zhu, L.; Lin, H.; Kazanowska, B. A.; Doherty, C. M.; Hill, A. J.; Gao, P.; Guo, R. Highly Selective and Permeable Microporous Polymer Membranes for Hydrogen Purification and CO<sub>2</sub> Removal from Natural Gas. *Chem. Mater.* **2018**, *30* (15), 5322–5332.
- (202) Li, Y.; Chung, T. S. Highly Selective Sulfonated Polyethersulfone (SPES)-Based Membranes with Transition Metal Counterions for Hydrogen Recovery and Natural Gas Separation. *J. Membr. Sci.* **2008**, *308* (1–2), 128–135.
- (203) Shao, L.; Low, B. T.; Chung, T. S.; Greenberg, A. R. Polymeric Membranes for the Hydrogen Economy: Contemporary Approaches and Prospects for the Future. *J. Membr. Sci.* **2009**, *327* (1–2), 18–31.
- (204) Conde, J. J.; Maroño, M.; Sánchez-Hervás, J. M. Pd-Based Membranes for Hydrogen Separation: Review of Alloying Elements and Their Influence on Membrane Properties. *Sep. Purif. Rev.* **2017**, *46* (2), 152–177.
- (205) Dube, S.; Gorimbo, J.; Moyo, M.; Okoye-Chine, C. G.; Liu, X. Synthesis and Application of Ni-Based Membranes in Hydrogen Separation and Purification Systems: A Review. *J. Environ. Chem. Eng.* **2023**, *11* (1), 109194.
- (206) Bernardo, G.; Araújo, T.; da Silva Lopes, T.; Sousa, J.; Mendes, A. Recent Advances in Membrane Technologies for Hydrogen Purification. *Int. J. Hydrogen Energy* **2020**, *45* (12), 7313–7338.
- (207) Roses, L.; Manzolini, G.; Campanari, S.; De Wit, E.; Walter, M. Techno-Economic Assessment of Membrane Reactor Technologies for Pure Hydrogen Production for Fuel Cell Vehicle Fleets. *Energy Fuels* **2013**, *27* (8), 4423–4431.
- (208) Lim, H.; Gu, Y.; Oyama, S. T. Studies of the Effect of Pressure and Hydrogen Permeance on the Ethanol Steam Reforming Reaction with Palladium- and Silica-Based Membranes. *J. Membr. Sci.* **2012**, *396*, 119–127.
- (209) Kanezashi, M.; Yada, K.; Yoshioka, T.; Tsuru, T. Design of Silica Networks for Development of Highly Permeable Hydrogen Separation Membranes with Hydrothermal Stability. *J. Am. Chem. Soc.* **2009**, *131* (2), 414–415.
- (210) Lei, L.; Lindbråthen, A.; Hillestad, M.; He, X. Carbon Molecular Sieve Membranes for Hydrogen Purification from a Steam Methane Reforming Process. *J. Membr. Sci.* **2021**, *627*, 119241.
- (211) Algieri, C.; Drioli, E. Zeolite Membranes: Synthesis and Applications. *Sep. Purif. Technol.* **2021**, *278*, 119295.
- (212) Liu, J.; Liu, C.; Huang, A. Co-Based Zeolitic Imidazolate Framework ZIF-9 Membranes Prepared on α-Al<sub>2</sub>O<sub>3</sub> Tubes through Covalent Modification for Hydrogen Separation. *Int. J. Hydrogen Energy* **2020**, *45* (1), 703–711.
- (213) Li, P.; Wang, Z.; Qiao, Z.; Liu, Y.; Cao, X.; Li, W.; Wang, J.; Wang, S. Recent Developments in Membranes for Efficient Hydrogen Purification. *J. Membr. Sci.* **2015**, *495*, 130–168.
- (214) Ghalei, B.; Wakimoto, K.; Wu, C. Y.; Isfahani, A. P.; Yamamoto, T.; Sakurai, K.; Higuchi, M.; Chang, B. K.; Kitagawa, S.; Sivaniah, E. Rational Tuning of Zirconium Metal–Organic Framework Membranes for Hydrogen Purification. *Angew. Chem.* **2019**, *131* (52), 19210–19216.
- (215) Kerscher, F.; Stary, A.; Gleis, S.; Ulrich, A.; Klein, H.; Spliethoff, H. Low-Carbon Hydrogen Production via Electron Beam Plasma Methane Pyrolysis: Techno-Economic Analysis and Carbon Footprint Assessment. *Int. J. Hydrogen Energy* **2021**, *46* (38), 19897–19912.
- (216) Salkuyeh, Y. K.; Saville, B. A.; MacLean, H. L. Techno-Economic Analysis and Life Cycle Assessment of Hydrogen Production from Different Biomass Gasification Processes. *Int. J. Hydrogen Energy* **2018**, *43* (20), 9514–9528.
- (217) Khojasteh Salkuyeh, Y.; Saville, B. A.; MacLean, H. L. Techno-Economic Analysis and Life Cycle Assessment of Hydrogen Production from Natural Gas Using Current and Emerging Technologies. *Int. J. Hydrogen Energy* **2017**, *42* (30), 18894–18909.
- (218) Cha, J.; Park, Y.; Briglijević, B.; Lee, B.; Lim, D.; Lee, T.; Jeong, H.; Kim, Y.; Sohn, H.; Mikulčić, H.; Lee, K. M.; Nam, D. H.; Lee, K. B.; Lim, H.; Yoon, C. W.; Jo, Y. S. An Efficient Process for Sustainable and Scalable Hydrogen Production from Green Ammonia. *Renewable Sustainable Energy Rev.* **2021**, *152*, 111562.
- (219) Ganeshan, P.; Vigneswaran, V. S.; Gowd, S. C.; KonduSamay, D.; Sanjay kumar, C.; Krishnamoorthy, N.; Kumar, D.; Juneja, A.; Paramasivan, B.; Raju, N. N.; Rajendran, K.; Pugazhendhi, A. How Does Techno-Economic Analysis and Lifecycle Assessment Help in Commercializing the Biohydrogen Supply Chain? *Fuel* **2023**, *341*, 127601.
- (220) Nasharuddin, R.; Zhu, M.; Zhang, Z.; Zhang, D. A Technoeconomic Analysis of Centralised and Distributed Processes of Ammonia Dissociation to Hydrogen for Fuel Cell Vehicle Applications. *Int. J. Hydrogen Energy* **2019**, *44* (28), 14445–14455.
- (221) Moraes, T. S.; Cozendey da Silva, H. N.; Zotes, L. P.; Mattos, L. V.; Pizarro Borges, L. E.; Farrauto, R.; Noronha, F. B. A Techno-Economic Evaluation of the Hydrogen Production for Energy Generation Using an Ethanol Fuel Processor. *Int. J. Hydrogen Energy* **2019**, *44* (39), 21205–21219.
- (222) Khamhaeng, P.; Laosiripojana, N.; Assabumrungrat, S.; Kim-Lohsoontorn, P. Techno-Economic Analysis of Hydrogen Production from Dehydrogenation and Steam Reforming of Ethanol for Carbon Dioxide Conversion to Methanol. *Int. J. Hydrogen Energy* **2021**, *46* (60), 30891–30902.
- (223) Byun, M.; Lee, B.; Lee, H.; Jung, S.; Ji, H.; Lim, H. Techno-Economic and Environmental Assessment of Methanol Steam Reforming for H<sub>2</sub> Production at Various Scales. *Int. J. Hydrogen Energy* **2020**, *45* (46), 24146–24158.
- (224) Kim, S.; Yun, S. W.; Lee, B.; Heo, J.; Kim, K.; Kim, Y. T.; Lim, H. Steam Reforming of Methanol for Ultra-Pure H<sub>2</sub> Production in a Membrane Reactor: Techno-Economic Analysis. *Int. J. Hydrogen Energy* **2019**, *44* (4), 2330–2339.
- (225) Khodabandehloo, M.; Larimi, A.; Khorasheh, F. Comparative Process Modeling and Techno-Economic Evaluation of Renewable Hydrogen Production by Glycerol Reforming in Aqueous and Gaseous Phases. *Energy Convers. Manage.* **2020**, *225*, 113483.

- (226) Martins, A. H.; Rouboa, A.; Monteiro, E. On the Green Hydrogen Production through Gasification Processes: A Techno-Economic Approach. *J. Cleaner Prod.* **2023**, *383*, 135476.
- (227) Ongis, M.; Di Marcoberardino, G.; Manzolini, G.; Gallucci, F.; Binotti, M. Membrane Reactors for Green Hydrogen Production from Biogas and Biomethane: A Techno-Economic Assessment. *Int. J. Hydrogen Energy* **2023**, *48* (51), 19580–19595.
- (228) Vuppaldadiyam, A. K.; Vuppaldadiyam, S. S. V.; Awasthi, A.; Sahoo, A.; Rehman, S.; Pant, K. K.; Murugavel, S.; Huang, Q.; Anthony, E.; Fennel, P.; Bhattacharya, S.; Leu, S. Y. Biomass Pyrolysis: A Review on Recent Advancements and Green Hydrogen Production. *Bioresour. Technol.* **2022**, *364*, 128087.
- (229) Hernández, B.; Blázquez, C. G.; Aristizábal-Marulanda, V.; Martín, M. Production of H<sub>2</sub> and Methanol via Dark Fermentation: A Process Optimization Study. *Ind. Eng. Chem. Res.* **2020**, *59* (38), 16720–16729.
- (230) Han, W.; Yan, Y.; Gu, J.; Shi, Y.; Tang, J.; Li, Y. Techno-Economic Analysis of a Novel Bioprocess Combining Solid State Fermentation and Dark Fermentation for H<sub>2</sub> Production from Food Waste. *Int. J. Hydrogen Energy* **2016**, *41* (48), 22619–22625.
- (231) Genç, Ş.; Koku, H. A Preliminary Techno-Economic Analysis of Photofermentative Hydrogen Production. *Int. J. Hydrogen Energy* **2024**, *52*, 212.
- (232) Yukesh Kannan, R.; Kavitha, S.; Preethi; Parthiba Karthikeyan, O.; Kumar, G.; Dai-Viet, N. V.; Rajesh Banu, J. Techno-Economic Assessment of Various Hydrogen Production Methods—A Review. *Bioresour. Technol.* **2021**, *319*, 124175.
- (233) Hosseinzadeh, A.; Zhou, J. L.; Li, X.; Afsari, M.; Altaee, A. Techno-Economic and Environmental Impact Assessment of Hydrogen Production Processes Using Bio-Waste as Renewable Energy Resource. *Renewable Sustainable Energy Rev.* **2022**, *156*, 111991.
- (234) Lepage, T.; Kammoun, M.; Schmetz, Q.; Richel, A. Biomass-to-Hydrogen: A Review of Main Routes Production, Processes Evaluation and Techno-Economical Assessment. *Biomass Bioenergy* **2021**, *144*, 105920.
- (235) Wu, N.; Lan, K.; Yao, Y. An Integrated Techno-Economic and Environmental Assessment for Carbon Capture in Hydrogen Production by Biomass Gasification. *Resour., Conserv. Recycl.* **2023**, *188*, 106693.
- (236) Frowijn, L. S. F.; van Sark, W. G. J. H. M. Analysis of Photon-Driven Solar-to-Hydrogen Production Methods in the Netherlands. *Sustainable Energy Technol. Assess.* **2021**, *48*, 101631.
- (237) Arcos, J. M. M.; Santos, D. M. F. The Hydrogen Color Spectrum: Techno-Economic Analysis of the Available Technologies for Hydrogen Production. *Gases* **2023**, *3* (1), 25–46.
- (238) Yu, M.; Wang, K.; Vredenburg, H. Insights into Low-Carbon Hydrogen Production Methods: Green, Blue and Aqua Hydrogen. *Int. J. Hydrogen Energy* **2021**, *46* (41), 21261–21273.
- (239) Zhou, Y.; Li, R.; Lv, Z.; Liu, J.; Zhou, H.; Xu, C. Green Hydrogen: A Promising Way to the Carbon-Free Society. *Chin. J. Chem. Eng.* **2022**, *43*, 2–13.
- (240) Pinsky, R.; Sabharwall, P.; Hartvigsen, J.; O'Brien, J. Comparative Review of Hydrogen Production Technologies for Nuclear Hybrid Energy Systems. *Prog. Nucl. Energy* **2020**, *123*, 103317.
- (241) Nasser, M.; Megahed, T. F.; Ookawara, S.; Hassan, H. Techno-Economic Assessment of Clean Hydrogen Production and Storage Using Hybrid Renewable Energy System of PV/Wind under Different Climatic Conditions. *Sustainable Energy Technol. Assess.* **2022**, *52*, 102195.
- (242) Grimm, A.; de Jong, W. A.; Kramer, G. J. Renewable Hydrogen Production: A Techno-Economic Comparison of Photoelectrochemical Cells and Photovoltaic-Electrolysis. *Int. J. Hydrogen Energy* **2020**, *45* (43), 22545–22555.
- (243) Shaner, M. R.; Atwater, H. A.; Lewis, N. S.; McFarland, E. W. A Comparative Technoeconomic Analysis of Renewable Hydrogen Production Using Solar Energy. *Energy Environ. Sci.* **2016**, *9* (7), 2354–2371.
- (244) Maurya, J.; Gemechu, E.; Kumar, A. The Development of Techno-Economic Assessment Models for Hydrogen Production via Photocatalytic Water Splitting. *Energy Convers. Manage.* **2023**, *279*, 116750.
- (245) Achour, Y.; Berrada, A.; Arechkik, A.; El Mrabet, R. Techno-Economic Assessment of Hydrogen Production from Three Different Solar Photovoltaic Technologies. *Int. J. Hydrogen Energy* **2023**, *48* (83), 32261–32276.
- (246) Touili, S.; Bouaichi, A.; Alami Merrouni, A.; Amrani, A.-i.; El Amrani, A.; El Hassouani, Y.; Messaoudi, C. Performance Analysis and Economic Competitiveness of 3 Different PV Technologies for Hydrogen Production under the Impact of Arid Climatic Conditions of Morocco. *Int. J. Hydrogen Energy* **2022**, *47* (74), 31596–31613.
- (247) Nikolaidis, P.; Poullikkas, A. A Comparative Overview of Hydrogen Production Processes. *Renewable Sustainable Energy Rev.* **2017**, *67*, 597–611.
- (248) Mohsin, M.; Rasheed, A. K.; Saidur, R. Economic Viability and Production Capacity of Wind Generated Renewable Hydrogen. *Int. J. Hydrogen Energy* **2018**, *43* (5), 2621–2630.
- (249) Qureshi, F.; Yusuf, M.; Tahir, M.; Haq, M.; Mohamed, M. M. I.; Kamyab, H.; Nguyen, H. H. T.; Vo, D. V. N.; Ibrahim, H. Renewable Hydrogen Production via Biological and Thermochemical Routes: Nanomaterials, Economic Analysis and Challenges. *Process Saf. Environ. Prot.* **2023**, *179*, 68–88.